
SYNTHESIS AND PHYSICAL CHARACTERISATION OF DOPED CONDUCTING POLYAROMATIC AMINES

Thesis submitted to the
Cochin University of Science and Technology
in partial fulfilment of the requirements
for the degree of

DOCTOR OF PHILOSOPHY
under the faculty of Science

G5602

by
M. J. JOSEPH

**DEPARTMENT OF APPLIED CHEMISTRY
COCHIN UNIVERSITY OF SCIENCE AND TECHNOLOGY
COCHIN – 682 022
INDIA**

DECEMBER 1995

CERTIFICATE

This is to certify that this thesis is an authentic record of the research work carried out by the author under our joint supervision, in partial fulfillment of the requirements for the degree of Doctor of Philosophy under the Faculty of Science of Cochin University of Science and Technology and further that no part thereof has been presented before for any other degree.

P. Madhavan Pillai

Professor P. Madhavan Pillai
(Supervising Teacher)
Professor and Head
Department of Applied Chemistry
Cochin University of Science and Technology
Kochi 682 022

Professor Jacob Philip
(Co-Guide)
Professor and Head
Department of Instrumentation (USIC)
Cochin University of Science and Technology
Kochi 682 022

Kochi - 22
28/12/1995

CONTENTS

PREFACE

CHAPTER 1

CONDUCTING POLYMERS - AN OVERVIEW	1
1. 1 INTRODUCTION TO ORGANIC CONDUCTORS	1
1. 2 CONDUCTING POLYMERS	2
1. 3 CHEMICAL SYNTHESIS OF CONDUCTING POLYMERS	3
1. 4 ELECTROCHEMICAL SYNTHESIS	5
1. 5 PLASMA POLYMERIZATION	7
1. 6 DOPING	7
1. 7 TRANSPORT PROPERTIES OF CONDUCTING POLYMERS	8
1. 8 MECHANISM OF ELECTRICAL CONDUCTION	12
1. 8a DC CONDUCTIVITY	13
1. 8b AC CONDUCTIVITY	21
1. 8c THERMOELECTRIC POWER	24
1. 9 WORK DONE IN THE THESIS	27
REFERENCES	29

CHAPTER 2

SYNTHESIS OF POLY AROMATIC AMINES	34
2. 1 INTRODUCTION	34
2. 2 CHEMICAL SYNTHESIS OF POLYAROMATIC AMINES	36
2. 3 POLYMERISATION MECHANISMS	38
2. 4 EXPERIMENTAL PROCEDURE	42
2. 5 SYNTHESIS OF POLYANILINE	43
2. 6 SYNTHESIS OF POLYANISIDINE	45
2. 7 COPOLYMERISATION	46
2. 8 PURIFICATION OF CONDUCTING POLYMERS	47
2. 9 DOPING	48
REFERENCES	49

CHAPTER 3

CHARACTERISATION OF POLYAROMATIC AMINES	53
3. 1 INTRODUCTION	53
3. 2 IR SPECTROSCOPY FOR POLYMER CHARACTERISATION	54
3. 2a. SAMPLE PREPARATION	56
3. 2b. RESULTS AND DISCUSSION	56
3. 3 NMR SPECTROSCOPY FOR POLYMER CHARACTERISATION	62
3. 3a. SAMPLE PREPARATION	63
3. 3b. RESULTS AND DISCUSSION	63
3. 4 UV SPECTROSCOPY FOR POLYMER CHARACTERISATION	68
3. 4a. SAMPLE PREPARATIONS	69
3. 4b. RESULT AND DISCUSSION	69
3. 5 X-RAY DIFFRACTION FOR POLYMER RESEARCH	74
3. 5a. WIDE-ANGLE X-RAY SCATTERING (WAXS)	75
3. 5b. SMALL ANGLE X-RAY SCATTERING (SAXS)	76
3. 5c. SAMPLE PREPARATION	77
3. 5d. RESULTS AND DISCUSSIONS	77
3. 6 THE PROPOSED STRUCTURES OF THE POLYMERS	80
REFERENCES	83

CHAPTER 4

ELECTRICAL TRANSPORT PROPERTIES OF POLYAROMATIC AMINES -I. DC AND AC CONDUCTIVITY	84
4. 1 INTRODUCTION	84
4. 2 DC CONDUCTION MECHANISM	86
4. 3 THEORY OF DC CONDUCTIVITY	89
4. 3a. CONDUCTION BY POLARONS	95
4. 3b. INTERSOLITON HOPPING CONDUCTION	96
4. 3c. TUNNELING CONDUCTION	97
4. 4 EXPERIMENTAL TECHNIQUE	103
4. 5 RESULTS AND DISCUSSION	106

4. 6	AC CONDUCTIVITY	124
4. 6a	ROLE OF VRH ON AC CONDUCTIVITY	126
4. 7	EXPERIMENTAL TECHNIQUE FOR AC CONDUCTIVITY	128
4. 8	RESULTS AND DISCUSSION	132
	REFERENCES	141

CHAPTER 5

ELECTRICAL TRANSPORT PROPERTIES OF POLYAROMATIC AMINES - II. THERMO ELECTRIC POWER **145**

5. 1	INTRODUCTION	145
5. 2	SIGNIFICANCE OF THERMOELECTRIC POWER	148
5. 3	EXPERIMENTAL METHOD	153
5. 4	RESULTS AND DISCUSSION	156
	REFERENCES	179

CHAPTER 6

THERMAL PROPERTIES OF CONDUCTING POLYMERS - POLYANILINE, POLYANISIDINE AND CO-POLYMERS **181**

6. 1	INTRODUCTION	181
6. 2	EXPERIMENTAL METHOD	187
6. 3	RESULTS AND DISCUSSION	191
	REFERENCES	195

CHAPTER 7

SUMMERY AND CONCLUSION **196**

PREFACE

Conducting polymers have emerged as a new class of electronic materials recently. They have attracted considerable attention as the investigations on these systems have generated entirely new scientific concepts as well as potential for new technology. Since these materials are polymers, they have highly anisotropic quasi-one-dimensional structures which make them fundamentally different from conventional inorganic semiconductors. Their chain like structure leads to strong coupling of the electronic states to conformational excitations peculiar to a one dimensional system. Electron processes in organic polymers cause modifications of chain geometry leading to strong electron-phonon coupling. The relatively weak interchain binding allows diffusion of dopant molecules into the structure while the strong intra chain C-C bonds maintain the integrity of the polymer. Several of the conjugated polymers exhibit very interesting nonlinear optical properties. A number of intrinsically insulating conjugated organic polymers can be doped to near metallic conductivities. The doping process involves exposure of the polymer to electron donors (such as alkali metals) or

electron acceptors (such as I_2 or AsF_5). The conductivity of organic polymers like polyacetylene, polyphenylenes, polyphenylene chalcogenides, polypyrrole etc. can be increased by several orders of magnitude by doping.

So far, maximum work has been done on polyacetylene because of its simple chain structure which allows extensive theoretical calculations and predictions to be made on their properties. But of late, more experimental as well as theoretical work are increasingly being devoted to nitrogen containing conducting polyaromatics such as polypyrrole, polyaniline etc. The conductivity and other properties of polyaromatics can also be modified substantially by doping . The interest in these materials is due to their potential applications in high energy density batteries, solar cells and novel electronic devices. Moreover, their properties are very exciting from the point of view of basic physics and chemistry. The area of conducting polymers is still a virgin field with plenty of scope for doing good work. Most of the work so far have been concentrated around a few materials such as polyacetylene, polypyrrole, polythiophene etc. The synthesis, characterization and investigation of the properties of many more conducting polymers, particularly polyaromatic amines, still remain to be done.

The unique properties of polyaromatic amines such as their charge conjugation asymmetry, high redox activity and the presence of nitrogen atoms in the conjugation path make them different from other conducting polymers. In this thesis we present the work we have done a few polyaromatic amines such as polyaniline, polyanisidine, and their copolymers. We have synthesised and characterized these materials. Selected physical properties of these materials have been studied and the effect of copolymerisation on the electrical properties of these materials have been investigated.

The thesis opens with an introductory chapter on the synthesis and physical properties of conducting polymers. This chapter is bifurcated into two parts, dealing with the synthesis and with the physical properties of conducting polymers. An introduction to organic conductors in general and conducting polymers in particular is given in this chapter. The techniques adopted for the preparation of these materials and their chemical, electrochemical and plasma polymerisation are briefly reviewed.

As has already been mentioned, conducting polymers have very exciting physical properties, particularly with regard to electrical conductivity. The general properties of these

materials are reviewed in Chapter 1. The electrical conductivity of these materials can be modified by doping and the mechanisms of electrical conduction are very peculiar and interesting. These aspects are also reviewed in this chapter. Further, work done by previous workers on dc conductivity, ac conductivity and thermoelectric power are reviewed here. Reference to the work done by earlier workers are cited at the end of the same chapter.

The work reported in the thesis basically is centered around the following conducting polymers: polyaniline, polyanisidine, and their copolymers. The details of the techniques used by us for synthesising these polyaromatic amines are described in Chapter 2 of the thesis. Chemical polymerisation techniques adopted by us for synthesising these materials are described in detail. Method of synthesising the copolymers is also described. The various methods adopted for purifying the materials and details of doping the polymer to make them electrically conducting are also discussed.

The various techniques used by us for characterizing the materials prepared and the results obtained are outlined in Chapter 3 of the thesis. The characterization methods used

by us include UV-Vis., FT-IR, NMR spectroscopy and X-ray diffraction studies. The details of all these techniques and experimental procedures are described in this chapter. The results obtained from each of the above characterization methods when applied to each of the materials under study are given and the results are discussed in each case.

Chapter 4 and 5 are devoted to details of the investigation of the electrical properties of the polyaromatic amines which we have studied. The theory of charge transport in polymeric conductors is outlined in Chapter 4. Details of dc conductivity, ac conductivity and thermoelectric power measurements on these samples are described. We have made these measurements on doped samples over a temperature range of 30K to 295K. Computer controlled measurement setups have been used in these studies. We have got some very interesting and new results and a detailed discussion of these results are given in Chapter 5. Measurements of the temperature variation of conductivity in some of these polymers are reported for the first time and so are the measurements on thermoelectric power. Our results on conductivity and thermoelectric power measurements enable us to predict the nature of the charge carriers in these materials upon doping.

In addition to electrical properties, we have studied selected thermal properties of our samples. The thermal diffusivity of the samples pelletized into disc form have been measured using the photoacoustic technique. The thermal diffusivity data are given in this chapter. A detailed description of the experimental technique used in these measurements, the results obtained and the analysis of the results are given in Chapter 6 of the thesis. The conclusions drawn from these studies are also given in this chapter. Only very limited work had been reported so far on the thermal properties of conducting polymers and our results forms the first of this kind on polyaromatic amines.

The general conclusions drawn by us from the results presented in earlier chapters of the thesis are presented in Chapter 7. This chapter also summarises the results presented in earlier chapters. The area of conducting polymers is very fascinating and there is plenty of scope for further research in this area. This aspect is also outlined in the last chapter.

We are in the process of communicating the results contained in this thesis to journals in the relevant area.

CHAPTER 1

CONDUCTING POLYMERS - AN OVERVIEW

1. 1 INTRODUCTION TO ORGANIC CONDUCTORS

Over the past 20 years, chemists have devoted much effort to synthesizing and characterizing organic conducting materials. The ability of these materials to undergo variations in electrical conductivity from insulating level to metallic conducting level is an exciting phenomenon and is proposed to have a large number of applications in electronic industry. Research in this field has lead to the discovery of a large number of semi conducting, metallic and even superconducting organic materials. In the field of organic semiconductors phthalocynine and metal phthalocynine are of prime importance since these materials are made use of in electrophotography, photochemical cells, photo voltaic cells etc. Among conducting organic materials, conducting polymers and organic charge transfer salts are the important ones form the application point of view. The doping of certain polymers with suitable reducing or oxidizing agents give rise to changes in conductivity from insulating to

metallic levels. Certain organic charge transfer salts show not only metallic conductivity, but also superconductivity under certain conditions. The recently discovered fullerenes, which exhibit high temperature superconductivity, are again molecules made of carbon atoms. The possibility of varying the conductivity from insulator to metallic levels in polymers has attracted a large number of scientists, not only chemists but also physicists and material scientists to explore the exciting possibilities in this field.

1. 2 CONDUCTING POLYMERS

The synthesis and quantitative investigation of electrical conductivity in organic polymers was revolutionized in 1977 with the observation of metallic conductivity in polyacetylene [1]. After the observation of metal like conductivity in polyacetylene (PA), very large number of conducting polymers have been synthesised using different methods of synthesis and doping. Among them polypyrrole, polythiophene, polyparaphynelene and polyaniline are the conducting polymers in which extensive studies have been carried out. Since the conductivity of these materials are known to depend on the method of synthesis, a large number

of preparation methods has been developed to improve the conductivity. Electrochemical, chemical and plasma polymerisation are the most notable and widely used techniques in this regard.

1. 3 CHEMICAL SYNTHESIS OF CONDUCTING POLYMERS

Conducting polymers are synthesized by the usual polymerization methods like chain or step growth polymerization as well as by special methods which are briefly discussed in the following paragraphs.

Polyacetylene (PA) was first synthesised by chain polymerization technique using Ziegler-Natta catalysts [2]. Free standing cis-PA film was prepared by polymerization of pure, dry acetylene gas at 195K using the titanium tetrabutoxide-triethyl aluminum catalyst system in toluene with Al:Ti in 4:1 ratio. All trans-PA was obtained by polymerization at 423K and using n-hexadecane as the solvent [3]. Polyacetylene was also prepared by a similar method using Lutinger catalyst (prepared by reduction of NiCo with sodium borohydeide) [4].

Polyacetylene synthesis using Ziegler-Natta catalyst is a widely accepted technique. But the fibrils in the film are randomly oriented which is not at all desirable for a polymeric material intended to exhibit high electrical conductivity. Hence modification of the catalyst or modification of the synthetic procedure using the same Ziegler-Natta catalyst changes very significantly the nature of the product in PA synthesis. Naarman et al [5] synthesised new PA using an $\text{AlEt}_3 / \text{Ti}(\text{OBu})_4$ catalyst dissolved in silicone oil which was heat treated at 393K for 2 hours before use. The materials obtained were homogeneous, highly regular and compact, crystalline, and defect free [5].

Polyheterocycles, namely polypyrrole and polythiophene previously prepared by electrochemical method are also now being synthesised by chain polymerization processes. Catalysts used are iron or copper perchlorates, chlorides etc. As in the electrochemical polymerization of these monomers, polymerization and doping are achieved simultaneously in these ionic chain growth polymerization also. However the polymers are obtained in the powder form.

In addition to chain growth polymerization methods, step growth polymerization methods are also performed for the synthesis of conducting polymers. These methods usually precede condensation reaction of bifunctional monomers to give a linear polymer. This polymerization technique has been used to synthesis quite a number of polymers containing heteroatom in the backbone. Polyphenylene sulphide is a well studied and commercially available polymer among those synthesised by step growth polymerization method [8]. The advantage of this method over chain growth polymerization is that it is possible to synthesis high molecular weight materials using this.

1. 4 ELECTROCHEMICAL SYNTHESIS

Electrochemical synthesis is regarded as a relatively simple method for the synthesis of conducting polymers. The beauty of this method is that polymerization in suitable electrolytic medium gives directly the desired doped polymer as a flexible free standing film. In this method, films are formed on the electrode surface by oxidative coupling and hence electrochemical stoichiometry is maintained [8]. In this respect the method is quite similar to the common electrochemical deposition of metal. It thus differs

basically from the common electroinitiated polymerization process where only chain initiation takes place either directly or indirectly by electrochemical means and chain polymerization takes place in bulk.

For the polymerization by the above method the monomer should be so chosen that (i) it possesses relatively low anodic potential ($< 2.1 \text{ V}$), (ii) its aromaticity should be maintained after substitution at suitable positions, and (iii) cation intermediate should be of intermediate stability, (iv) the solvent should have poor nucleophilic character, and finally, (v) the electrode should be such that it is not oxidised concurrently with the monomer [8].

The well studied polymers, polypyrrole (PPY) and polythiophene (PTh) are usually prepared by electrochemical polymerization. Attempts have been made to synthesis other polymers from aniline [10] or phenol [11] and more recently, benzene and other aromatic hydrocarbons [12] are electrochemically polymerised to produce conducting polymer systems.

1. 5 PLASMA POLYMERIZATION

Plasma polymerization is a useful and effective method for preparing ultra thin, uniform polymer layers that strongly adhere to an appropriate substrate. Electric glow discharge is used to create low temperature or cold plasma required for the process. The main advantage of this method is that it is a one step process that eliminates the various steps necessary for conventional coating processes.

1. 6 DOPING

Conducting polymers generally exhibit poor electrical conductivity in the virgin state and behave as insulators. Only polyacetylene shows semiconducting behaviour in the virgin state. The virgin polymer need to be treated with suitable oxidising or reducing agents to remarkably enhance their conductivities. The method has been termed doping in analogy to similar phenomenon associated with inorganic semiconductors. But the process and mechanism of doping as applied to the above two classes of materials differ widely in significance.

Doping of conducting polymers involve random dispersion or aggregation of dopant in molar concentration in the disordered substrate. The dopant concentration may be as high as 50% [13]. Also, incorporation of the dopant molecules in the quasi-one dimensional polymeric systems considerably distort the chain order resulting in a local reorganization of the polymer [14].

Besides, the mechanism of doping is also different in the two cases [15]. Doping of inorganic semiconductors generates either holes in the valence band or electrons in conduction band, whereas doping of a polymer results in the formation of conjugational defects viz soliton, polaron or bipolarons in the polymer chain [16].

1. 7 TRANSPORT PROPERTIES OF CONDUCTING POLYMERS

A number of papers have been published on the transport properties of conducting polymers. However there are still several points on which different workers disagree regarding the mechanism of charge transport in conducting polymers. This is largely due to the complex structural and morphological forms that conducting polymers exhibit. They are disordered materials, whose charge transport can usually

be considered as a percolation process. Conducting pathways have to be formed through the sample in order to make the current flow. The special nature of the charge carriers (solitons, polarons, bipolarons) in these materials reflects the role and importance of electron-phonon interaction, but in addition, the Coulombic interaction between electrons also may play a significant role. There is also the question of the dimensionality, since in principle a conjugated carbon chain is a one-dimensional conductor. Interchain charge transfer may, however, often make the charge transport appear three dimensional. Another important factor contributing to the complexity of the problem is doping, which usually influences the structure as well as the electrical properties strongly.

Theoretical calculations have demonstrated that the intrinsic transport properties of highly doped conjugated polymers are metallic [17]. However, even the most conductive and best-oriented samples studied so far still show semiconductive temperature dependence of dc and ac conductivities. The highest room temperature conductivity, of the order of 100000 S cm^{-1} , has been obtained in stretch-oriented trans-PA doped with iodine [18], while theoretical estimates give values that are one or two orders of

magnitude higher [19]. This indicates that the conductivity is still limited by structural defects and or interchain charge transfer. Detailed experiments have shown that the transport in highly doped conducting polymers can usually be described by models considering small conducting islands separated by resistive barriers. The charge transport then occurs via hopping of the carriers across these barriers and quantum mechanical tunneling through the barriers.

Lightly doped or undoped conducting polymers show strong temperature dependence for conductivity. The room temperature conductivity is low and the electrical properties resemble those of insulators or poor semiconductors. The charge carrier transport is described as occurring via hopping between localized solitonic, polaronic or bipolaronic states. The electrical properties of moderately doped samples are typically the most difficult to interpret, because there may be several transport processes acting in parallel.

Investigations on the electrical transport properties have been carried out not only in PA but also on a very large number of other conducting polymers. Figure 1.1 shows the structure of some of the well studied conducting polymers.

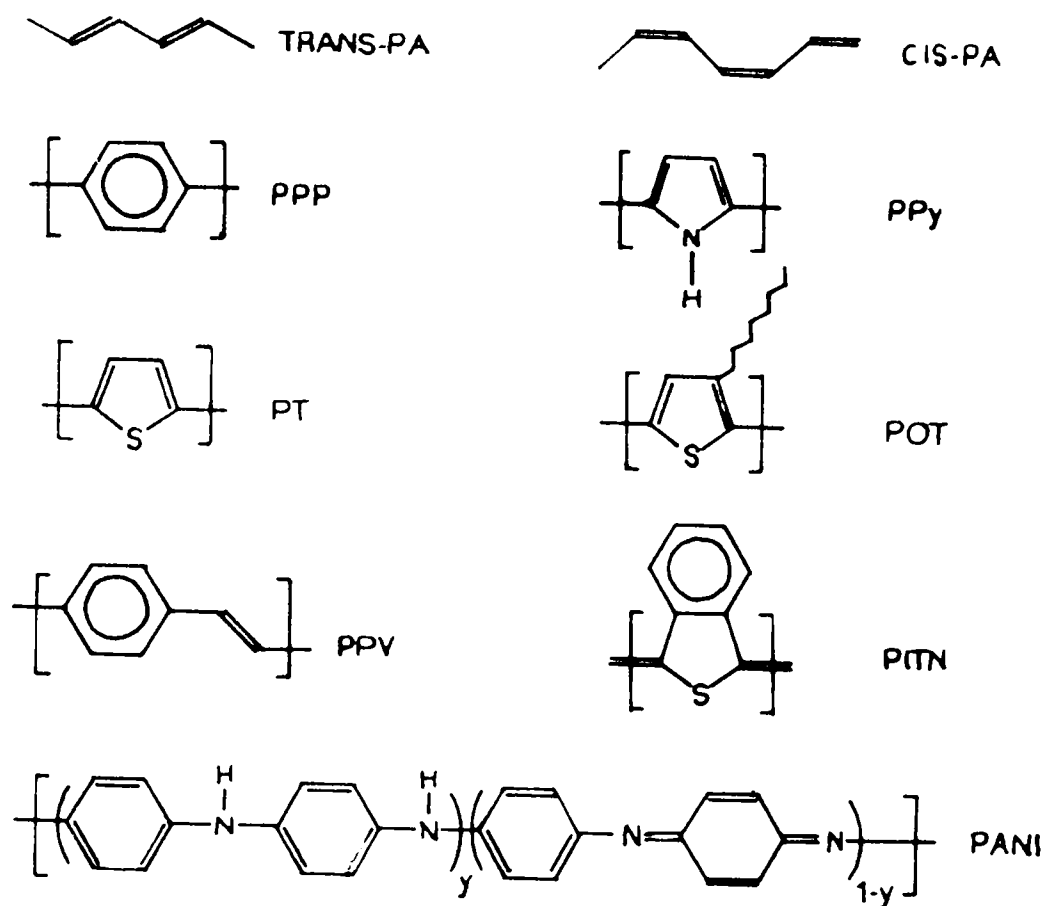


Figure 1.1. Structure of various conducting polymers. The following abbreviations have been used: trans-polyacetylene (trans-PA), cis-polyacetylene (cis-PA), polyparaphenylene (PPP), polypyrrole (PPy), polythiophene (PT), poly(3-ocylthiophene) (POT), polyphenylenevinylene (PPV), polyisothianaphthene (PITN), polyaniline (PAN).

Among them, polyaniline family of conducting polymer has attracted much attention, since, it provides a means of systematically studying the electronic structure of polymer as a function of both the number of electrons and the number of protons on the polymer chain. The understanding of the electronic state of this polymer with protonation is of great interest in the attempts to unveil the physics of the same and other polymer system containing heteroatoms [20,21,22,23,24].

1. 8 MECHANISM OF ELECTRICAL CONDUCTION

It is well known that conducting polymers have a lot of properties in common with amorphous materials due to their feasibility for different conformation, dangling bonds etc., although a certain amount of crystallinity also exists for some polymers [25]. Recent advances in the understanding of the effects of disorder on electrical and transport properties in amorphous semiconductors have provided some deep insight into the problem of transport in doped and undoped polymers.

Experimental data of electrical properties can only be properly explained if a model for the electronic structure

is available. It is well known after the pioneering work of Bloch that crystals have a universal energy band structure. For crystalline semiconductors, the main features of the energy distribution of the density of states are the presence of sharp structures in the valence and conduction bands, and their abrupt termination at the valence band maximum and conduction band minimum. The sharp edges in the density of states create a well defined energy gap. Within the band, the wave functions are extended. In amorphous solids, the long range order is absent and the short range order determine the energy band structure and charge transport. The concept of the density of states is very well applicable to noncrystalline solids as well [26,27,28].

1. 8a. DC CONDUCTIVITY

Even though conducting polymers show metallic level of conductivity, the temperature dependence of conductivity is not metal like. In most of the conducting polymers, the dependence is like that of a semiconductor. The semiconductor like behaviour of the conductivity has been explained on the basis of the existence of potential barriers between highly conducting regions. These barriers

have been suggested to be conjugational defects, or other inhomogeneities in the polymer chain. The charge carriers will have to hop over or tunnel through the potential barriers. Since tunneling by itself is a temperature independent process, the temperature dependence of the conductivity must arise from other processes influencing the charge transfer between highly conducting regions. The models of Sheng take into account the charging energy of conducting regions [29] or the random thermal motion of charge carriers on both sides of the tunnel junction [30], and the derived transport characteristics have been the most successful ones in describing the conductivity of highly doped conjugated polymers.

When the size of highly conducting regions or islands are sufficiently small (less than about 20 nm), the energy required to move an electron from an electrically neutral island become significant. If the voltage between two adjacent islands is small compared with $kT/|e|$, charge carriers can be generated only by thermal activation, making conductivity temperature dependent and limited by only the charging energy. The charge carriers will then percolate along the path with least resistance. The conductivity varies with temperature as [30],

$$\sigma = \sigma_0 \exp \{-(T_0/T)\}^{1/2} \quad (1.1)$$

where σ_0 and T_0 are material constants.

If the size of the highly conducting regions is larger than about 20 nm, charging energy becomes negligible. Sheng's second model for inhomogeneous conductors is based on fluctuation-induced tunnelling of charge carriers between highly conducting islands. This model applies to larger conducting regions, typically of the order of a micrometer. The theory assumes that the random thermal motion of the charge carriers within the conducting islands induces a randomly alternating voltage across the gap between neighboring islands. When the potential barrier formed by the gap is assumed to be parabolic, a simple expression can be derived for the temperature dependence of the conductivity [31], given by

$$\sigma = \sigma_1 \exp \{-T_2/(T_2+T)\} \quad (1.2)$$

T_1 and T_2 are material constants dependent on the width and height of the tunneling barrier. T_1 is typically greater than 100K and T_2 ranges from a few K to several tens of K.

The models for charging energy limited and thermal fluctuation induced tunneling have proved to be appropriate for describing the transport properties of highly doped conducting polymers for many reasons. Effects such as doping resulting in inhomogeneously distributed dopants, fibrillar morphology, interchain transport, transport through grain boundaries etc. can very well be accounted for by these models. The various morphological and structural forms taken by conducting polymers because of changes in dopant, doping level, dedoping, compensation and processing may, however, also result in the applicability or combination of other transport models, such as the hopping models. The granular metal type behavior, i.e. tunneling between highly conducting regions having metallic properties, is still the most commonly observed transport property in doped conducting polymer, with the exception of new highly conducting trans-PA at higher temperatures.

The values of the conductivity at zero temperature is a distinguishable difference between tunneling and hopping conduction. Being phonon assisted tunneling between localized electronic states, the hopping conductivity vanishes as the temperature falls to zero. In the case of

tunneling conduction, the conductivity does not extrapolate to zero because the tunneling process itself is temperature independent, depending only on the shape and height of the potential barrier separating the carriers. However, limitations caused by charging effects in tunneling between smaller metallic particles can also force the conductivity to zero when no thermal energy is available.

Each state can have only one electron of each spin direction in the hopping conduction process. If the localization is very strong, an electron will jump to the nearest state, and this nearest neighbour hopping conductivity will be proportional to the Boltzmann factor, $\exp(-W/k_B T)$, where W is the difference between the energies of the two states. If localization is less strong, an electron can jump to sites for which the activation energy is smaller but which can reside further away, i.e the conduction occurs by variable range hopping. As the temperature is decreased, fewer states fall within the allowed energy range and the average hopping distance increases. As a result, the hopping probability and, thus, conductivity decrease. The temperature dependence of variable range hopping (VRH) conductivity is [32].

$$\sigma = \sigma_2(T) \exp \{-(T_3/T)\}^{1/(d+1)} \quad (1.3)$$

where d indicates the dimensionality, and

$$T_3 \propto (a^d N(E_F))^{-1} \quad (1.4)$$

where $N(E_F)$ is the density of states and a denotes the localization length. The prefactor $\sigma_2(T)$ is more slowly varying than the exponential factor. Hence the logarithm of the conductivity is proportional to $T^{-1/4}$, $T^{-1/3}$, $T^{-1/2}$ for three, two and one dimensional conduction, respectively. Because the resistance of the traversed route can be optimized, the temperature dependence of the conductivity is strong compared with nearest neighbour hopping.

Over the years, the theory of variable range hopping has been successful in describing the transport properties in a variety of disordered semiconductors, as well as in conducting polymers, despite the many approximations and simplifications made in deriving the equations. Further work has, for example, included the Coulomb interaction between localized electrons [33], which changes the exponent from $1/4$ to $1/2$ in above equation for three dimensions. Another

modification, the model of anisotropic variable range hopping [34] developed for conducting polymers, assumes that the wave function is less localized in the direction of the conjugated chain, so that hops in chain direction are favoured. Taking this realistic assumption into account has generally resulted in improved agreement with experimental data.

Since the theory of variable range hopping was originally developed for amorphous semiconductors, it ignores the extraordinary nature of charge carriers in conjugated polymers. The intersoliton hopping model was proposed by Kivelson [35] to account for, for example, the experimentally observed large thermopower and the strong temperature dependence of the ac conductivity in lightly doped trans-PA, whose features are in contradiction to variable range hopping. The theory assumes inter chain transport to occur by hopping between neutral and charged soliton states at isoenergetic levels. Neutral solitons are mobile along the carbon chain, while charged soliton are pinned next to dopant ions. Their roles are interchanged in the hopping process. The temperature dependence of the dc conductivity can be approximated by a simple power law:

$$\sigma = A T^i$$

(1.5)

where A is a constant. The power index i lies typically around 10 or above. The intersoliton model has also been modified for the case of interpolyaronic conduction in conducting polymers with a non degenerate ground state [36], in which case the hopping takes place between a polaron and a bipolaron, both pinned by the counter ions. The concept of bipolaron hopping introduced by Chance et al. [37] has been applied to the case of undoped trans-PA by Townsend and Friend [38]. In this model, pairs of solitons with the same charge state (analogous to bipolarons) are suggested to hop from one chain to another. First one of the charge is transferred and two polarons are formed in the two adjacent chains. The bipolaron hopping is then completed by the second charge following the first.

We can see from the above discussion that a good number of models describing hopping transport in conducting polymers as well as amorphous semiconductors have been proposed, but there is still no general agreement on the detailed mechanism of hopping. For example, Emin and Skotheim [39] have argued that the observation of conductivity which

varies as $\exp(-T^{-1/4})$ is not a necessary evidence for variable range hopping, but can also arise from the elemental jump rates of the hopping sites. Also serious questions on the validity of intersoliton hopping have been raised by Nagi and Rendell [40] based on the anomalous phonon coupling function assumed in the model.

1. 8b AC CONDUCTIVITY

The frequency dependent conductivity is conventionally divided as arising from two contributions, σ_{dc} and $\sigma_{ac}(\omega)$, whose sum constitutes the measured conductivity. It has been found experimentally in a variety of disordered materials that $\sigma_{ac}(\omega)$ increases with frequency and the frequency dependence can be fitted to a power law given by

$$\sigma_{ac}(\omega) = B \omega^s \quad (1.6.)$$

with B, a constant and s typically around 0.8. The power law can also be derived theoretically on the basis of the pair approximation [41] by treating the hops as transitions between occupied and vacant sites near the Fermi energy. The extended pair approximation [42] takes also into account the environment of each pair of hopping sites. Other

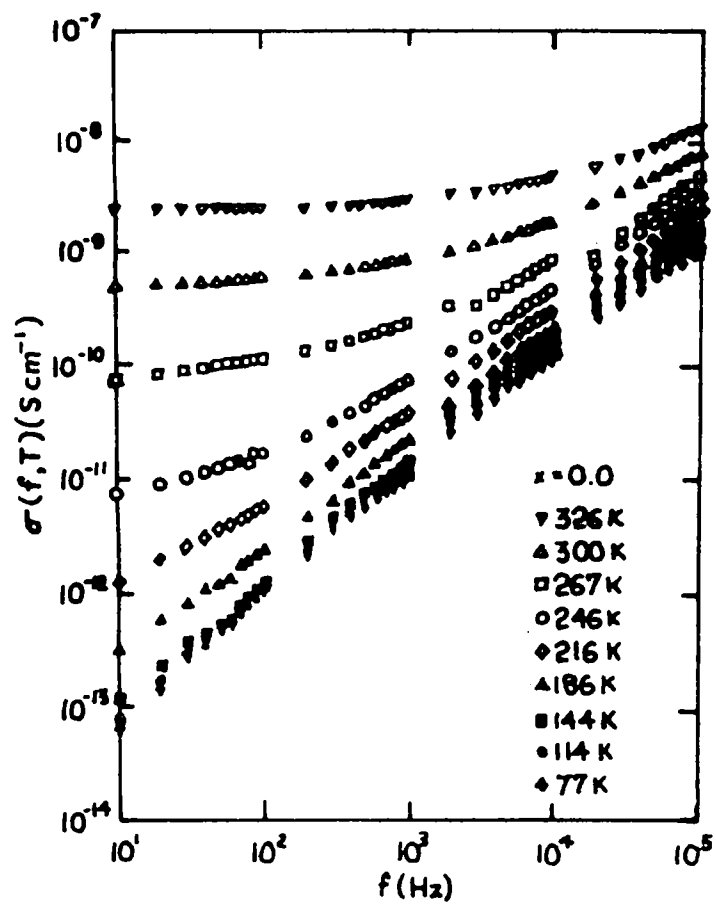


Figure 1.2. The frequency dependence of the conductivity of undoped emeraldine-base PANI.

suggested types of hopping as well as tunneling between metallic islands also adopt a similar functional form for $\sigma_{ac}(\omega)$ [43,44]. The frequency dependence of conductivity in Kivelson's intersoliton hopping is based on the pair approximation, but the temperature dependence of σ_{ac} is generally stronger in Kivelson's model than in other theories of hopping in a distribution of states near the Fermi level. The intersoliton model has been applied successfully to the analysis of experimental ac conductivity data from trans PA [45].

Figure 1.2. shows the frequency dependence of the conductivity different temperatures for undoped Polyaniline (PANI) in its emeraldine base form [46]. The conductivity varies in good agreement with above equation at low temperatures, but in this case the temperature dependence of $\sigma_{ac}(\omega)$ is relatively weak and the temperature dependence of σ_{dc} is too strong to be described by the intersoliton hopping model. The increase in dielectric constant at low frequencies coincides with the tendency towards frequency independent conductivity and was interpreted as three dimensional hopping among fixed polaron states. The

behaviour shown in Figure 1.2. is commonly observed also in other conjugated polymers in their undoped or lightly doped forms.

1. 8c THERMOELECTRIC POWER

Thermoelectric power in the case of hopping conduction is still not very well understood and different authors give different results [32,47]. In general, the thermoelectric power S for hopping conduction is given by [32]

$$S(T) = (k_B T / 2 e k_B T) \left[\frac{d \ln f(E) g(E) \mu(E)}{dE} \right] \quad (1.7)$$

where W is the range of energy contributing to the conduction, $f(E)$ is the energy distribution function of the conduction electron, and $\mu(E)$ is their mobility. According to Mott and Davis [32] W is assumed to be the hopping energy. For the inter-chain hopping in quasi-one-dimensional variable range hopping, $W \sim k_B(T_0 T)^{1/2}$ so that

$$S(T)_{\text{inter}} \approx (k_B^2 T_0 / e) \left[\frac{d \ln f(E) g(E) \mu(E)}{dE} \right]_{E_F} \\ \sim \text{constant} \quad (1.8)$$

and for the intrachain hopping, $W \sim k_B T_0$, so that

$$S(T)_{\text{intra}} \approx (k_B^2 T_0^2 / e T) \left[\frac{d \ln f(E) g(E) \mu(E)}{dE} \right]_{E_F} \sim 1/T \quad (1.9)$$

The total thermopower will have contribution from both interchain and intrachain hopping and have the temperature dependence given by

$$S(T) = S_0 + B/T \quad (1.10)$$

For metallic conduction $W \sim k_B T$ so that we have the well known linear relation

$$S(T) \propto T \quad (1.11)$$

for three dimensional VRH, $W \sim k_B (T T_0^3)^{1/4}$ so that [32]

$$S(T) \propto T^{1/2} \quad (1.12)$$

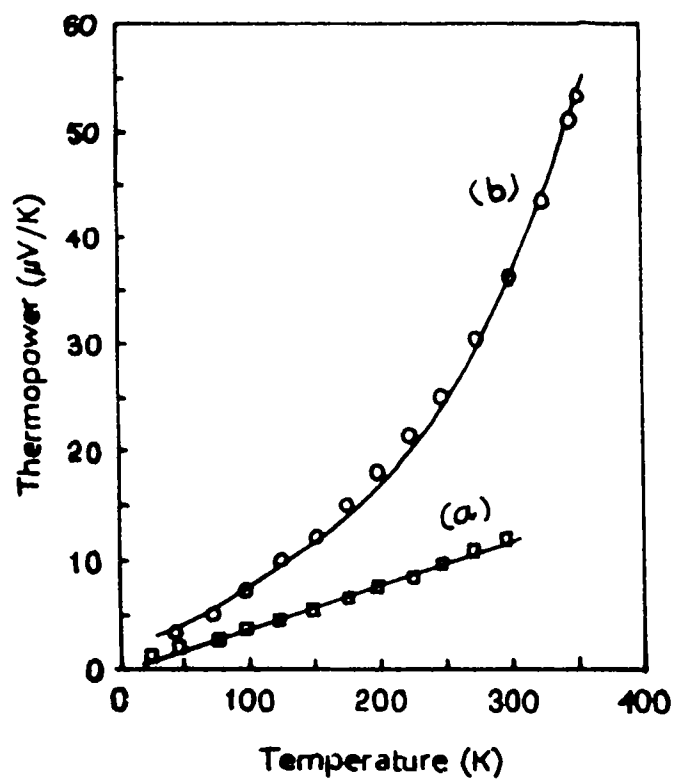


Figure 1.3. Temperature dependence of the thermopower in FeCl_3 -doped electrochemically prepared film of PT (a) and an FeCl_3 -doped pressed pellet of PPP (b).

The thermoelectric power measurement in doped conducting polymers usually show metallic properties, ie thermopower increase linearly with temperature, since as a zero current measurement, the thermopower is not largely influenced by the tunneling barriers separating the highly conducting islands [48]. A typical linear temperature dependence of the thermopower is shown in Figure 1.3.

The data shown are for a free standing electrochemically prepared and highly doped film of polythiophene [49]. Similar behavior has been observed in doped trans-PA [50] and PANI [51]. The upper curve in Figure 1.3. shows the corresponding characteristics for an FeCl_3 doped, pressed pellet of Polypyrrole (PPY). In this case the behaviour is linear but, as shown by the fit, it can still be successfully explained by a model which assumes that the material consist of metallic strands separated by this potential barrier [52].

1. 9 WORK DONE IN THE THESIS

In this thesis we present the work done by us on the transport properties of selected conducting polymers

polyaniline, polyanisidine, and their copolymers. These polymers have been prepared by the chemical polymerization method and made conducting by doping with HCl. The samples have been pelletized in to disc form for measurements. The dc and ac electrical conductivity and thermoelectric power of all the samples have been measured over a wide temperature range from 30K to room temperature with automated experimental setups. The results are interpreted based on different models. The thermal diffusivity of the samples have been measured using the photoacoustic technique. The details of the work done, results obtained and discussion of the results are described in the following chapters.

REFERENCES

1. H. Shirakawa and S. Ikeda *Polym. J.*, 2 (1971) 231.
2. J. C. M. Chien, *Polyacetylene Chemistry, Physics and Materials Science* (Academic Press, New York 1984).
3. T. Ito, H. Shirakawa and S. Ikeda, *J. Polym. Sci. Chem. Ed.*, 12 (1974) 11
4. G. Lieser, R. Wegner, W. Muller and J. V. Enkelmann, *Macromol. Chem.*, 1 (1980) 621.
5. H. Naarman and N. Theophilou, *Synth. Metal.*, 22 (1987) 1.
6. K. Idel, E. Ostlinning, W. Koch and W. Hetz, *Ger. Pat.* 3312, 254 (1984): *Chem Abstr.* 102 (1985) 149975.
7. G. B. Street, T. C. Clark, K. Kroun, P. Pfluger, J. F. Rabolt and R. H. Geiss, *Polymer Prepr. (Am. Chem. Soc. Polym., Chem.)* 23 (1982) 117.
8. A. F. Diaz and Bargon, *Handbook of Conducting Polymers*, T. A. Skotheim (Ed) (Marcel Dekker, New York 1986)
9. A. Watanabe, K. Mori, Y. Iwasak and Y. Nakamura, *J. Chem. Soc. Chem. Commun.*, (1987) 3.
10. N. Oyama, T. Ohsaka, T. Hirokawa and T. Suzuc *J. Chem Soc. Chem. Commun.*, (1987) 1133.

11. D. C. Trivedi, *J. Chem. Soc. Chem. Commun.*, (1989) 544.
12. J. E. Formmer and R. R. Chance, *Encyclopedia of Polymer Science and Engineering*. J.I.Kroschwitz (Ed) (Wiley, New York 1986) p462.
13. T. J. Lewis. *Faraday Discuss. Chem. Soc.*, 88 (1989) 189.
14. A. G. Macdiarmid, R. J. Mammone, J. R. Krawczye and S. J. Porter, *Mol. Cryst. Liq. Cryst.*, 105 (1984) 89.
15. S. Roth. *Mater. Sci. Forum.*, 21 (1987) 10.
16. L. Pietronero, *Synth. Metal.*, 8 (1983) 225.
17. H. Naarman and N. Theophilou, *Synth. Met.*, 22 (1987)1.
18. S. Kivelson and A. J. Heeger, *Synth. Metal.*, 22 (1979) 747.
19. S. Stafstrom, J. L. Breads, A. J. Epstein, H. S. Woo, D. B. Tanner, W. S. Huang and A. G. MacDiarmid, *Phys. Rev. Lett.*, 59 (1987) 1464.
20. H. Kuzmany, N. S. Sariciftci, H. Neugebauer and A. Neckel, *Phys. Rev. Lett.*, 60 (1987) 212.
21. H. Y. Choi and E. J. Mele, *Phys. Rev. Lett.*, 59 (1987) 2188.
22. J. Langer, *Solid State Commun.*, 26 (1987) 839.
23. I. Webman, J. Jortner, and M. H. Cohen, *Phys. Rev.*, B16 (1977) 2959.
24. S. Stafstrom, R. Riklund and K. A. Chao. *Phys. Rev.*,

B26 (1982) 4691

25. N. F. Mott and E. A. Davis *Electron Process in Noncrystalline Solids* (Clarendon, Oxford 1979).
26. P. A. Lee and T. V. Ramakrishnan *Rev. of Mod. Phys.*, 57. (1985) 287.
27. P. Nagels, *Top. Appl. Phys.*, 36. (1979) 114.
28. P. Sheng, *Phys. Rev.*, B21 (1980) 2186.
29. P. Sheng and J. Klafter. *Phys. Rev.*, B27 (1983) 2583.
30. P. Sheng, E. K. Sichel and J. I. Gittleman *Phys. Rev. Lett.*, 40 (1978) 1197.
31. A. L. Efros and B. J. Shklovski *J. Phys C.*, 8 (1975) 407.
32. S. Roth, H. Bleier and W. Pukaacki, *Farady Discuss. Chem. Soc.* , 88 (1989) 223.
33. S. Kivelson, *Phys. Rev.*, B25 (1982) 3798.
34. P. Kuivalainen, H. Isotalo, P. Yli Lahtiand C. Holmstrom, *Phys. Rev.*, B31 (1985) 7900.
35. R. R. Chance, J. L. Bredas and R. Silbey *Phys. Rev.*, B29 (1984) 4491.
36. P. D. Townsend and R. H. Friend , *Phys. Rev.*, B40 (1989) 3112.
37. D. Emin in T. A. Skotheim (Ed) *Hand book of Conducting polymers* (Marcel Dekker, New York, 1986) 915
38. K. L. Nagi and R. W. Rendell, in T. A. Skotheim (Ed)

Hand book of Conducting polymers,(MarcelDekker, New York.1986)

39. M. Pollak and T. H. Geballe, Phys. Rev., 122 (1961) 1742.
40. S. Summerfield and P. N. Butcher J. Phys. C., 16 (1983) 295.
41. A. J. Epstein in T. A. Skotheim (Ed) Hand book of Conducting polymers (Marcel Dekker New York. 1986)
42. W. Rehwald, H. Kiess and B. Binggeli. Z. Phys., B68 (1987) 143.
43. A. J. Epstein, H. Rommelmann, M. Abkowitz and H. W. Gibson. Phys Rev. Lett., 47 (1981) 1549, Mol. Cryst. Liq. Cryst., 77 (1981) 81.
44. F. Zuo, M. Angelopoulos, A. G. MacDiarmid and A. J. Epstein, Phys. Rev., B39 (1989) 3570.
45. P. Nagels in M. H. Brodsky (Ed) Amorphous Semiconductors (Springr Verlag 1979)
46. J. R. Cooper, B. Alavi, L. W. Zhou, W. P. Beyerman and G. Gruner, Phys. Rev., B35 (1987) 18.
47. J. E. Osterholm, P. Passiniemi, H. Isotalo and H. Stubb, Synth. Met.,18 (1987) 213.
48. W. W. Park. A. J. Heeger M. A. Druy and A. G. MacDiarmid,J. Chem. Phys.,73 (1980) 446.
- 51 49. F. Zuo, M. Angelopoulos, A. G. MacDiarmid and A. J.

Epstien Phys. Rev., B38 (1987) 3475.

- 50. P. Kuivalainen, H. Isotalo and H. Stubb. Phys.Stat.
Sol.,122 (1984) 791.**

CHAPTER 2

SYNTHESIS OF POLY AROMATIC AMINES

2. 1 INTRODUCTION

The successful synthesis of polyacetylene and its subsequent doping to make it electrically conducting polymer have raised great interest because of their many possible applications [1,2]. These materials have already been the subject of numerous reviews [3,4]. One of these polymers in particular polyaniline, (PANI) has been the center of considerable scientific interest in recent years. Even though these polymers have been known for the last 150 years, the electrical conductivity was noticed only in 1980. After 1980, extensive research is being carried out to overcome the problems related to synthesis, structure modification and electrical transport studies on polyaniline [5,6,7,8,9,10.]. The number of publications on the subject of PANI is becoming greater and greater. On one hand these may probably be linked to the numerous possible applications envisaged for conducting polymers and, on the other hand, to the fact that aniline is a cheap product and PANI is a very

stable material. This polymer differs substantially from other conducting polymers due to its charge conjugation asymmetry, both carbon ring and nitrogen atoms are within the conjugation path, and convertibility of insulating state to metallic state is possible by means of protonation to the $-N=$ sites. This is different from conventional doped polymer in that there is no change in the number of electrons in the polymer chain. Thus the physics and chemistry of these polymers differ from the other conventional conducting polymers.

The fundamental questions that arise concern with the polymerisation, the structure of the material in its oxidation states, the redox mechanism, the electronic and ionic conduction mechanism, the role of the doping ions, residual water and solvation. Workers in the field have still not completely understood all the observed phenomena and the existing models need to be elaborated even more, in order to explain the experimental results. The influence of light, in particular, on the behaviour of PANI proves to be very complex [11]. Even though the complexity and confusion on these materials are still existing, large number of studies are going on in PANI and its derivatives and analogs. Among them polyanisidine, is a new one which shows

very good solubility due to the methoxy group in the chain [12]. In this chapter we present the work done on the chemical synthesis of polyaniline, polybenzidine polyanisidine and the co polymers of aniline, anisidine and benzidine

2. 2 CHEMICAL SYNTHESIS OF POLYAROMATIC AMINES

Various chemical oxidising agents have been used by different authors to polymerise aromatic amines. Potassium dichromate, ammonium persulphate or peroxydisulphate, hydrogen peroxide, ceric nitrate and ceric sulphate are some of the examples of oxidising agents used for the synthesis of conducting polyaromatic amines in general and polyaniline in particular [7,13,14,15]. It has been noted that the polymer quality very much depends on the oxidising agent and a degradation of the polymer occurs if the quantity is too high. The polymerisation reaction is mainly carried out in acidic medium in most of the the reported work [13,14,15]. The pH value very much affects the quality of the polymer. Using utetic mixtures of hydrofluoric acid and ammonia, the polymer can be synthesised even below a pH value 0 and polymers obtained under these conditions has been reported to be of much better quality [16]. Most of the work was

done in aqueous media in the case of polyaniline. However, these polymers and their derivatives can also be prepared in organic media [17].

The works of Jozefowicz et al. [18] have shown that the oxidation of aniline by a chemical oxidant can occur even at ambient temperature. In any case, the reaction takes place with the rate of reaction being dependent on the temperature usually in the range 0-80⁰C. And it had been noted that the enthalpy of reaction is high and it does not vary within the range 0 -77⁰C or with the concentration of aniline but varies with the concentration of the oxidising agent. It is also noted that the activation energy does not depend on the reaction conditions [18]. The author concludes that the reaction of aniline can be broken down into two stages.

i) A slow a thermic stage which is dependent on pH, temperature and concentration of the reactant. Dissolved oxygen in the solvent has no influence on the reaction in contrast to other oxidising species which decrease the induction period; this stage obeys the Arrhenius law between 0 and 50⁰C

ii) A fast exothermic stage which is temperature dependent and varies only slightly with the concentration of oxidant. In general, the polymer synthesised by the above method is isolated from the reaction medium by filtration. The precipitate is then washed and conditioned using an appropriate solvent.

2. 3 POLYMERISATION MECHANISMS

The wide variety of methods employed for the preparations of PANI lead to the formation of products whose nature and properties differ greatly. As a result of this, in many of the studies carried out on PANI and its derivatives, a multitude of polymerisation mechanisms have been proposed by different authors.

According to most authors, the first step in the oxidation of aniline is the formation of a radical cation as shown in Figure 2.1a. The formation of radical cation is independent on the pH of the synthesis medium, and is the governing criteria for the polymerisation reaction. This radical cation is resonance stabilized and can be represented by the following canonical forms as shown in Figure 2.1b.

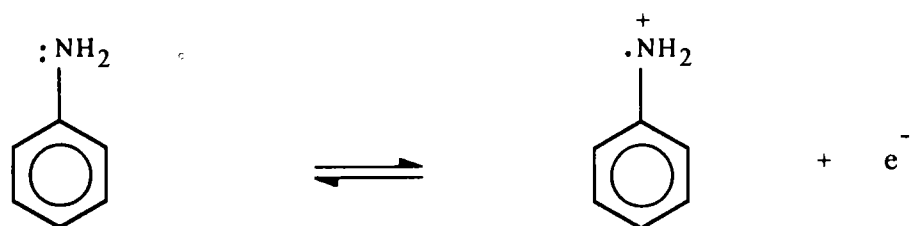


Figure 2.1a: Oxidation of aniline

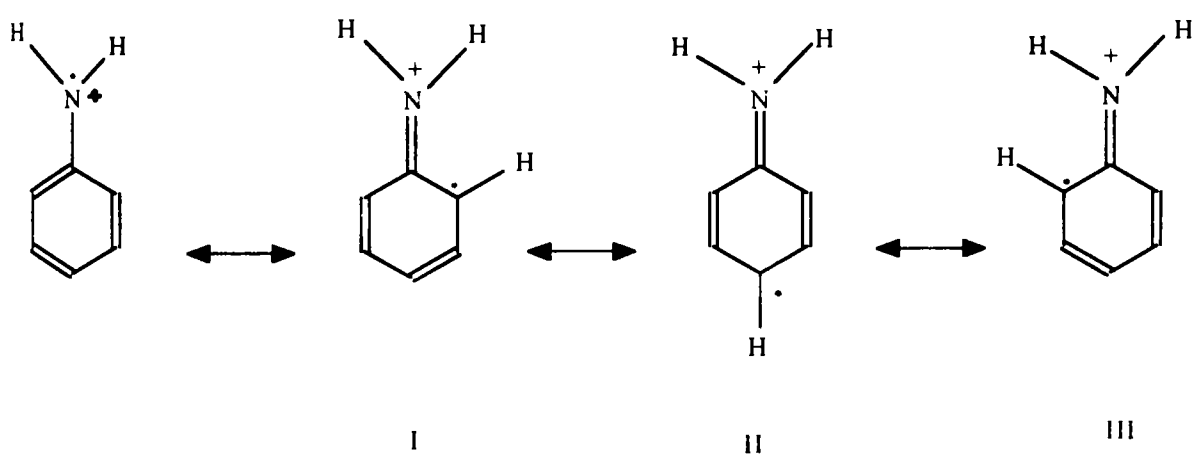


Figure 2.1b: Canonical forms of resonance stabilised radical cations

Mohilner[19] was the first to assert that in sulfuric acid medium, the oxidation of aniline is an electrochemical reaction, mainly resulting in para coupled chains. However, Bacon and Adams [20] as well as Wawzonek and Mac Intyre [21] showed that the oxidation of aniline or its para substituted derivative in acid or acetonitrile medium give rise to the formation of benzidines and PADPA, by a process which is pH dependent. These reaction products result from tail to tail and head to tail coupling respectively with elimination of the para group to the amino group. This is established by the Raman studies by Holze [22]. The polymerisation mechanism is shown in Figure 2.1c.

Nevertheless, Breitenbach and Hecker [23,24] propose that the oxidation mechanism of aniline in acetonitrile/pyridine medium is similar to that in acid medium as described by Mohilner [19]. The base removes a proton from the radical cation forming a neutral radical which is oxidised to give the nitrenium cation. This nitrenium cation can attack the aniline to yield PADPA. More recently, Volkov et al. [25] have confirmed these conclusions by carrying out studies on the oxidation products of aniline in acetonitrile medium using classical and multiple reflection IR spectroscopic and XPS methods. The spectra of the anodic oxidation product of

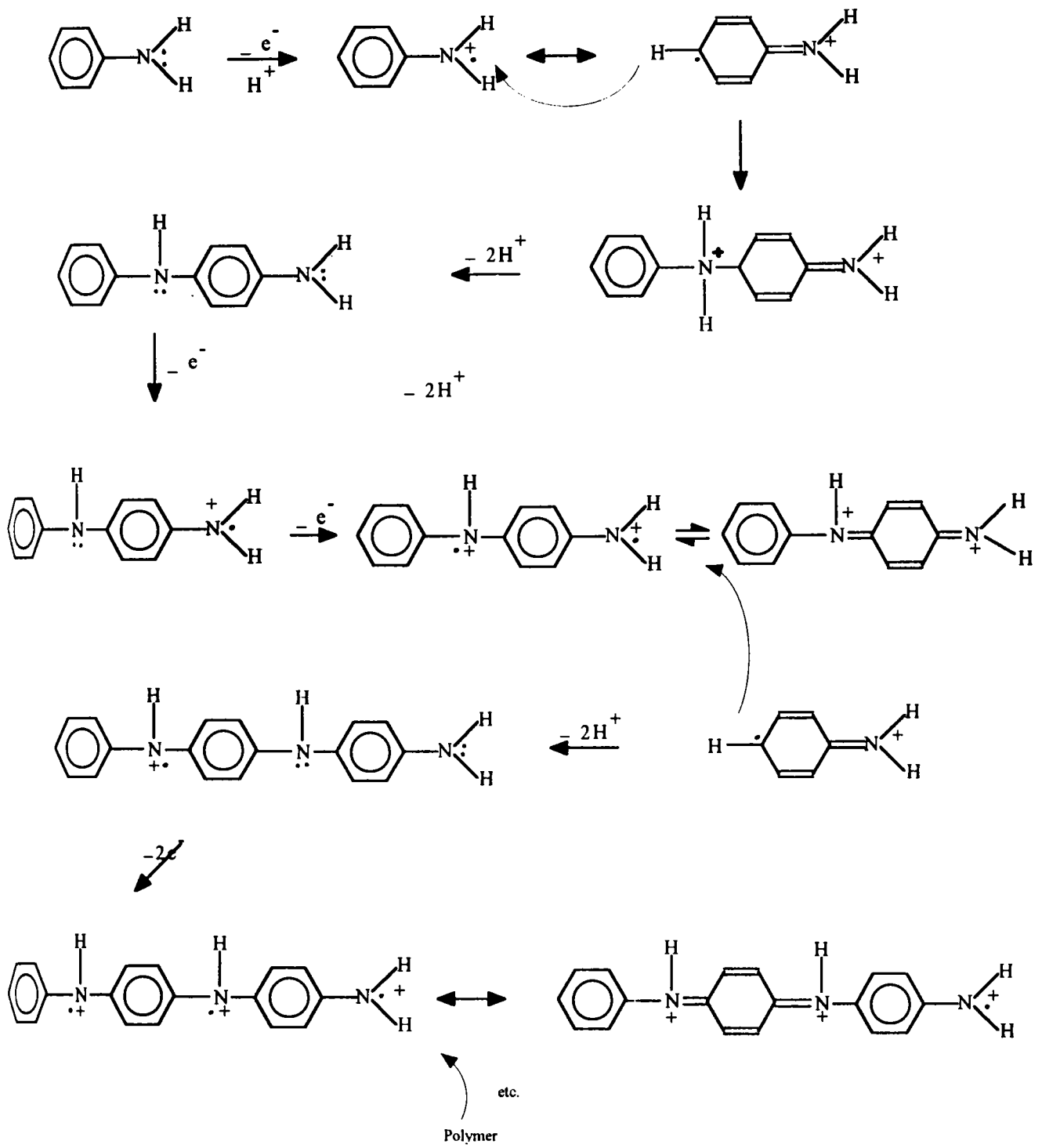


Figure 2.1c: Reaction mechanism for radical cation coupling of aniline leading to the formation of a linear polymer

aniline is identical to those of the chemically prepared polyaniline.

Ohsaka et al. [26] highlight the difference in the behaviour of the oxidation products of aniline prepared in sulfuric acid medium (pH=1), phosphoric acid medium (pH=7), and in acetonitrile solution. The characteristic of the head to head coupling is observed only in the spectra corresponding to the products prepared under neutral or basic conditions. These authors have attributed the head to tail configuration to the aniline oxidation products prepared in acidic medium.

Genies et al. [9] have recently undertaken a spectroscopic study of the polymerisation mechanism of aniline in utetic mixtures of hydrofluoric acid and ammonia. This study has permitted them to demonstrate that at low oxidation potentials the PANI formed results from the polymerisation of the monomer radical cation.

2. 4 EXPERIMENTAL PROCEDURE

The results reported on the properties of polyaniline considerably differ depending on the method of preparation

[27-30]. Various factors contribute to such discrepancies. In chemically prepared samples factors like the oxidant used to bring about the polymerisation, the ratio of the monomer to oxidant, the temperature at which the oxidation is carried out, the post treatment given to the crude material like washing, doping, and drying affect the properties. Some times, samples prepared by the same method also significantly differ in properties. One of the factors which invariably affects the electrical properties is retention of moisture by doped samples. The chemical polymerisation also leads to some oligomeric impurities [31].

In the experimental procedure followed in this work, meticulous care was taken to purify the monomers to remove the oligomeric residues from the crude polymer and to maintain identical conditions for post preparative treatment.

2. 5 SYNTHESIS OF POLYANILINE

a. Purification of aniline

Commercially available aniline contains traces of aromatic hydrocarbons and nitrobenzene. On storing aniline, it

develops a dark colour probably due to air oxidation. Hence aniline was purified as described below using recommended methods [32]. Aniline was dissolved in 6M HCl. Any precipitate of aniline hydrochloride was dissolved by stirring with more of water. The solution was extracted with toluene to remove neutral and acidic impurities present. The aniline hydrochloride solution was rendered alkaline with 40 % caustic soda. The oily liquid that get separated out was removed, dried over solid sodium hydroxide and distilled. The middle fraction which distilled out at 184 to 188 °C was collected.

b. Polymerisation of Aniline

Polyaniline was synthesised according to the following procedure. The purified aniline (15.83 g) was added to 500 ml of 1M HCl in a three necked round bottom flask. The oxidant solution, (200 ml of 1M HCl and 9.13 g of ammonium peroxydisulphate $((\text{NH}_4)_2\text{S}_2\text{O}_8)$ was added slowly from a dropping funnel while stirring the mixture at 0°C. The reaction mixture was stirred for 4 hours. The precipitated polyaniline was filtered and then washed with distilled water. The product was subjected to purification using the procedure described at the end this chapter.

2. 6 SYNTHESIS OF POLYANISIDINE

a. Purification of anisidine

o-Anisidine was purified by vacuum distillation. Reagent grade anisidine was vacuum distilled and the fraction collected at 225⁰C on redistillation was used for polymerisation .

b. Polymerisation of *o*-Anisidine.

Polyanisidine was synthesised chemically by oxidative polymerisation. *o*-Anisidine was vacuum distilled before use. 20.93g of *o*-anisidine (0.17 mol) was dissolved in 500 ml 1M HCl and cooled in an ice bath at 0⁰C. 9.13 g of ammonium peroxydisulfate (0.04 mol) were dissolved in 200 ml 1M HCl and cooled to 0⁰C and placed in a separating funnel above the *o*-anisidine solution to facilitate drop-wise addition. The ammonium peroxydisulphate solution was slowly introduced in to the *o*-anisidine solution over an approximately 10 minute period with constant stirring. After 4 hours of stirring at 0⁰C, the solid polyanisidine was filtered out, washed with distilled water and subjected to purification as described later.

2. 7 COPOLYMERISATION

a. Co polymer of aniline and anisidine

The synthesis of the co polymer of aniline and anisidine was done using the procedure of polyaniline synthesis. Purified monomers were taken in equimolar ratio and dissolved in 500 ml 1M HCl. The solution was kept cooled to 0°C. The ammonium peroxydisulphate solution was also cooled to same temperature and added slowly to the monomer solution with continuous stirring for about 4 hours. The precipitate was filtered and washed with distilled water and subjected to purification

b. Co polymer of aniline and benzidine

15.49 g of benzidine was dissolved in 250 ml 1M HCl and cooled to 0°C. Then 15.83 g of aniline was also dissolved in 250 ml of 1M HCl and cooled to a temperature around zero. The two solutions were mixed together and stirred well at around 0°C and then 18.26 g ammonium persulphate solution in 1M HCl was added drop wise. The mixture was kept for four hours with continuous stirring. Then the precipitate was

filtered and washed with distilled water. The material was subjected to purification.

c. Co polymer of anisidine and benzidine.

20.93 g of anisidine is dissolved in 250 ml 1M HCl and cooled to a temperature of 0°C. Then 15.49 g of benzidine is dissolved in 250 ml of the same concentration of HCl and cooled to 0°C. Then both solution were mixed together and stirred in a continuous manner. Then the cooled ammonium persulphate solution is added in to the mixture drop wise. The mixture is kept in the vessel for a period of 4 hours. Then precipitate is filtered and washed with distilled water. and subjected to purification.

2. 8 PURIFICATION OF CONDUCTING POLYMERS

Every method described for the synthesis of conducting polymers cited in the above section results in the contamination of the product with unreacted materials and byproducts. The polymer formed itself is mixture of oligomers. Common purification technique such as acid, alkali or solvent washing is used for the initial purification of the product.

The polymer salt obtained from the vessel was dried well and powdered. The powder form of polymer was stirred with 1M HCl so as to eliminate any monomer present in the polymer. The polymer was filtered out and washed with plenty of distilled water. The material was filtered out and dried again. The dried polymer sample is again powdered well and subjected to soxhlet extraction. The material is continuously extracted with THF about 48 hours, since all the monomers and oligomers present in the sample will be washed out. The extracted sample contains high molecular weight polymers.

2. 9 DOPING

It has been observed by earlier workers [12,15] that doping of polyaniline from moderately concentrated HCl results in the incorporation of chlorine atom to the aromatic ring. For this reason, the purified polymer was subjected to doped with HCl of up to one molar concentration. Finely powdered polymer sample was shaken with 200 ml of HCl of appropriate concentration for 24 hours. The protonated material formed was filtered without the aid of solvent, sucked dry by drawing air using a water pump. It was dried in vacuum oven at 80⁰C, and then stored in a dry vacuum desiccator.

REFERENCES

1. T. Ito, H. Shirakawa and S. Ikeda, *J. Polym. Chem. Ed.*, 12 (1974) 11.
2. C. K. Chiang, C. R. Fincher, Y. W. Park, A. J. Heeger, H. Shirakawa, E. J. Luis, S. C. Gau and A. J. MacDiarmid, *Phys. Rev. Lett.*, 39 (1977) 1098.
3. E. M. Genies, M. Lapkowski and C. Tsintavis, *New J. Chem.*, 12 (1988) 181.
4. R. L. Greene and G. B. Street, *Science.*, 228 (1984) 651.
5. A. Volkov, G. Tourillon, P. C. Lacaze and J. E. Dubois, *J. Electroanal.*, 115 (1980) 279.
6. C. M. Carlin, L. J. Kepley and A. J. Bard, *J. Electrochem. Soc.*, 132 (1985) 353.
7. A.G. MacDiarmid, J. C. Chiang, M. Halpern, W. S. Hung, S. L. Mu, N. L. D. Somasiri, W. Wu and S. I. Yaniger, *Mol. Liq. Cryst.*, 121 (1985) 173
8. A. G. MacDiarmid, N. L. D. Somasiri, W. R. Salaneck, I. Lundstrom, B. Liedberg, M. A. Hassan, R. Erlandsson and P. Konrasson, *Springer Series in Solid State Sciences*, Vol. 63, Springer, Berlin, 1985, p218.

9. E. M. Genies and C. Tsintavis, *J. Electroanal. Chem.*, 195 (1985) 109.
10. J. P. Travers, J. Chroboczek, F. Devreux, F. Genoud, M. Nechtschein, A. A. Syed, E. M. Genies and C. Tsintavis, *Mol. Cryst., Liq. Cryst.*, 121 (1988) 61.
11. E. M. Genies and M. Lapkowski, *Synth. Met.*, 24 (1988) 61.
12. David MacInnes, Jr. *Synth. Met.*, 25 (1988) 237.
13. E. M. Genies C. Tsintavis and A. A. Syed, *Mol. Cryst., Liq. Cryst.*, 121 (1985) 181.
14. R. L. Hand and R. FNelson, *J. Electrochem. Soc.*, 125 (1978) 1059.
15. R. L. Hand and R. F. Nelson, *J. Am. Chem. Soc.*, (1974) 850.
16. Fr. Patent No. EN 8307958 (1983); U. S. Patent No. 698183 (1985)
17. A. Watanabe, K. Mori, M. Mikuni, Y. Nakamura and M. Matsuda, *Macromolecules*, 22, (1989) 3323
18. L. T. Yu, M. S. Borreden, M. Jozefowicz, G. Belorgey and R. Buvet, *J. Polym. Sci.*10 (1987) 353.
19. D. M. Mohilner, R. N. Adams and W. J. Argersinger, *J. Am. Chem. Soc.*,84 (1962) 3618.

20. J. Bacon and R. N. Adams, *J. Am. Chem. Soc.*, 90 (1968) 6596.
21. S. Wawzonek and T. W. MacIntyre, *J. eLECTROCHEM. SOC.*, 114 (1967) 1025.,(1972) 1350.
22. R. Holze, *J. Electronal. Chem.*, 224 (1971) 253.
23. M. Breitenbach and K. H. Hecker, *J. Electroanal. Chem.*, 29 (1971) 309.
24. M. Breitenbach and K. H. Hecker, *J. Electroanal. Chem.*, 33 (1971) 45; 43 (1973) 267.
25. A. Volkov, G. Tourillon, P. C. Lacaze and J. E. Dubois, *J. Electroanal. Chem.*, 115 (1980) 279.
26. T. Ohsaka, Y. Ohnuki, N. Oyama, G. Katagiri and K. Kamisako, *J. Electroanal. Chem.*, 161 (1984) 399.
27. J. Tang, X. Jing, B. Wang and F. Wang, *Synth. Met.*,24 (1988) 231.
28. K. L. Tan, B. T. G. Tan, S. H. Khor, K. G. Neoh and E. T. Kang, *J. Phys. Chem. Solids.*, 52 (1991) 673.
29. A. Andreatta, Y. Cao, J. Chaing and A. J. Heeger, *Synth. Met.*,26 (1988) 383.
30. V. G. Kulkarani, L. D. Campbell and W. R. Mathew, *Synth. Met.*, 30 (1989) 321.

31. J. J. Langer, *Synth. Met.*, 35 (1990) 295.
32. D. D. Perrin, W. L. F. Armarego and D. R. Perrin,
Purification of Laboratory Chemicals, 2nd edn. Pergamon
press, (1980).

CHAPTER 3

CHARACTERISATION OF POLYAROMATIC AMINES

3. 1 INTRODUCTION

The polymer related problems which can be solved by spectroscopy are many and varied. They may concern chemical aspects and chain structure, tacticity 'mer' sequence distribution, chain branching or structure of radicals. They may concern physical aspects, eg chain orientation, crystallinity, crystal thickness, miscibility of polymers, Chain conformation and chain dynamics etc. In conducting polymer research spectroscopic methods are extensively used for chemical characterisation and structure determination of the polymer molecules, effect of doping on the polymer chain. The different spectroscopic methods which we have used to characterise the polyaromatic amines are described below.

Conducting polymers are generally insoluble in common solvents. So the characterisation of conducting polymers were extremely difficult compared with the usual polymers.

The π electron conjugation in this class of polymers causes cross linking and the materials were highly intractable. Hence the molecular weight determination, most important tool of characterisation of polymers cannot be applied to this polymers generally. However analytical techniques such as FTIR, NMR, UV-Visible spectroscopy and XRD etc. were used to determine the molecular structure, crystalline nature etc of these materials.

3. 2 IR SPECTROSCOPY FOR POLYMER CHARACTERISATION

The list of useful applications of IR spectroscopy in polymer science is almost endless. Characterisation of chemical structure is one of the most important uses. Here we just give an introduction of IR spectroscopy in chemical characterisation.

IR Spectroscopy can be used to asses the number average molar mass in polymer by assessing the end group. However it is not applicable to conducting polymers because of π electron conjugation and the extraordinary nature of cross linking in this class of polymers, even though molecules with low molecular mass can be assessed using IR spectroscopy. One advantage of this method is that the

polymer need not be dissolved prior to the analysis. It is also not useful in branched polymers.

Stereo regularity (tacticity) can also be determined by IR spectroscopy for some polymers. Their spectra of isotactic and syndiotactic polymers show several absorption peaks which are absent in the spectrum of atactic polymers. However, the spectra of the two in the molten states are generally the same.

Hydrogen bonds are the strongest secondary bonds in polymers. They appear in several important polymers; eg polyamides. They play a vital role in certain miscible polymer blends. Their effects on the IR spectrum is well known. In polyamides, the vibrational stretching frequency of hydrogen bonded -OH- and -NH- group are shifted to lower values compared to the non hydrogen bonded analogous. The vibration frequencies of the -NH- group drops 3450 cm^{-1} to 3300 cm^{-1} . A similar shift of the absorption peaks may indicate specific interaction between different polymers, which is an important reason for miscibility.

3. 2a. SAMPLE PREPARATION

Liquids studied by IR spectroscopy are examined as thin films between two IR transparent plates or as solutions in IR transparent solvent. Solid polymers may be studied in solution using any one of the transparent solvent. The solvent may also cast films on a crystal of NaCl an the optimum thickness depends on the IR absorption of the polymer. Insoluble polymers are generally studied by making in to the form of a discs after grinding the polymer sample 1%(w/w) with IR transparent potassium bromide. In our study we use both technique. The polymers were cast in to thin films by means of mulling it with nujol on a KBr plate. The KBr disc is prepared by grinding the polymer with spectroscopic grade KBr and applying a pressure of 10 tons using KBr die and press. The spectra of the solvent of the monomers were taken by casting thin films on the KBr plate directly.

3. 2b. RESULTS AND DISCUSSION

a) Polyaniline

The spectra of the monomer and polymer are shown in figure 3.2. The monomer spectra shows the NH stretching frequencies

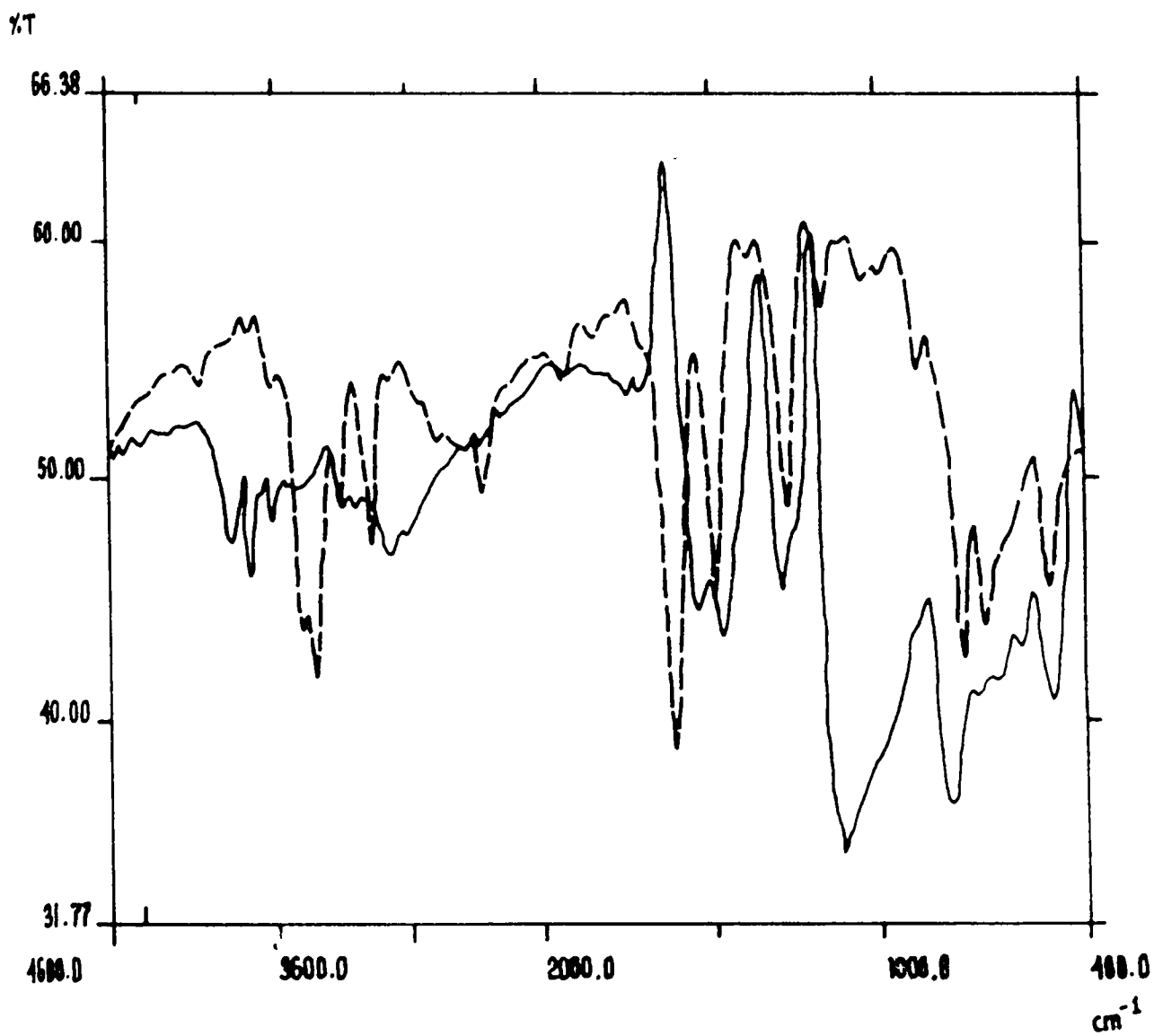


Figure 3.2: FTIR. Spectra of aniline and polyaniline.

(---) Aniline (—) Polyaniline

at 3438,3362 and 3220 cm^{-1} The NH bending frequency is observed at 1617 cm^{-1} (strong or medium). In doped polyaniline the observed broad band at 3300-2800 cm^{-1} but extending to 2300 cm^{-1} indicative of NH stretching frequency of an amine salt. The corresponding NH bending frequency observed at 1543 cm^{-1} . This indicates considerable modifications of the monomer structure. The IR spectrum is indicative of the polyaniline structure as already reported.[1,3,4,5,6]

b) Polyanisidine

The IR spectra of the anisidine and polyanisidine are shown in figure 3.3. For anisidine the NH stretching band is observed at 3459,3368 and 3200 cm^{-1} and the bending frequency is observed at 1613 cm^{-1} . The bands observed 1227 and 1034 cm^{-1} are indicative of C-O-C stretching. For doped polyanisidine a broad band between 3403 cm^{-1} extending up to 2200 cm^{-1} is an indication of secondary amine salt. The NH bending frequency is observed at 1568 cm^{-1} . The absorption observed at 1207 and 1014 cm^{-1} is the indication of C-O-C stretching. The spectra of polyanisidine is similar to the reported in reference [2].

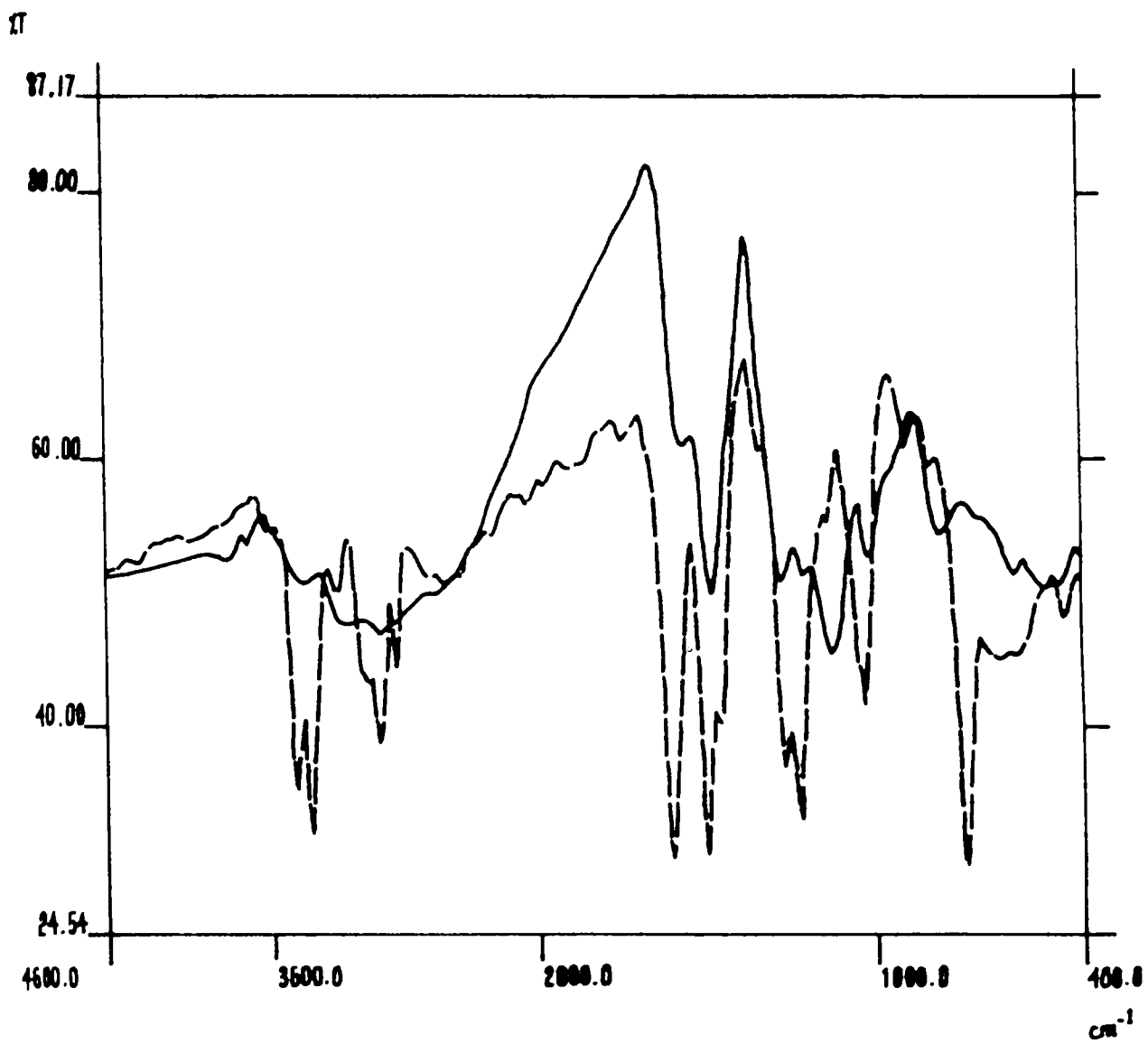


Figure 3.3: FTIR Spectra of anisidine and polyanisidine.

(- - -) Anisidine (——) Polyanisidine

c) Co polymer of aniline and anisidine

The spectrum of the doped co polymer containing aniline and anisidine is shown in figure 3.4. The broad band absorption between 3300 to 2200 cm^{-1} corresponds to NH stretching and 1579 cm^{-1} corresponds to NH bending is observed in the co polymer spectrum indicating a secondary amine salt. The frequency observed at 1207 and 1015 cm^{-1} is an indication of C-O-C stretching.

d) Co polymer of aniline and benzidine

The spectrum of the co polymer containing aniline and benzidine is shown in figure 3.4. Absorption at 3430 to 2360 cm^{-1} is an indication of an NH stretching frequency of primary and secondary amine salts. The NH bending frequency is observed at 1562 cm^{-1} . This indicate the presence of both primary amine and secondary amine residues in the polymerised molecules.

e) Co polymer of anisidine and benzidine

The spectrum of the polymer containing anisidine and benzidine is shown in figure 3.4. No prominent absorption due to NH stretching frequency are observed in the IR

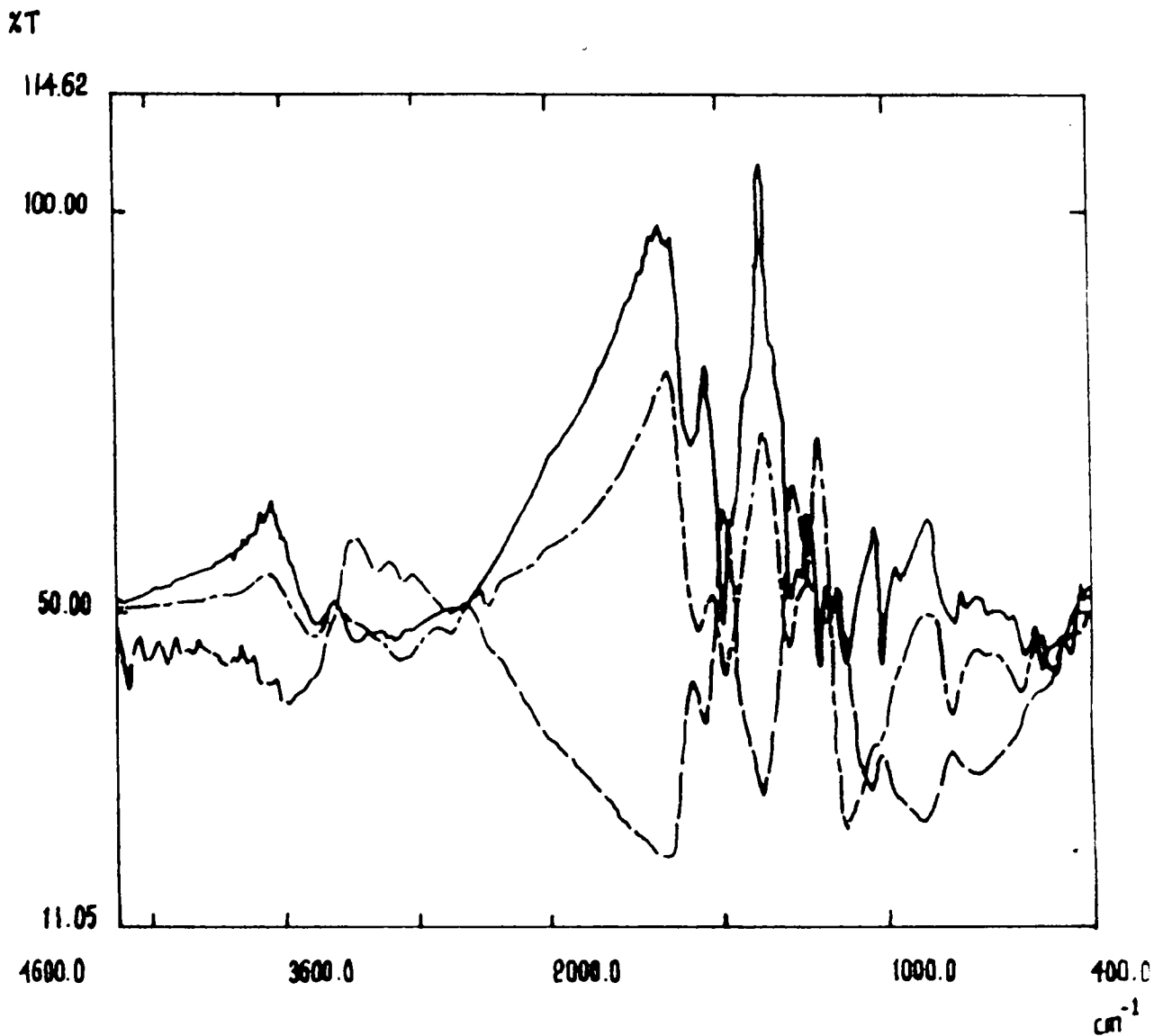


Figure 3.4: FTIR. Spectra of copolymers.

- (————) Co polymer of aniline and anisidine
- (- - -) Co polymer of aniline and benzidine
- (— · —) Co polymer of anisidine and benzidine

spectrum. However there is an indication that there are absorptions corresponding to C=N (1662 cm^{-1}) and NH bending (1568 cm^{-1}) in the molecules.

3. 3 NMR SPECTROSCOPY FOR POLYMER CHARACTERISATION

NMR spectroscopy is the primary method for the assessment of the chemical structure of the polymer characterisation of tacticity and chain branching in polymers. The head to tail configuration and sequence distribution of monomers in co-polymers are two good examples of problems solved by using NMR spectroscopy. The broad line NMR line shape provide information about both structure and segmental mobility. Broadening is mainly due to the spin-spin interaction which, when the spin (ie polymer segments) are immobile leads to a considerable broadening of the resonance line . Polymers of more liquid like nature exhibit more narrow resonance lines.

In a molecule containing many atoms the field on any one of these is attend by the presence of the others.

$$\Delta E = 2\mu(H_0 + H_L)$$

where H_L is the local field with strength 5-10 gauss. It is these changes that are important in NMR Characterisation.

3. 3a. SAMPLE PREPARATION

In order to take solution spectra the sample should be dissolved in an ideal solvent. The solvent should contain no protons in its structure and be inexpensive, low boiling nonpolar and inert. Carbon tetrachloride is an ideal solvent if the sample is sufficiently soluble in it. The most widely used solvent is deuterated chloroform. However our samples do not dissolve in any of the above solvent so we dissolved the sample in deuterated dimethyl sulphoxide and the spectra are recorded.

3. 3b. RESULTS AND DISCUSSION

The proton magnetic resonance spectra of the doped polymers show poor resolutions. However all the polymers containing anisidine show methoxy peaks around 3.9 -3.8 ppm. Also a group of aromatic peaks were observed in between 6.9 to 8.2ppm. The complicated set of peaks as shown in figure 3.5a to 3.5d may be due to polymer chain containing both benzenoid and quinoid rings.

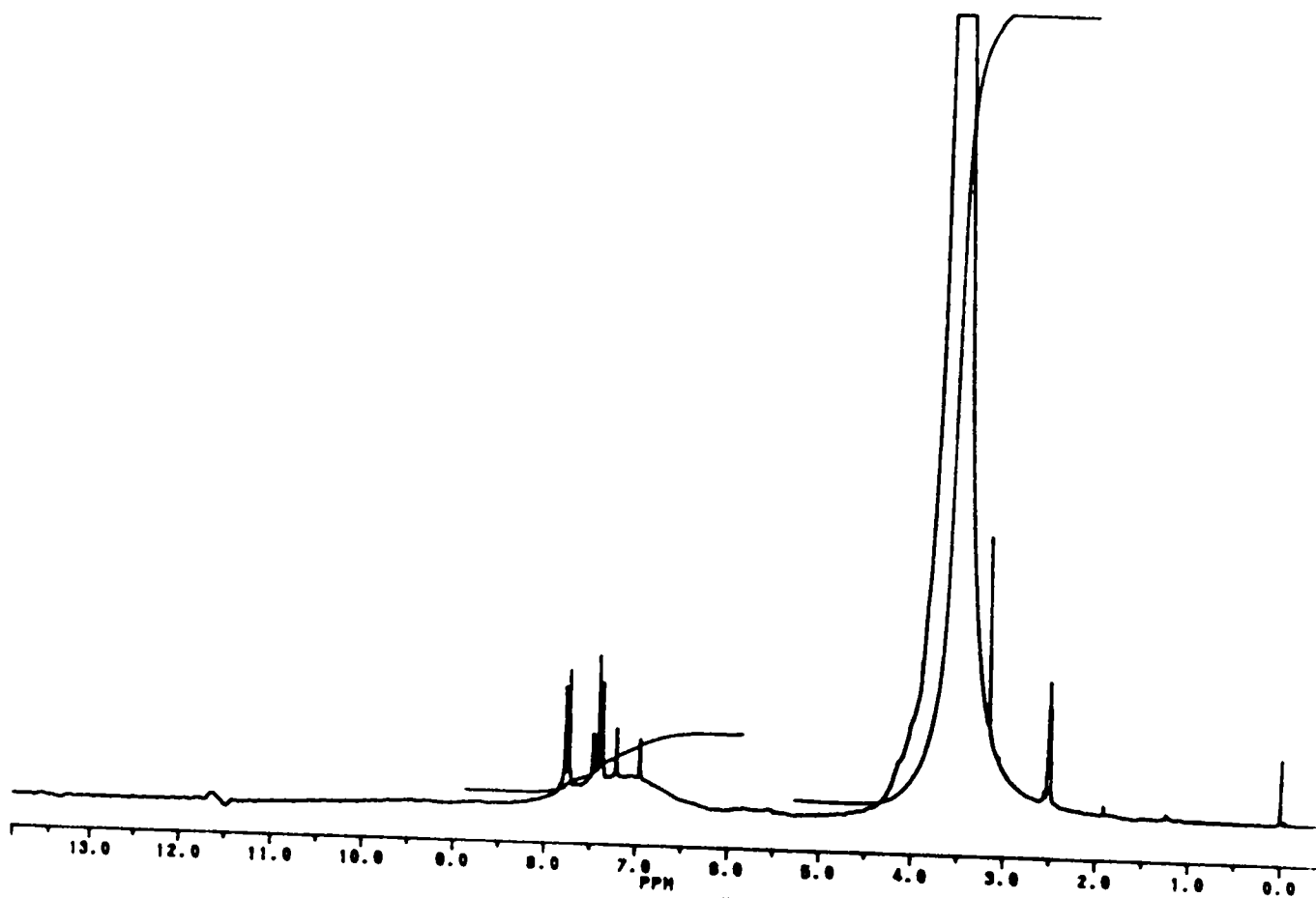


Figure 3.5a: ^1H NMR. Spectrum of polyanisidine.

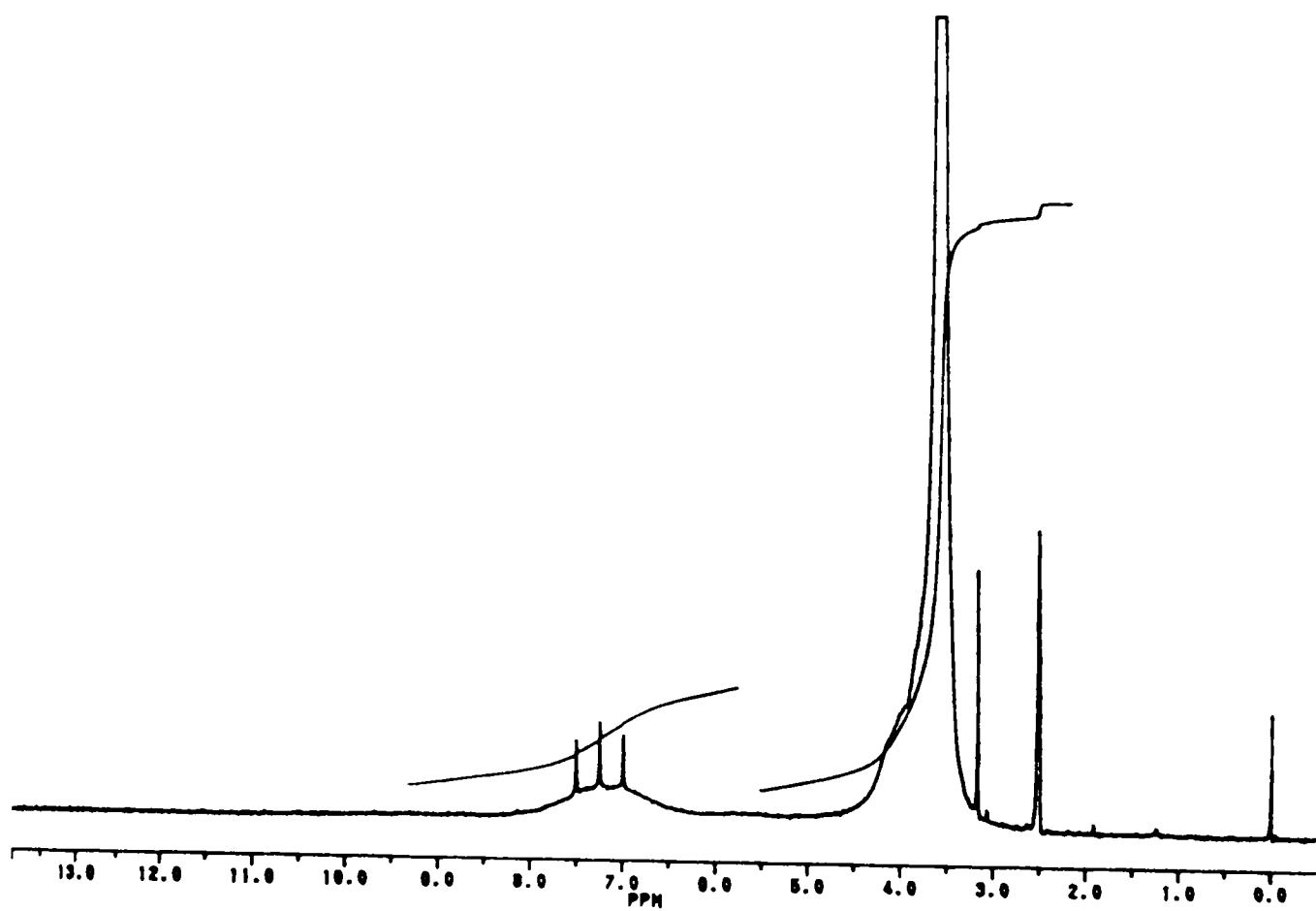


Figure 3.5b: ^1H NMR. Spectrum of co polymer of aniline and anisidine.

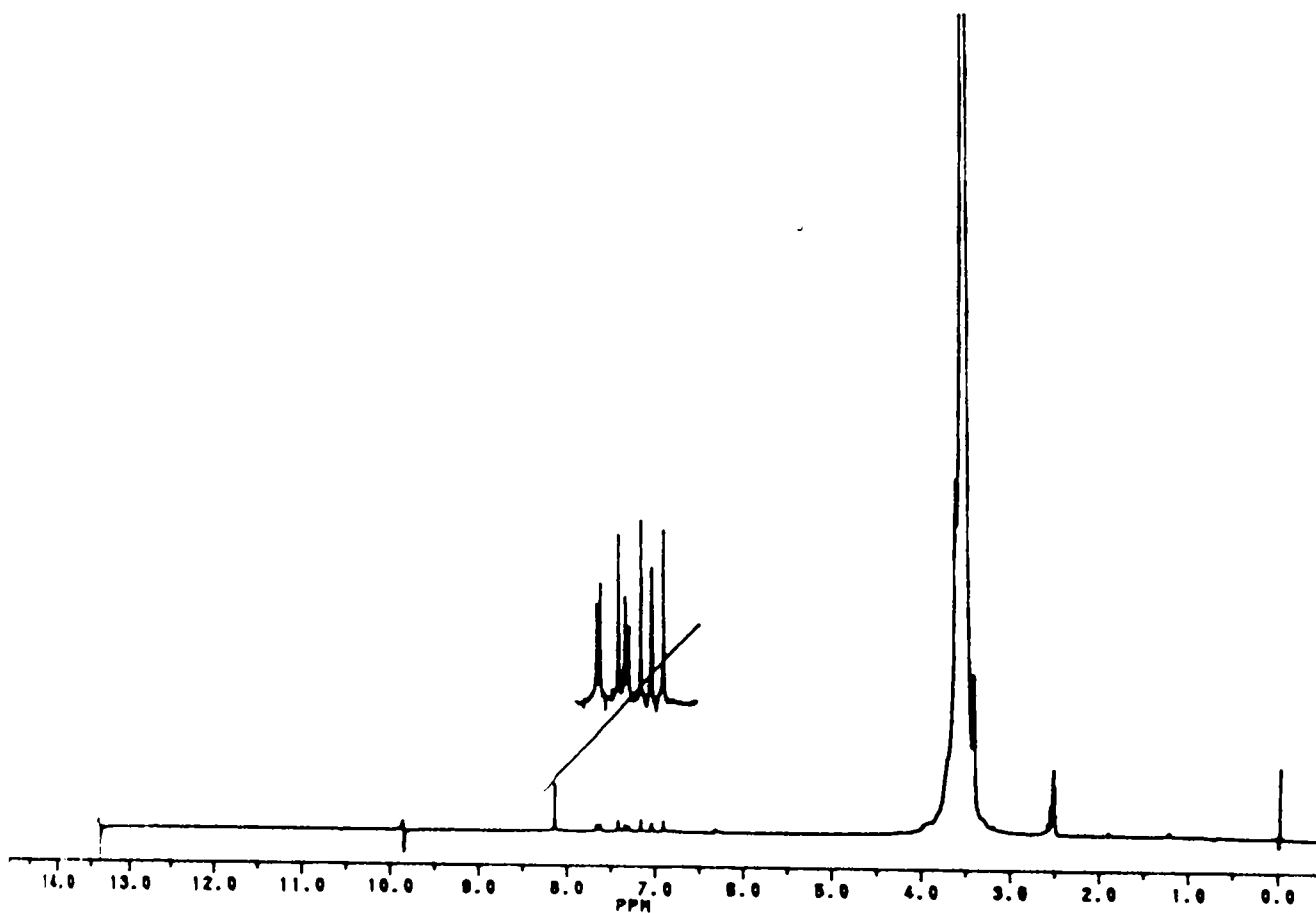


Figure 3.5c: ^1H NMR. Spectrum of co polymer of aniline and benzidine.

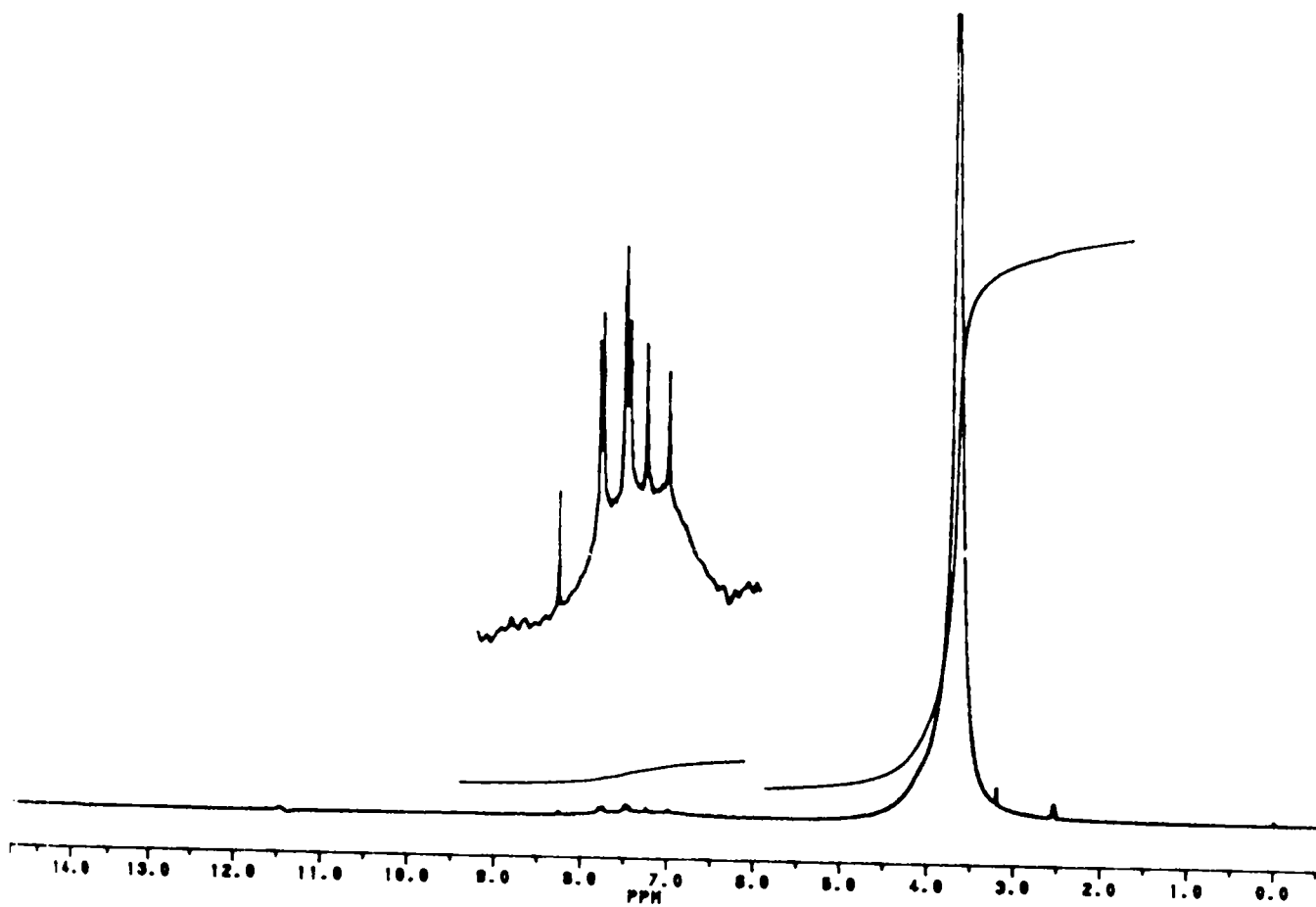


Figure 3.5d: ^1H NMR. Spectrum of co polymer of anisidine and benzidine.

3.4. U V SPECTROSCOPY FOR POLYMER CHARACTERISATION

Molecular absorption in ultra violet and visible region of the spectrum is dependent on the electronic structure of the molecules. Absorption of energy is quantised, resulting in the elevation of electrons from orbital in the ground state to higher energy orbital in an excited state . For many electronic structures, the absorption does not occur in the readily accessible portion of the ultraviolet region . In practice, ultraviolet spectrometry is limited to conjugated system for the most part.

Bands attributed to $\pi \rightarrow \pi^*$ transitions appear in the spectra of molecules that have conjugated π systems such as butadiene. Such absorptions also appear in the spectra of aromatic molecules possessing chromophoric substitutions. These $\pi \rightarrow \pi^*$ transitions are usually characterized by high molar absorptivity, $\epsilon_{\max} > 10000$.

B-Bands are characteristic of the spectra of aromatic or heteroaromatic molecules. Benzene shows a broad absorption band, containing multiple peaks or fine structure, in the near ultraviolet region between 230 and 270 nm. The fine structure arises from vibrational sub levels affecting the

electronic transitions. When a chromophoric group is attached to an aromatic ring, the B bands are observed at longer wavelengths than the more intense $\pi \rightarrow \pi^*$ transitions.

3. 4a. SAMPLE PREPARATIONS

In order to take solution spectra the sample should be dissolved in a ideal solvent. Many solvents are available for use in the ultraviolet region. Three common solvents are cyclohexane, 95% ethanol, and 1,4 -dioxane. Since our samples are not dissolved in any of the above solvents and so we dissolved in DMSO and a base line correction was applied to chart the spectrum.

3. 4b. RESULT AND DISCUSSION

The uv-vis spectra of monomers and polymers were shown in Figure 3.6a -3.6d. All the monomer shows strong absorption in between 290 to 295nm. Aniline shows strong absorption at 293nm and when polymerised the absorption shifts from 293 to 316nm. The additional peaks at 608nm observed in the spectrum may be due to doping. This an indication of the extend conjugation and polymerisation of the monomer. The

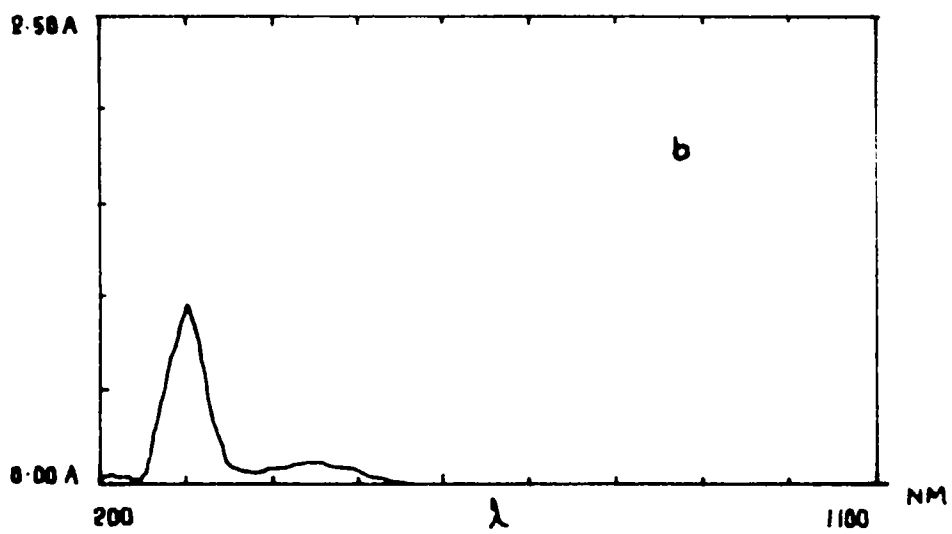
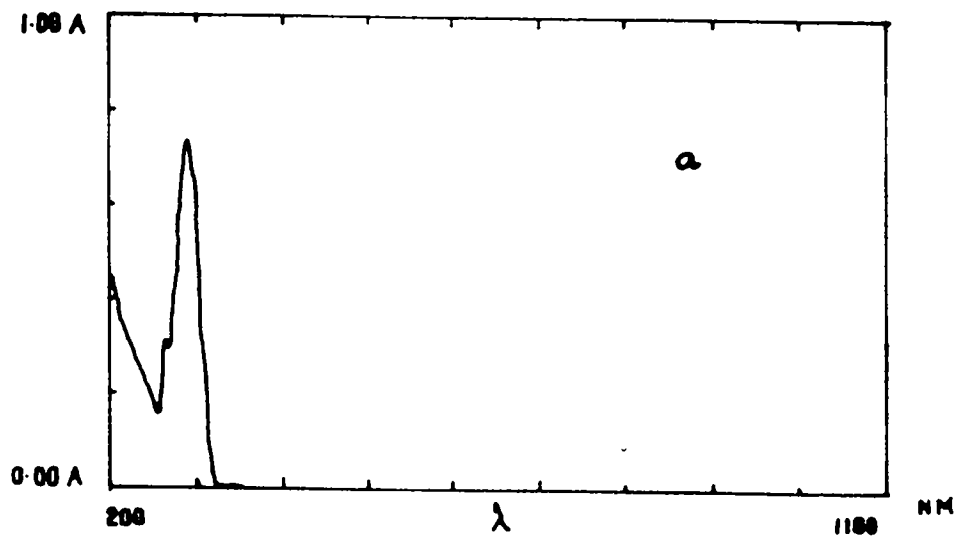


Figure 3.6a: UV-vis.Spectra of (a) Aniline,
(b) polyaniline.

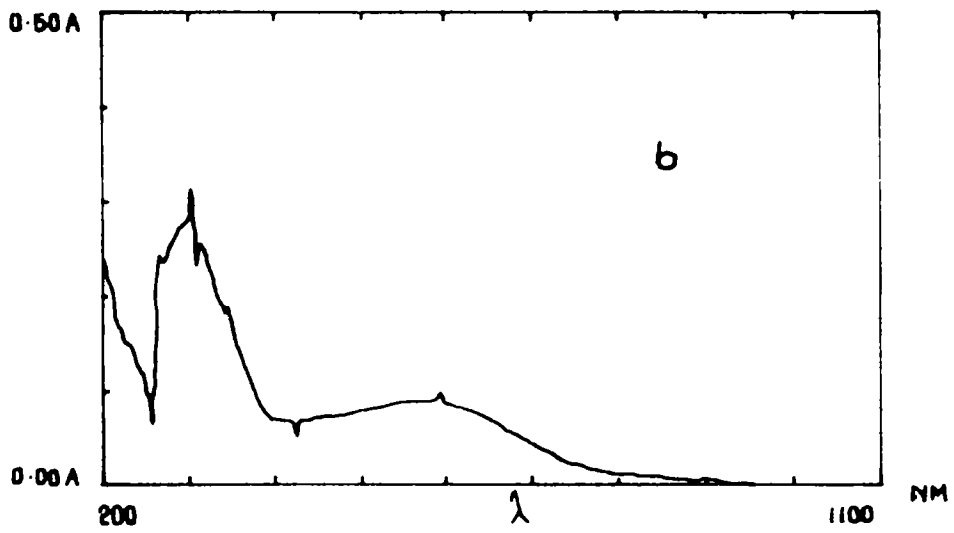
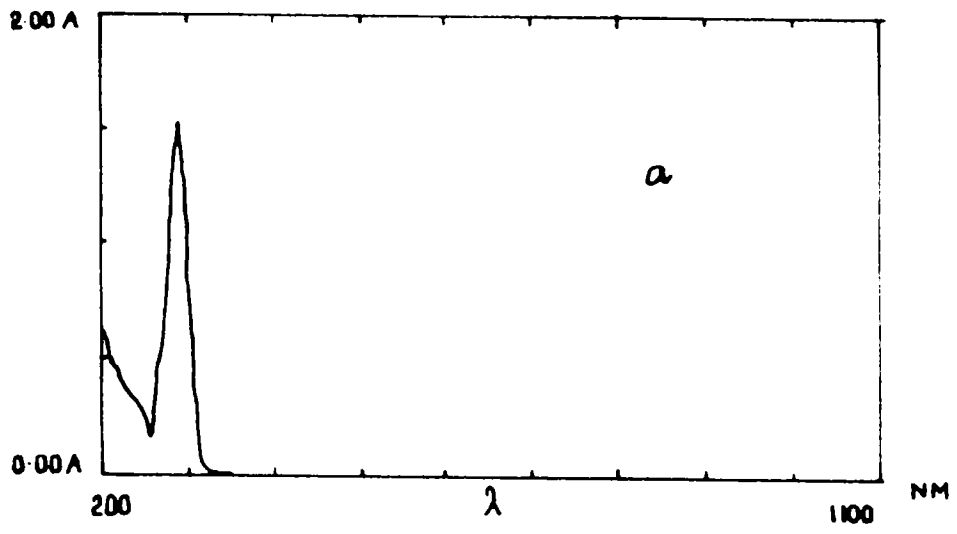


Figure 3.6b: UV-vis.Spectra of (a) Anisidine, (b) polyanisidine.

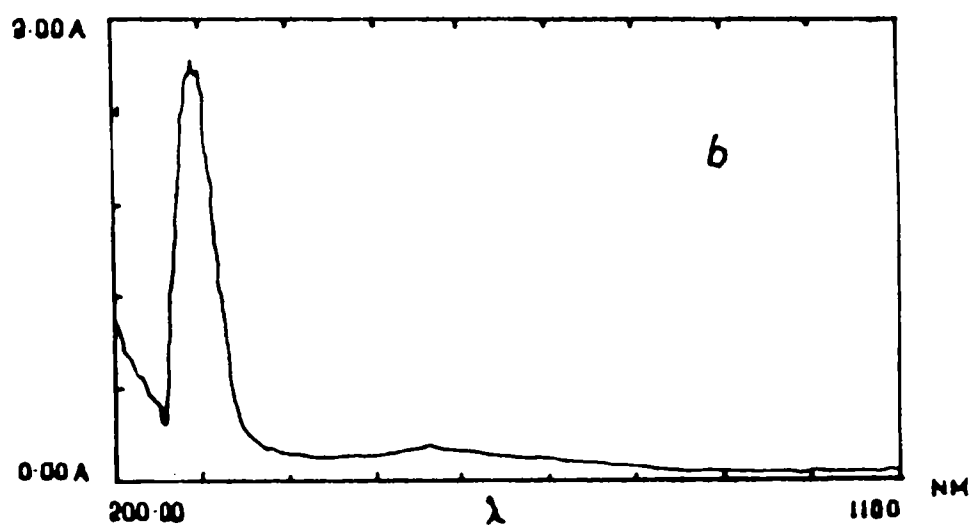
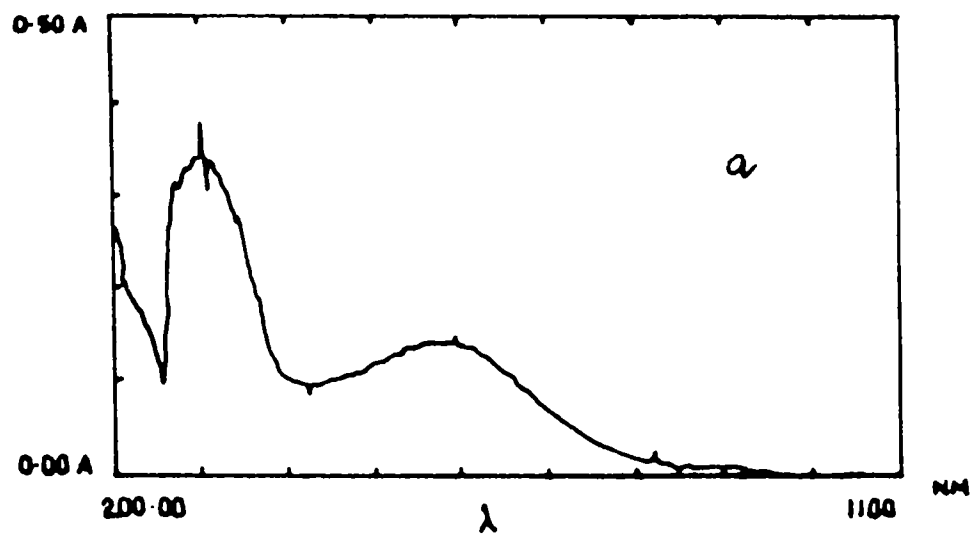


Figure 3.6c: UV-vis.Spectra of (a) co polymer of aniline and Anisidine, (b) co polymer of aniline and benzidine.

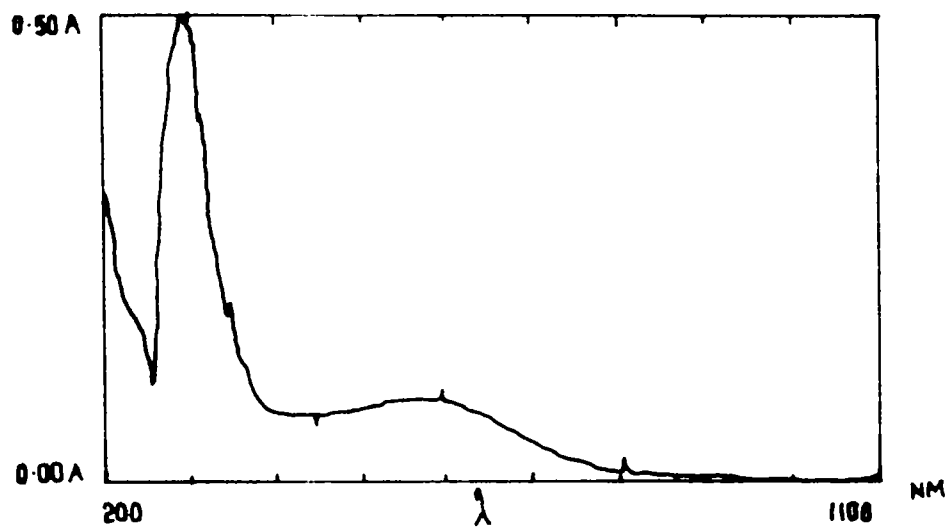


Figure 3.6d: UV-vis.Spectra of co polymer of anisidine and benzidine.

monomer absorption peak at 290nm shifted to 305nm in the case of polyanisidine. The additional peak in this case is observed at 592nm. The co polymer containing aniline and anisidine shows strong absorption at 305nm. In addition to it there are two peaks appearing at 597nm and 821nm. This may be due to the structural modifications in the co polymer. The co- polymer containing aniline and benzidine shows only two absorption peaks. The peaks at 294nm may be due to the benzidine in the polymer and the peak at 560 may be as due to the doping effect. In the case of co polymer containing anisidine and benzidine there are three peaks as in the case of co polymer contain anisidine and aniline. The peaks appear at 306 ,595 and at 806nm. So we assume that the very weak absorption peaks appearing at 821 and 806nm may be due to the structural modification of the polymer due to methoxy group.

3. 5 X-RAY DIFFRACTION FOR POLYMER RESEARCH

The diffraction of x-rays by crystals is a particularly well documented field. The crystalline characterisation of the solid materials were based on the Bragg's equation $2 d \sin\theta = n \lambda$ where n is the order of diffraction and d is the lattice parameter and λ is the wave length used for the

diffractions. In polymer research generally two kinds of x-ray diffractions methods were used. They are discussed in the following paragraphs.

3. 5a. WIDE-ANGLE X-RAY SCATTERING (WAXS)

Wide-angle x-ray scattering (WAXS) refers to studies of scattering at relatively large angles. When making use of Bragg's equation with λ is ≈ 0.15 nm: $d = 0.075/\sin\theta$, where for large scattering angles (2θ) yields distances smaller than 1nm. A scattering angle (2θ) of 36° corresponds to $d = 0.3$ nm. WAXS is used for the assessment of crystal unit cell structure, ie cell identification and the measurement of cell dimensions (a,b and c).

The important applications of WAXS in polymer research are described as follows. First of all, WAXS provides direct evidence of the physical structure. The polymer can be considered as semi crystalline provided that sharp Bragg reflections are observed. A diffuse scattering pattern indicates that only short range order is present. The polymer is probably fully amorphous. However, it is possible that it is liquid crystalline with a nematic mesomorphism. WAXS is the standard method for the

assessment of crystallinity. The assessment of unit cell of polymers with un known crystal structure, and the determination of the unit cell dimensions of polymers with known cell type are important uses of WAXS data. WAXS is also used to record strains in the crystalline phase in stressed samples. The broadening of the diffraction peaks provides information about crystal size and internal disorder.

3. 5b. SMALL ANGLE X-RAY SCATTERING (SAXS)

Small-angle X-ray Scattering (SAXS) is concerned with scattering phenomena occurring at small angles, typically less than a few degrees. The most important requirement is a very good collimation of the x-ray beam. There are several methods used: pinhole collimation and slit collimation.

SAXS is used for the assessment of superstructures in both crystalline and liquid crystalline polymers. The so called SAXS long period of semi crystalline polymers is the repeating distance in the stacks of lamellar crystals. The long period includes one crystal thickness and one amorphous interlayer thickness. It is thus possible to calculate the

crystal thickness from the long period simply by multiplication with the volume crystallinity. Smectic polymers show a layered structure which is readily detected in a SAXS camera. The repeating distance is commonly in the range 2-5nm. It is possible in a Statton camera to detect both the wide-angle reflections originating from the interchain spacing and the low angle reflections arising from the layering. Micro voids created by fracture phenomena have also been assessed by SAXS.

3. 5c. SAMPLE PREPARATION

For x-ray diffractions either powder or solid sample can be used. For the present investigations we use thin disc of polymers made by pelletising the polymer by applying pressure of 10 tones.

3. 5d. RESULTS AND DISCUSSIONS

Oxidation of neutral PANI to yield the quinoid structure generates new molecular orbitals, distorting the original structure of the more reduced form. Furthermore, molecular configurations may be altered on excitation or ionization during spectroscopic studies, thus complicating data

interpretation. One of the greatest barriers limiting the information abstracted using x-ray diffraction is the amorphous character of this polymer. The covalent bonding between monomeric units in polymer chains considerably restricts energetically feasible periodic packing arrangements in polymer charge-transfer complexes when compared with molecular charge-transfer complexes. The difficulties that arise in interpreting structural data on PANI can be somewhat avoided by studying short oligomers, the composition of which is less variable and the geometric structures of which are more accessible. The resulting model studies yield information that may not be completely transferable to the long polymers but can be, nevertheless, be indicative. The x-ray diffraction patterns of our samples are shown in Figure 3.7. The amorphous character of the polymers is evident from the patterns. However peaks appeared in the case of polyaniline and its co polymer containing benzidine is an indication of the presence of crystallinity. From the figure it can also be seen that polyanisidine and its co polymer containing aniline are fully amorphous in character. The amorphous character of the co polymer is an indication of the structural disorder of these materials due to the two dimensional coupling of monomers.

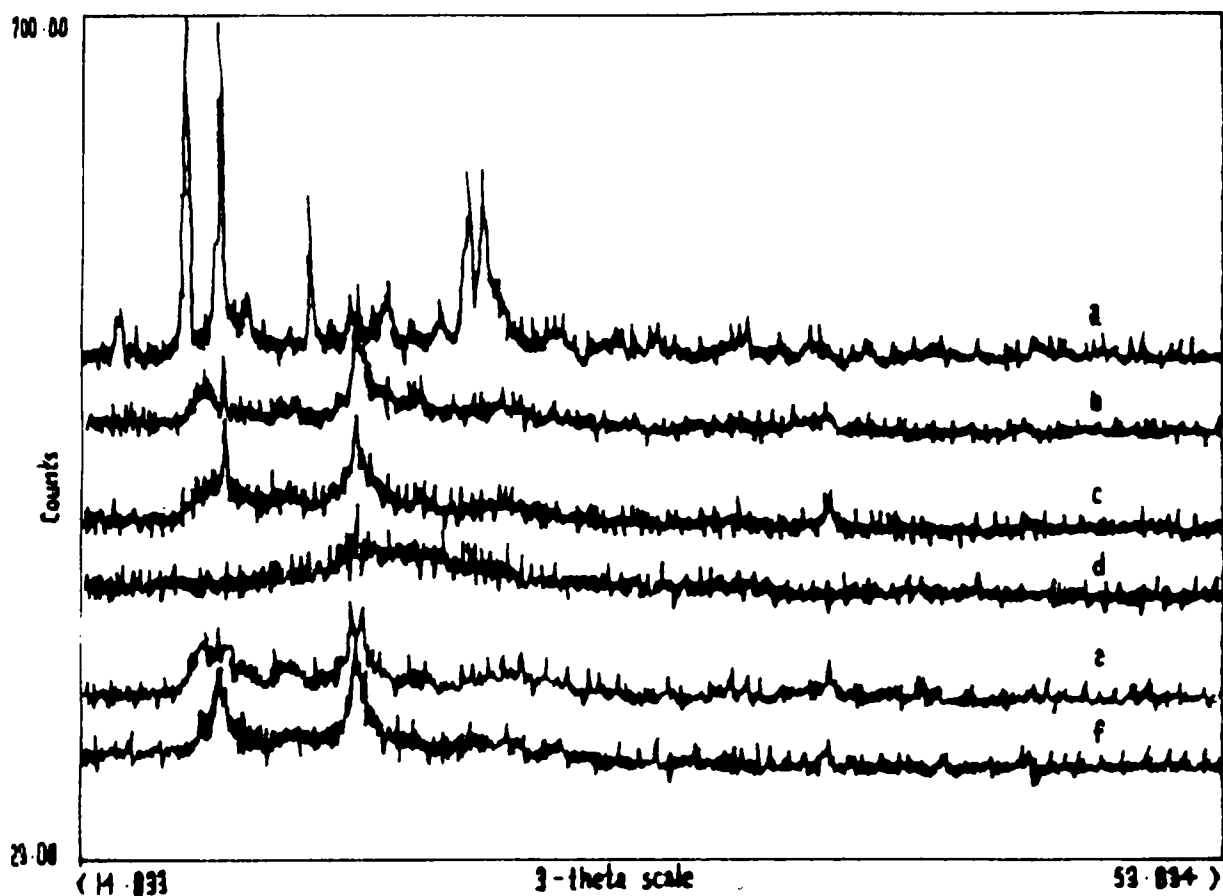


Figure 3.7: X-Ray diffractions of (a) Polyaniline (b) Polyanisidine (c) Polybenzidine (Electrochemically polymerised form) (d) Co polymer of aniline and anisidine (e) Co polymer of aniline and benzidine (f) Co polymer of anisidine and benzidine.

3. 8 THE PROPOSED STRUCTURES OF THE POLYMERS

From results of all the characterisation techniques adopted on our samples, we propose the following structures for them. The structure of the polyaniline and polyanisidine appears to be the same as reported by various authors as shown in Figure 3.8a and 3.8b. The co polymers show different structures. In the case of co polymer having aniline and anisidine one of the arrangements possible is shown in Figure 3.8c. In the co polymer containing aniline and benzidine, the aniline may be attached to benzidine either linearly as shown in Figure 3.8d. or two dimensionally as shown in Figure 3.8d1. The polymer containing anisidine and benzidine may also have the structures as shown in Figure 3.8e.or 3.8e1.

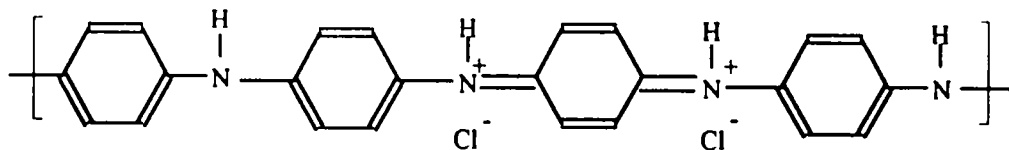


Fig. 3.8a: Structure of Doped polyaniline

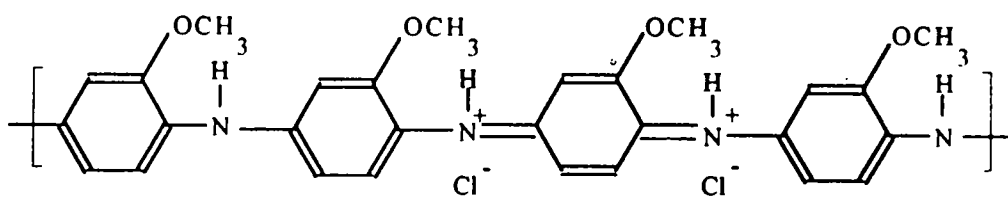


Fig. 3.8b: Structure of Doped polyanisidine

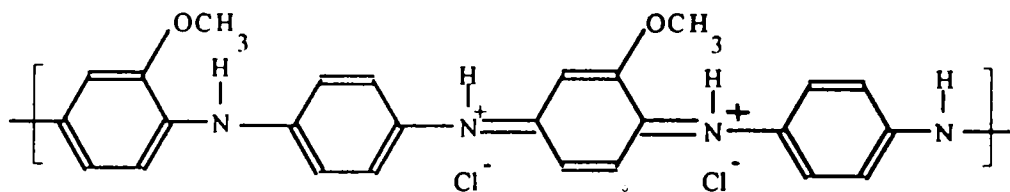


Fig. 3.8c: Structure of Doped co-polymer of aniline and anisidine

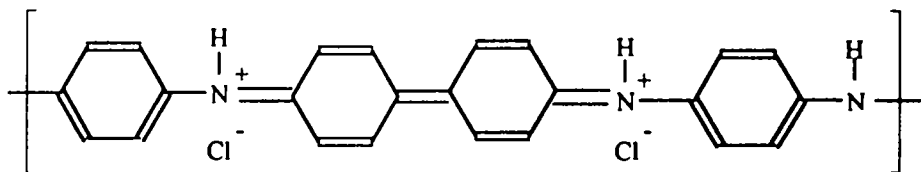


Fig. 3.8d: Structure of Doped co-polymer of aniline and benzidine

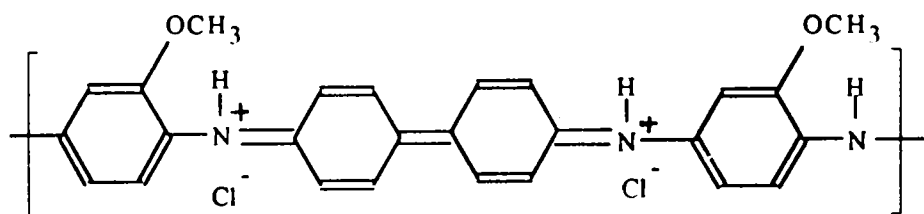


Fig. 3.8e: Structure of Doped co-polymer of anisidine and benzidine

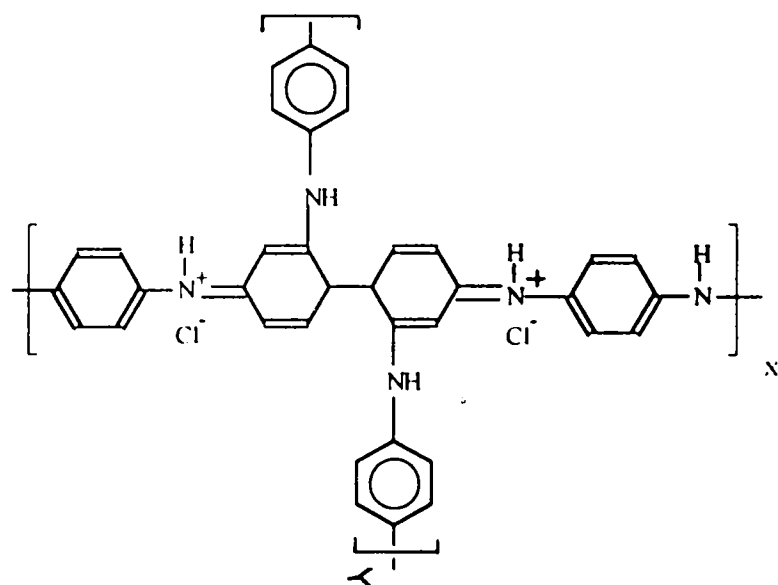


Figure 3.8d1: Probable structure of co-polymer resulting from two-dimensional polymerisation of aniline and benzidine

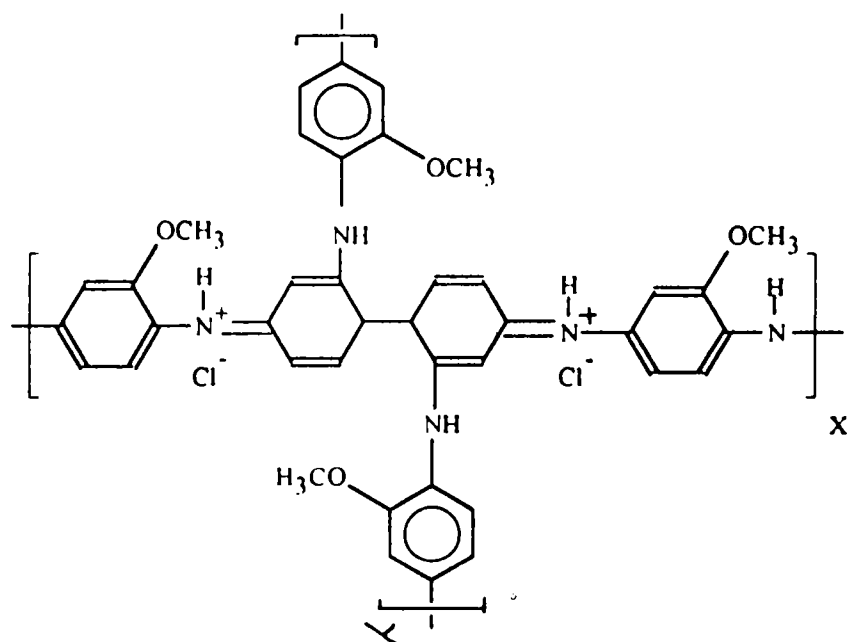


Figure 3.8e1: Probable structure of co-polymer resulting from two-dimensional polymerisation of anisidine and benzidine

REFERENCES

1. T. Ohsaka et al., *J. Electroanal. Chem.*, 161 (1984) 399.
2. I. H. C. Mattoso, S. K. Manohar., A. G. MacDermid and A. J. Epstein., *J. Poly. Sci. Part A. Poly. Chem.* 1227 (1995) 1227.
3. S. K. Manohar and A. G. MacDermid. *Synth. Metals.*, 29 (1989) E349.
4. R. P. McCall, M. G. Roe, J. M. Ginder, T. Kusumoto and A. J. Epstein., *Synth. Metals.*, 29 (1989) E433.
5. Issei Harada, Yukio Furukawa and Fumitaka Ueda., *Synth. Metals.*, 29 (1989) E303.
6. S. C. K. Misra and Subhas Chandra., *Indian Journal of Chemistry.*, 33A (1994) 583.

CHAPTER 4

ELECTRICAL TRANSPORT PROPERTIES OF POLYAROMATIC AMINES - I. DC AND AC CONDUCTIVITY

4. 1 INTRODUCTION

The first conductivity studies on the oxidation products of aniline indicated that these materials have interesting electronic properties. Pohl and Engelhardt [1], Parini [2] and Maleev [3] quoted the first values for conductivity as ranging from 10^{-13} to $10 \text{ ohm}^{-1} \text{ cm}^{-1}$. There has, however, been difficulty in reproducing these values. Systematic studies on the relationship between conductivity of polyanilines, (PANI) their mode of synthesis and their physico-chemical properties have enabled Jozefowicz and his co workers [4,5,6] to reduce the discrepancies in the results (eg: reproducibility within 10% in the case of the conductivity of polyaniline). This was achieved by a well defined synthesis method which simply involves the oxidation of aniline by ammonium persulfate in sulphuric acid at pH value 1, which yielded a material having a conductivity of $100 \text{ ohm}^{-1} \text{ cm}^{-1}$. Jozefowicz et al. [7,8] also established simple

relationships between the conductivity and chemical potential for the species present in the solid matrix, as function of the degree of protonation and hydration of the polymer. The conductivity of PANI prepared electrochemically in neutral, phosphoric or basic (acetonitrile/pyridine) media is much weaker, being in the range 10^{-15} to 10^{-14} ohm⁻¹cm⁻¹. It has been shown that the polymer formed at 0°C is more ordered and hence more conductive in the metallic region than that synthesised at 30 °C [9].

From conductivity measurements and NMR spectroscopic investigations, Travers et al. [10] have observed that the polymer exhibits a metal-to-insulator transition which is a function of the pH. The conductivity of the polymer is 5 ohm⁻¹cm⁻¹ when the polymer is previously equilibrated at pH value 6. MacDiarmid et al. [11,12,13,14] has also described a variation in the conductivity of both chemically and electrochemically prepared polymers with the pH of the aqueous solution to which the polymer were exposed before drying. The polymer exhibits a conductivity 1 ohm⁻¹cm⁻¹ when it is equilibrated at a pH between -1 and +1 , and 10 ohm⁻¹cm⁻¹ when it is equilibrated at a pH between 5 and 6. Elsewhere they indicate that the conductivity of the polymer

is a function of the level of doping, with a value of $1 \text{ ohm}^{-1} \text{ cm}^{-1}$ for 0% to 10% doping. Measurements carried out by Brahma [15] revealed that PANI doped with iodine exhibits a conductivity four order of magnitude greater than the undoped polymer. It has also been observed by Kitani et al [16] that the resistance is no longer measurable after the polymer has been treated with a base such as sodium hydroxide.

Wrighton et al. [17] and Glarum and Marshall [18] have carried out in situ conductivity measurements on PANI in aqueous sulfuric acid solution as a function of the applied potential. They observed a minimum in the resistance between 0.3 and 0.5 V and two insulator-conductor transitions in the ranges of 0.0-0.15 V and 0.65-0.8 V.

4. 2 DC CONDUCTION MECHANISM

The mechanisms on the formation of metallic state and charge conduction in conducting polymers have been the subject of intensive research since the report of an insulator to metal transition occurring upon p or n type doping of polyacetylene [19], and the subsequent proposal that the defect states such as solitons and polarons play an

important role in their electrical transport properties[20,21,22,23,24]. The electronic states and conduction mechanism of emeraldine form of polyaniline have been of particular interest [25,26]. This polymer differs from conventional conducting polymers in that the number of electrons on the polymer chain are kept constant while the number of protons are varied. Recent experimental results on the emeraldine base and salt have demonstrated that there is an insulator to metal transition with protonation. The metallic state was proposed as due to the formation of polaronic bands [25,27,28,29].

The experimental results on DC transport, AC transport, and thermopower measurements made on the polyaniline demonstrate that there are two regimes of protonation; one at light doping in which case the transport is dominated by hopping motion of charged carriers, and the other at heavy doping in which the system becomes a granular polymeric metal with the metallic islands surrounded by insulating layers, and the charge conduction is through charging energy limited tunneling between metallic regions [30,31].

The schematic diagram of the chemical bonding of the emeraldine base before and after protonation is

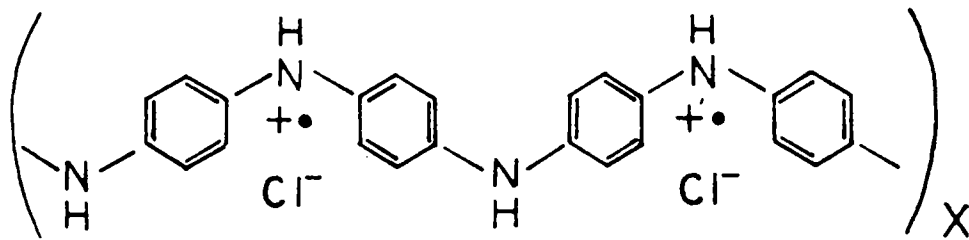
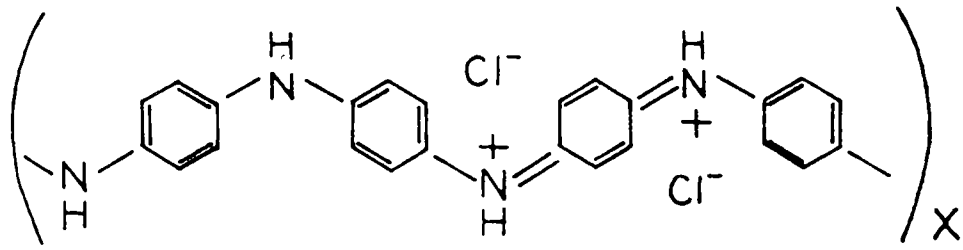


Figure 4.1: Schematic diagram of a polaron and a bipolaron

schematically shown in figure 4.1, depicting the possible defect states such as neutral polarons, charged polarons and bipolarons. Because of the thermodynamic equilibrium condition, these defect states are at equilibrium distribution with each other. Similar phenomena have been proposed to exist in pure and doped polyacetylene system where neutral and charged solitons and polarons coexists in all stages of doping process.

4. 3 THEORY OF DC CONDUCTIVITY

The essential features of Davis and Mott's model for the band structure of amorphous semiconductors are the existence of narrow tails of localised states at the extremities of the valence and conduction bands and a band of localised levels near the middle of the gap. Accordingly there are three different conduction channels [32,33] as outlined below.

a) Extended state conduction: Conductivity is due to electrons excited beyond the mobility edges E_c in to extended states. Assuming a constant density of states N_c and constant mobility μ_c , one gets

$$\sigma = eN(E_c)k_b\mu_c \exp \{-(E_c - E_F)/k_B T \} \quad (4.1)$$

b) Conduction in band tails: If the wave functions are localised, conduction can occur by thermally activated hopping. Every time an electron hops from one localised state to another state, it will exchange energy with a phonon with energy $W(E)$. It may be expected that the mobility will be thermally activated,

$$\mu_{hop} = \mu_0 \exp [-W(E)/k_B T] \quad (4.2)$$

Assuming a power dependence for the density of states, one finds

$$\sigma_{hop} = \sigma_0 (k_B T/\Delta E) C \exp [-(E_A - E_F + W)/k_B T] \quad (4.3)$$

c) Conduction in localised states at Fermi energy: if the Fermi energy lies in a band of localised states, as predicted by Davis and Mott's model, the carriers can move between the states via a phonon assisted tunneling process. We shall follow the original derivation. For this mechanism

let us consider an electron that is scattered by phonons from one localised state to another. The probability p that an electron will jump from one states to another is determined by the following three factors.

1) The probability of finding of a phonon with an excitation energy equal to the energy difference between the states, W , is given by a Boltzmann distribution $\exp(-W/k_B T)$.

2) The attempt frequency ν_{ph} , which can not be greater than the maximum phonon frequency (in the range of $10^{12} s^{-1}$ - $10^{13} s^{-1}$).

3) The probability of an electron transfer from one state to another. This factor depends on the overlapping of wave function and should be given by $\exp(-2\alpha R)$. Here R is the jumping distance, which at high temperatures equals to the intersite spacing, and α is the transfer integral between the two sites, which is representative of the rate of fall of a wave function at a site. If overlapping is large, the $\exp(-2\alpha R)$ becomes of the order of one.

The probability p that an electron will jump can then be expressed as

$$p = \nu_{ph} \exp [(-2\alpha R - W)/k_B T] \quad (4.4)$$

By making use of Einstein's relation

$$\mu = eD/k_B T \quad (4.5)$$

with $D = (1/6)pR^2$, the conductivity can be written as

$$\sigma = (1/6)e^2 R^2 N(E_F) \nu_{ph} \exp[(-2\alpha R - W/k_B T)] \quad (4.6)$$

As the temperature is lowered the number and the energy of phonons decrease, and the more energetic phonon assisted nearest neighbor hops will progressively become less favorable. Carriers will tend to hop to a larger distances in order to find sites which lie energetically closer than the nearest neighbors. This mechanism is the so called variable range hopping. The factor $\exp [(-2\alpha R - W/k_B T)]$ will not have a maximum value for nearest neighbors. In order to find the most probable hopping distance, Mott used an optimization procedure and the conductivity is found as

$$\sigma = \sigma_0(T) \exp [-(T_0/T)^{1/4}] \quad (4.7)$$

with

$$\sigma_0(T) = e^2/2(8\pi)^{1/2} \nu_{ph} [N(E_F)/\alpha k_B T]^{1/2} \quad (4.8)$$

and

$$T_0 = 16\alpha^3/k_B N(E_F) \quad (4.9)$$

In principle, α and $N(E_F)$ can be evaluated from the slope of a plot of $\ln \sigma(T)$ vs $T^{-1/2}$ and the prefactor $\sigma_0(T)$ if one assumes a reasonable value for ν_{ph} .

The above equation is for three dimensional system. With the same argument one can find that the exponent of the temperature dependent conductivity is different for different dimensions, or σ is proportional to $\exp(-A/T^n)$. For 3-D systems, the exponent (n) is 1/4 and for 1-D systems it is 1/2 [6].

It should be mentioned that Mott's derivation of variable range hopping model is under several simplified assumptions: energy independence of the density of states at E_F ; neglect of correlation effects in the tunneling process; omission of multiphonon processes; and the neglect of electron-phonon and electron-electron interactions. Efros and

Shklovskii [34] and many other subsequent workers showed that under certain assumptions long range Coulomb interaction should lead to a conductivity of the form.

$$\sigma = \sigma_0 \exp(-A/T^{1/2}) \quad (4.10)$$

The analysis, confirmed by computer calculations [34], is as follows. Consider an empty and an occupied state at a distance R from each other with energies E_a and E_b above and below the Fermi level respectively. The energy required to move an electron from one to the other is

$$E_a - E_b - e^2/kR \quad (4.11)$$

Around any one of the states there is sphere of volume

$$(4\pi/3)R^3 = (4\pi/3)(e^2/k\epsilon)^3 \quad (4.12)$$

with $\epsilon = E_a - E_b$, where we can define the one electron density of states $N(E)$ seen by the electron introduced or taken away from the material. Calculation shows a decrease in the $N(E)$ at Fermi level [7]. By optimizing the most probable jumping distance, one can find easily the $\sigma \propto \exp(-A/T^{1/2})$ dependence rather than $\exp(-A/T^{1/4})$ in the case of constant

density of states at the Fermi level.

4. 3a. CONDUCTION BY POLARONS

When a charge is introduced in to the conduction bands of a perfect ionic crystal, it may be energetically favorable for it to move in a spatially localised level, accompanied by a local deformation in the previously perfect ionic arrangement that serves to screen its field and reduces its electrostatic energy [35,36,37]. A polaron can move by hopping from one lattice site to an equivalent one, which can only be created with a similar distortion surrounding it. The deformation energy comes from phonons. Therefore, the conduction of polarons is phonon assisted tunneling between nearby sites [32]. From Einstein's relation we can write

$$\sigma = ne\mu = ne^2 D/k_B T = n e^2 a^2 p_1 p_2 / k_B T \quad (4.13)$$

with

$$p_1 = \nu_{ph} \exp(-W/k_B T) \quad (4.14)$$

The probability of finding a nearby site with the an

equivalent distortion, W , is related to polaron binding energy by $W = E_p/2$ and

$$P_2 = 2\pi/h\nu_{ph} (\pi/Wk_B T)^{1/2} t^2 \quad (4.15)$$

is the probability of charge transfer. Then one can get [6]

$$\sigma = (\pi n^2 a^2 t^2 / k_B T h\nu_{ph}) (\pi/Wk_B T)^{1/2} \exp(-W/k_B T) \quad (4.16)$$

4. 3b. INTERSOLITON HOPPING CONDUCTION

For a lightly doped polyacetylene it has been proposed by Kivelson et al [38,39] that inter soliton hopping might play an important role in the charge conduction process. The theory is predicated in the presence of both a charged soliton and a neutral soliton, both of which are situated near dopant ions, referred to as impurity sites. The requirement of a dopant ion near the neutral soliton is to minimize the energy cost for the electron transfer from one site to another. The formula derived by Kivelson is

$$\sigma = (Ae^2 \gamma(T) \xi / k_B T) \cdot (\xi / R_0^2) \cdot [y^0 y^+ / (y^0 + y^+)^2] \exp(-2BR_0/\xi) \quad (4.17)$$

where A and B are dimensionless constants, y^0 and y^+ are the fractions of occupied neutral and charged soliton sites respectively, R_0 is the average separation between dopant ions and ξ is the three dimensional electronic decay length, $\gamma(T)$ is the electron-phonon coupling constant. The main predications of this model for conductivity are the following:

- 1) The dopant concentration does not affect temperature dependence of conductivity.
- 2) Conductivity varies as $\sigma \propto T^{z+1}$ which is a slower function of T than $\exp(-E_b/k_B T)$.

4. 3c. TUNNELING CONDUCTION

The above discussed mechanisms are for homogeneous media, which means that the localised states such as solitons, polarons, and bipolarons are randomly distributed over the specimen. There are, however, conduction mechanisms, different from the above ones, which apply to composite materials such as conducting particles embedded in

insulating matrix [40]. For these system, the charge carriers are delocalised and free to move over a distance very large compared to the atomic dimensions of the conducting particles. The electrical conduction in these media is dominated by carrier transfer between conducting segments rather than between localised states as we have discussed earlier. Two kinds of transport mechanisms have been developed by Sheng and co workers [41,42]. One is called charging energy limited tunneling for small metallic particles. The other is by a thermally modulated tunneling between large metallic particles. These models are described below.

a) The charging energy limited tunneling[41] can be derived as follows. When an electron is transferred from one conducting island to another, the capacitor consisting of these two grains is charged. Such a process of a charge carrier generation requires a certain amount of charging energy E_c , which can be pictured as stored in the fields of the charged pair. From dimensional analysis, E_c has to have the form

$$E_c = e^2 F(s/d) \quad (4.18)$$

where e is the electronic charge, d is the size of a grain,

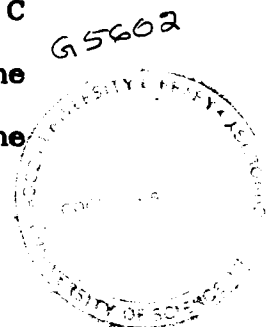
s is the separation between grains, and F is a function whose form depends on the shape and arrangement of the grains and on the interaction between grains. The existence of E_c directly implies that the thermal equilibrium density of charge carriers, whose generation requires charging energy E_c and should be proportional to Boltzman factor $\exp[-(E_c/2k_B T)]$. One plausible assumption is that for a certain concentration of doping, the ratio (s/d) is a constant whose value depends only on x. And it follows that $x s E_c = C$ (constant) where x is the hopping integral. Since the conductivity is the product of mobility, charge, and the density of charge carriers, one can write

$$\sigma \propto \exp [-(E_c/k_B T) - 2xs] = \exp [-(E_c/k_B T) - (2C/E_c)] \quad (4.19).$$

It is easily seen that σ is a peaked function of E_c with a maximum occurring at

$$E_c = (4k_B T C)^{1/2} \quad (4.20)$$

In granular metals where there is a distribution of E_c , the dominant contribution would come from these carriers with maximized E_c . Therefore, the dominant contribution to conductivity is given by



$$\sigma = \sigma_0 \exp [-2 (C/k_B T)^{1/2}] \quad (4.21)$$

One feature of charging energy limited tunneling model is that the generation of charged carriers can come from either temperature activation or application of an external electric field. When the voltage difference between two neighboring grains is larger than E_0/e , a pair of positive and negative charged grains can be generated. In the high field limit where $e\Delta V \gg k_B T$, the generation rate would only depend on the tunneling rate $\exp(-2\kappa s)$. The maximum contribution will come from grains with the shortest separation. From the assumption $2\kappa s E_0 = \text{Constant } (C)$, one gets

$$\sigma \propto \exp (12\kappa s) = \exp (-2\kappa C/2\kappa\Delta V) = \exp (-E_0/E) \quad (4.22)$$

with $E_0 = C/ew$. One can calculate w , the grain size, if T_0 is known from DC conductivity data, as

$$w = k_B T_0 / 4eE_0 \quad (4.23)$$

b) Thermal fluctuation modified tunneling [42] is proposed for a system with metallic islands, the charge density fluctuations within each island being negligible. A direct

consequence of large size of conducting regions is that the charging energy required to remove an electron from a neutral aggregate is completely negligible, in sharp distinction to the conduction in granular metals where the charging energy plays an important role. Therefore, charge transfers in this case can be regarded as tunneling between two bulk conductors. Assuming that the tunnel barrier is in the form of a plane parallel junction of area A and separation w , the barrier potential of the ion is of the form

$$V(x) = V_0 - 4V_0 x^2 / w^2 \quad (4.24)$$

where x is defined as the centre of the junction. The tunneling current density can be calculated using WKB methods as

$$j(E) = j_0 \exp [-(\pi x w / 2)(E/E_0 - 1)^2] \quad (4.25)$$

where $E_0 = 4V_0 / ew$ and $x = (2mV_0 / h^2)^{1/2}$

There are two possible sources for the electrical field. One is the applied electrical field E_a and the other possibility is that there is a thermal fluctuation voltage given by

$(k_B T/C)^{1/2}$ with $C = A/4\pi w$, the capacitance of the junction. The total electric field across the junction is the sum of the two. Since the thermal electric field can be in both directions, at a fixed and small applied field, $E_a < E_t$, and the net forward current is given by

$$\Delta j = j(E_a + E_t) - j(E_a - E_t) \quad (4.26)$$

With thermal average, one can get the dominant conductivity as

$$\sigma = \sigma_0 \exp(-T_1/T + T_0) \quad (4.27)$$

with

$$T_1 = wAE_0^2 / 8\pi k_B \quad (4.28)$$

and

$$T_0 = AE_0^2 / 4\pi^2 \times k_B \quad (4.29)$$

Here T_1 is a measure of the energy required to move an electron across the insulating gap and T_0 is a temperature much below which the conductivity reduces to a temperature

independent tunneling.

The high electric field behavior can be obtained as

$$j(E) = j_0 \exp \{-a(T)[(E_A/E_0)-1]^2\} \quad (4.30)$$

where

$$a(T) = T_1/(T+T_0) \quad (4.31)$$

4. 4 EXPERIMENTAL TECHNIQUE

The conductivity of emeraldine form of polyaniline changes from $10^{-10} \text{ ohm}^{-1} \text{ cm}^{-1}$ to $10^2 \text{ ohm}^{-1} \text{ cm}^{-1}$ with protonation. The emeraldine form of polyaniline shows the highest achieved conductivity for the polyaromatic amine family of polymers. We have performed DC conductivity measurements as a function of temperature of polyaniline, polyanisidine and co polymers of aniline and anisidine, aniline and benzidine and anisidine and benzidine. These polymers were prepared under same conditions described in chapter 2 and were doped with 1M HCl. The measurements were performed on pressed pellets of the samples.

Resistance is measured using the four probe technique. It is measured using Schlumberger multimeter using an in built current source, where ranges of 0.1 KOhm to 1000 MOhm are provided. 0.1, 1, 10, 100 and 1000 KOhm ranges have been use for four terminal technique and 10 to 1000 MOhm ranges for a special ratio method. The temperature is measured using a platinum RTD. The resistance of the RTD is then converted in to corresponding temperature (Kelvin) using an equation which has been formulated after linearization of its characteristic curve.

A locally available IEEE card PCL-231 from Dynalog has been used to automate the setup. The software is in GWBASIC. Low temperature has been achieved with the closed cycle Helium refrigerator developed and fabricated at CAT for IUC DAE Facilities at Indore. A block diagram of the experimental setup used for conductivity measurements is shown in the Figure 4.2. The system has been cooled to the lowest possible temperature and then allowed to warm up. Measurements have been taken during warm up. The dimensions of the sample have been measured. The resistivity and the conductivity has been calculated from the resistance data at each temperature.

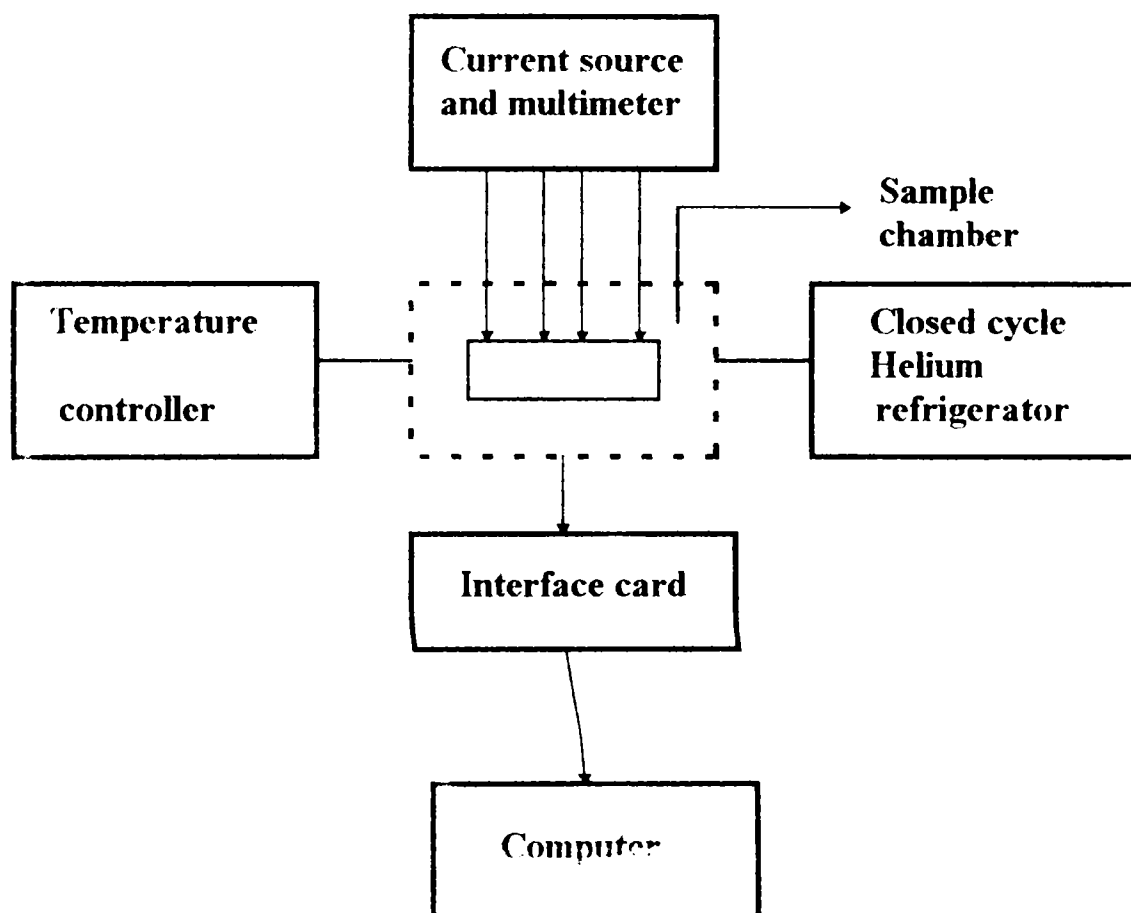


Figure 4.2: Block diagram of the experimental setup used for dc conductivity measurements.

4. 5 RESULTS AND DISCUSSION

Figures 4.3a to 4.3e show plots of dc conductivity as a function of temperature for all the polymers and co polymers. The conductivity of polyaniline increases with temperature in a linear fashion up to room temperature. However, the temperature dependence of conductivity of polyanisidine and all the co polymers containing anisidine show two different regions. In the first region, the conductivity is almost independent of temperature at certain range of temperature which is different for polyanisidine and its co polymers. In the second region, the conductivity increase with temperature as in the case of polyaniline. In the co polymer containing aniline and benzidine, the variation of conductivity with temperature is highly complicated. At above 125 K, it shows an anomalous behaviour. The occurrence of two regions in the case of polyanisidine and all the co polymers containing anisidine is attributed to the different conduction mechanisms.

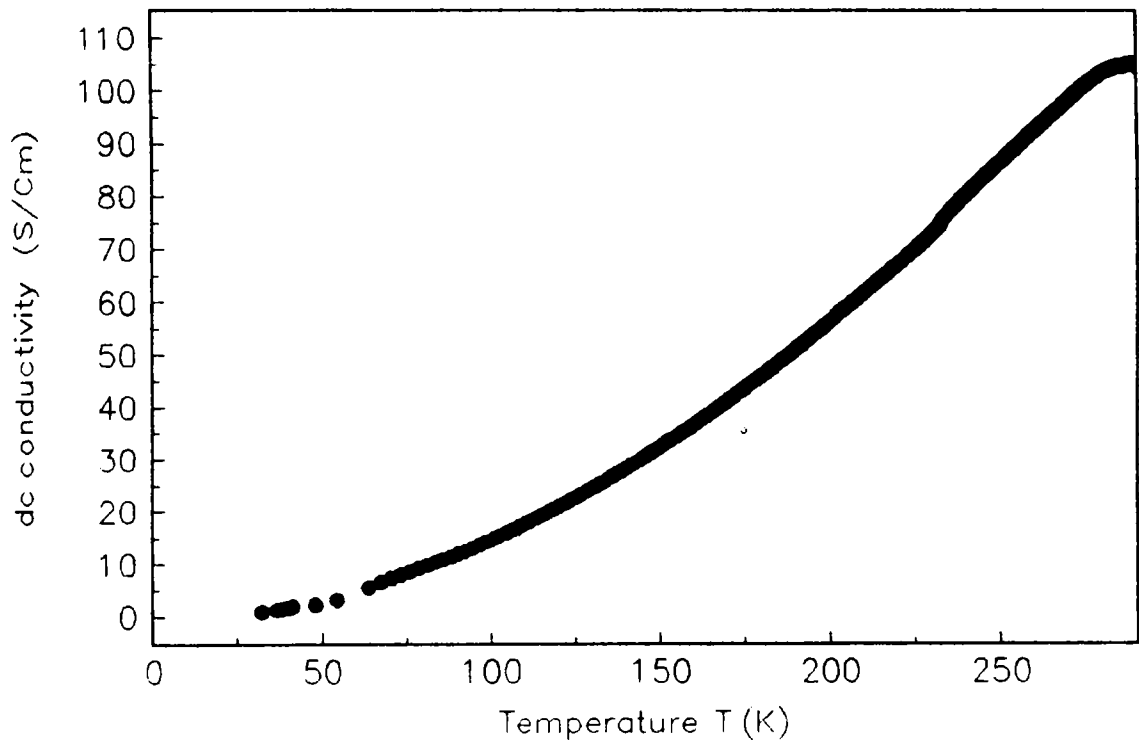


Figure 4.3a: Conductivity versus temperature plot for doped polyaniline.

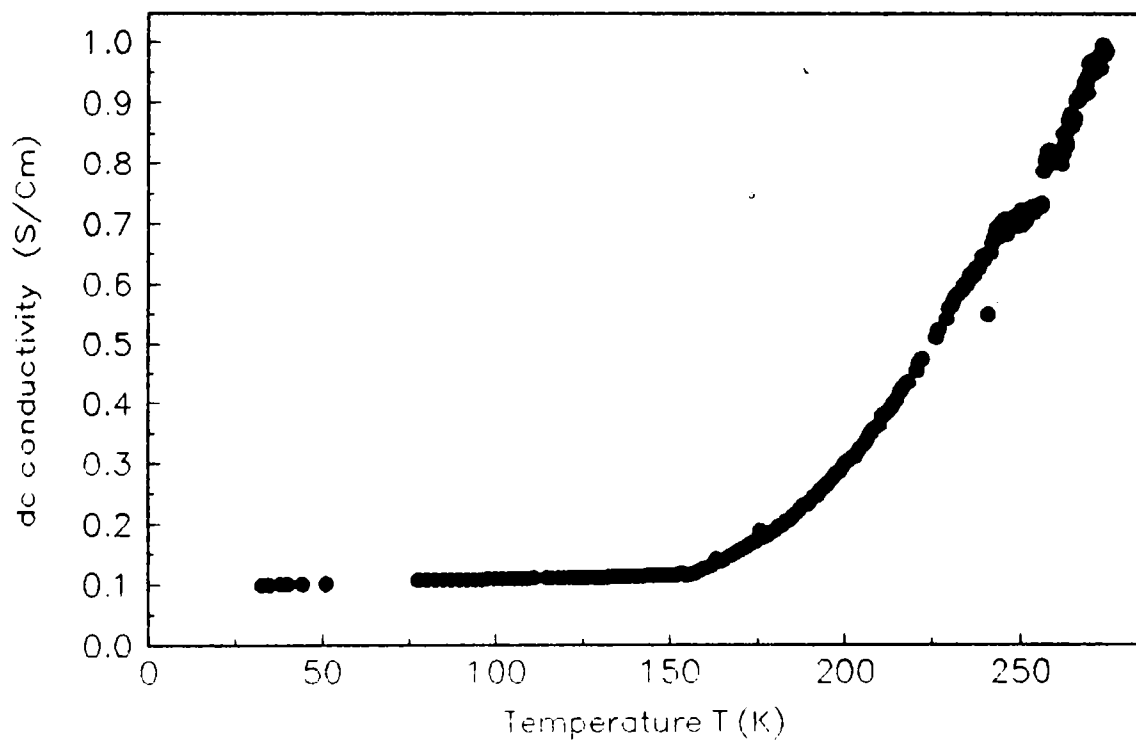


Figure 4.3b: Conductivity versus temperature plot for doped polyanisidine.

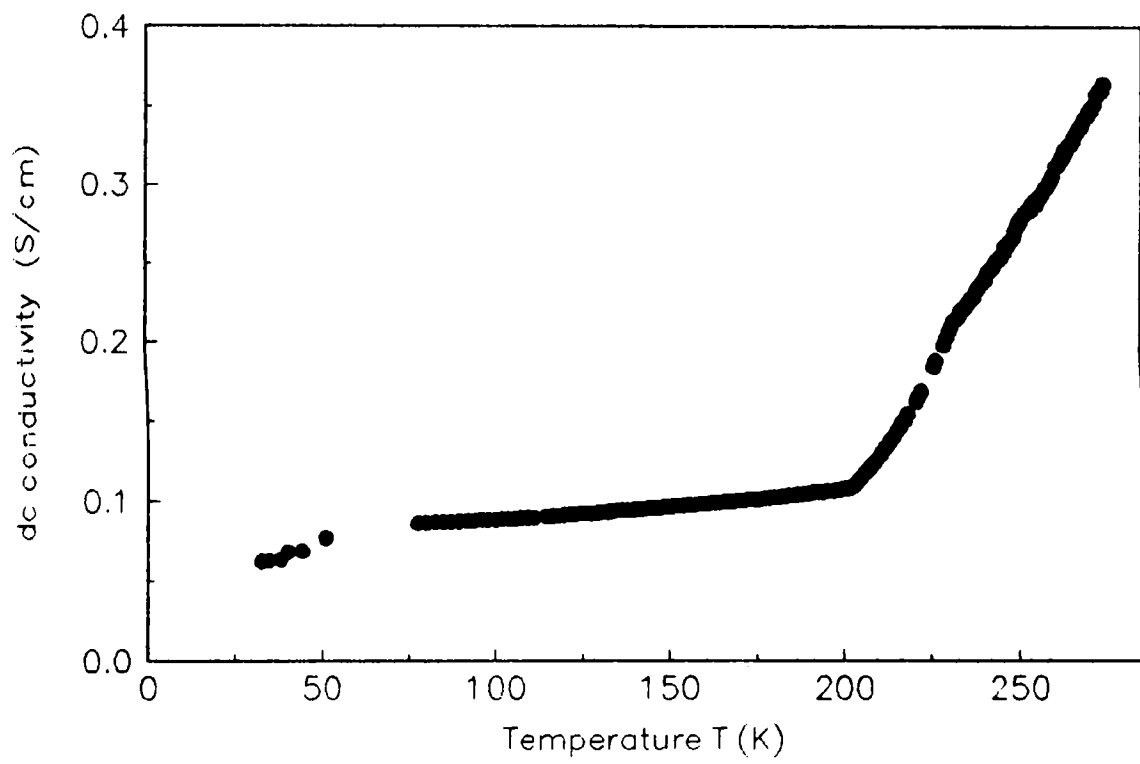


Figure 4.3c: Conductivity versus temperature plot for doped co polymer of anisidine and aniline.

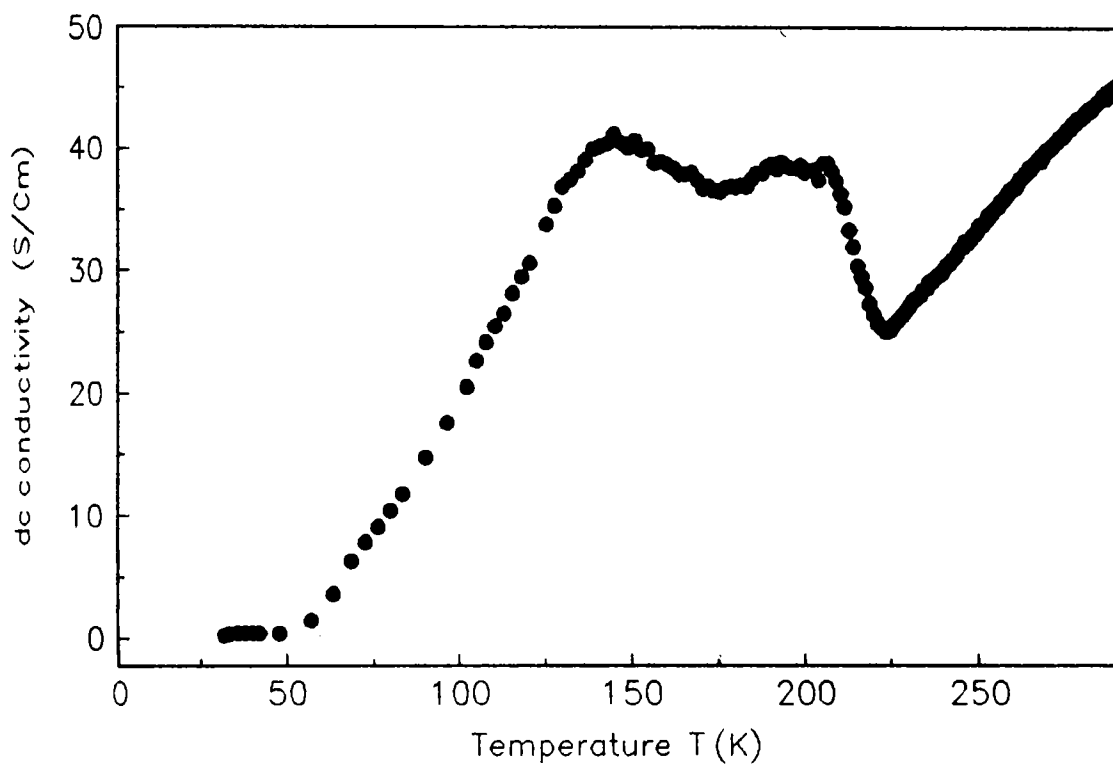


Figure 4.3d: Conductivity versus temperature plot for doped co polymer of aniline benzidine.

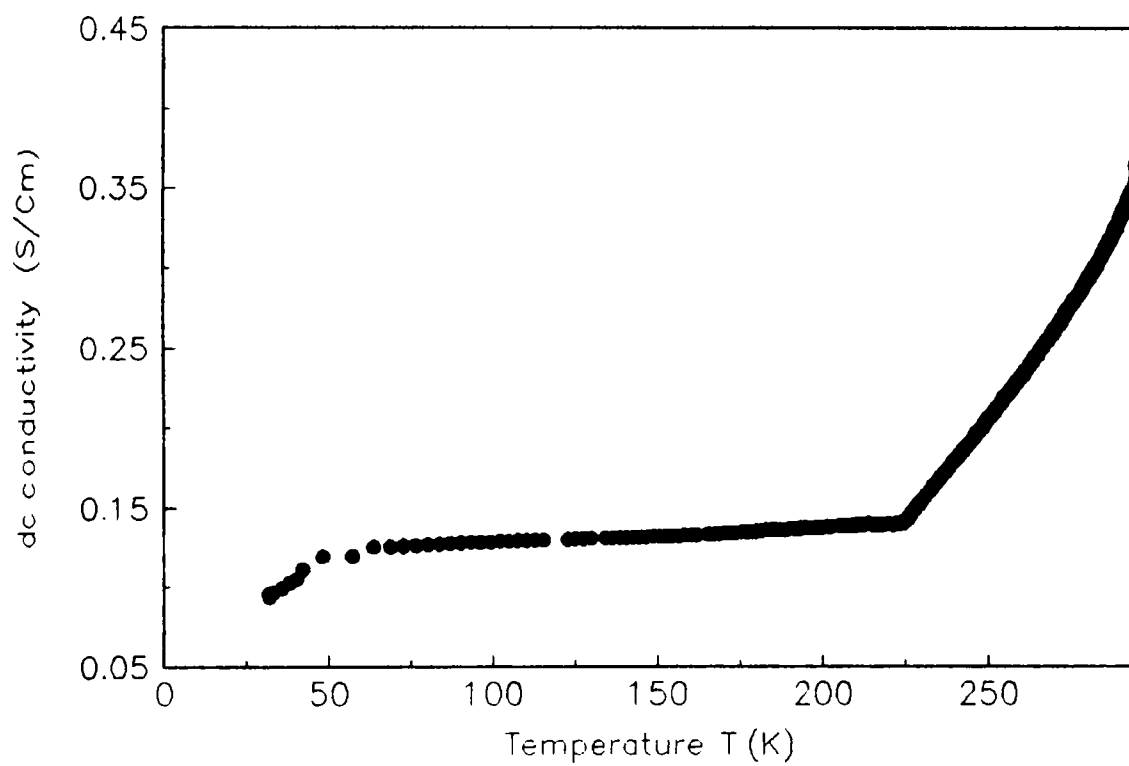


Figure 4.3e: Conductivity versus temperature plot for doped co polymer of anisidine and benzidine.

For semiconductors it is normally expected that the conductivity is thermally activated which means that the charge carriers are thermally excited to the conduction band, with the number density of carriers following a Boltzmann distribution and a linear dependence for log conductivity with $1/T$. The activation energy E_a is found to be T dependent. The activation energy is a monotonically increasing function of temperature and a decreasing function of doping concentration. The decrease in activation energy at low temperature suggest that the charge carriers are able to move around with lesser energy cost at low temperature implying that Mott's variable range hopping may play an important role. Figure 4.4a to 4.4e show the log conductivity versus $1/T$ plot of all the polymers and co polymers we have studied. It is easy to note that there is no linear dependence in any of these cases. So it is clear that the conduction mechanism is very much different from that of one dimensional hopping.

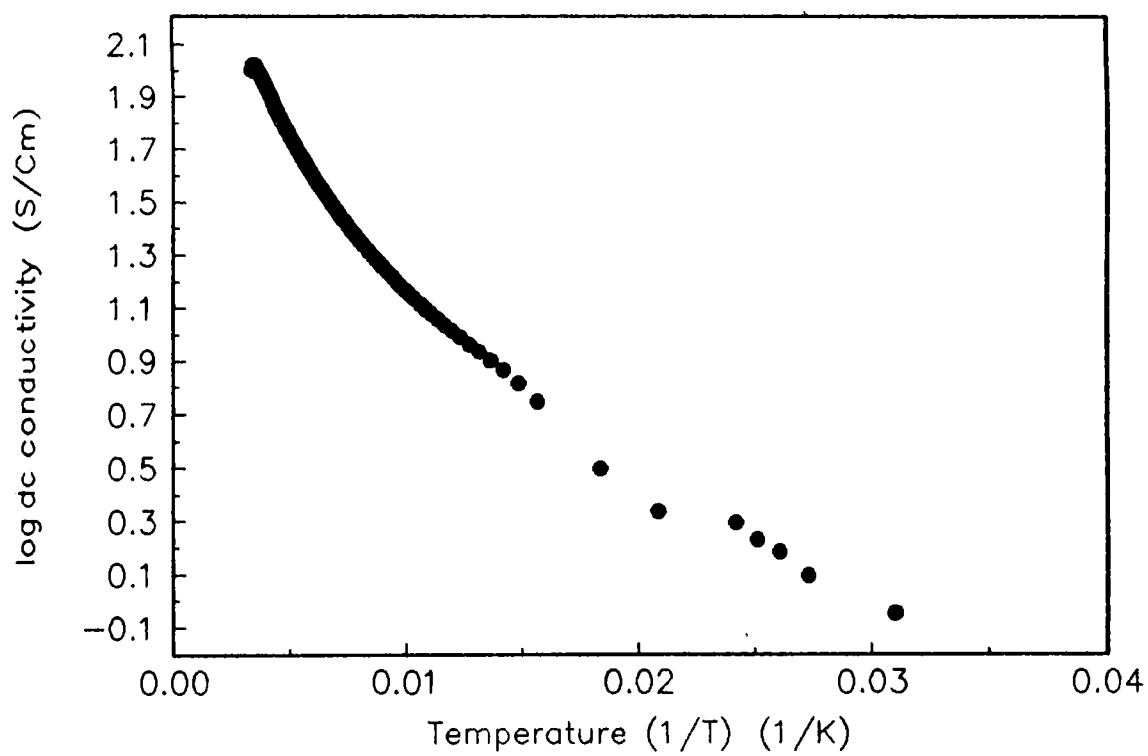


Figure 4.4a: Log conductivity versus 1/T plot for doped polyaniline.

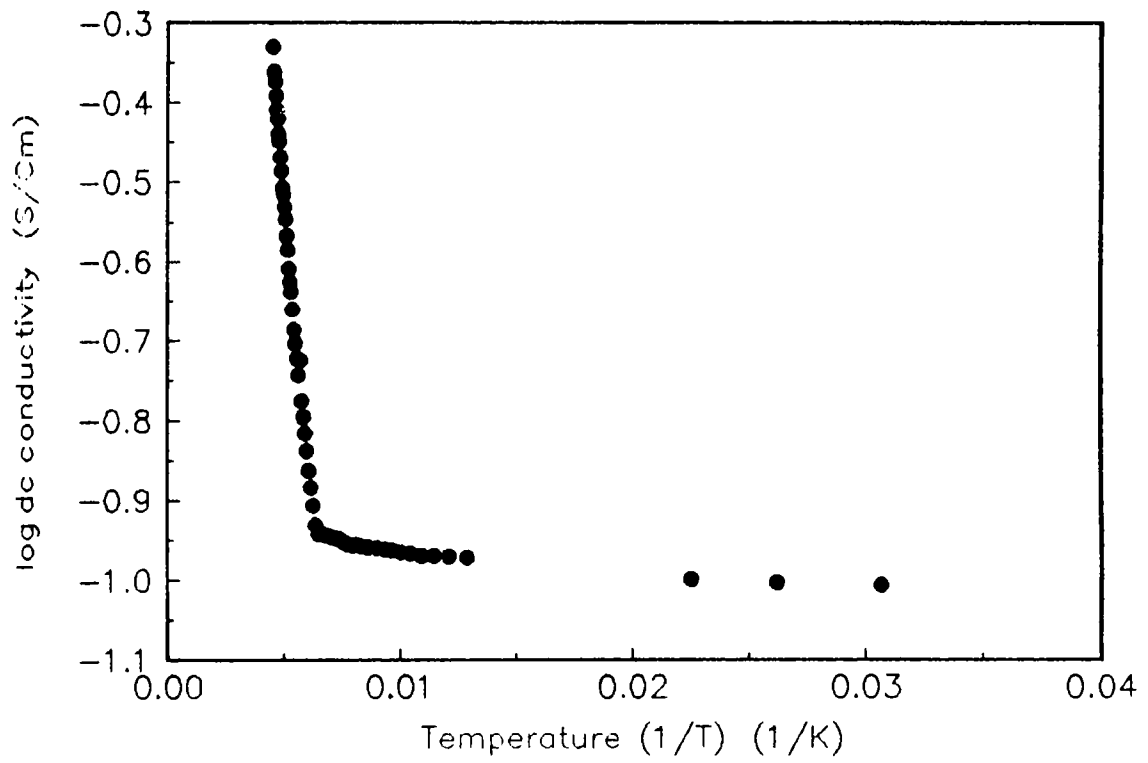


Figure 4.4b: Log conductivity versus 1/T plot for doped polyanisidine.

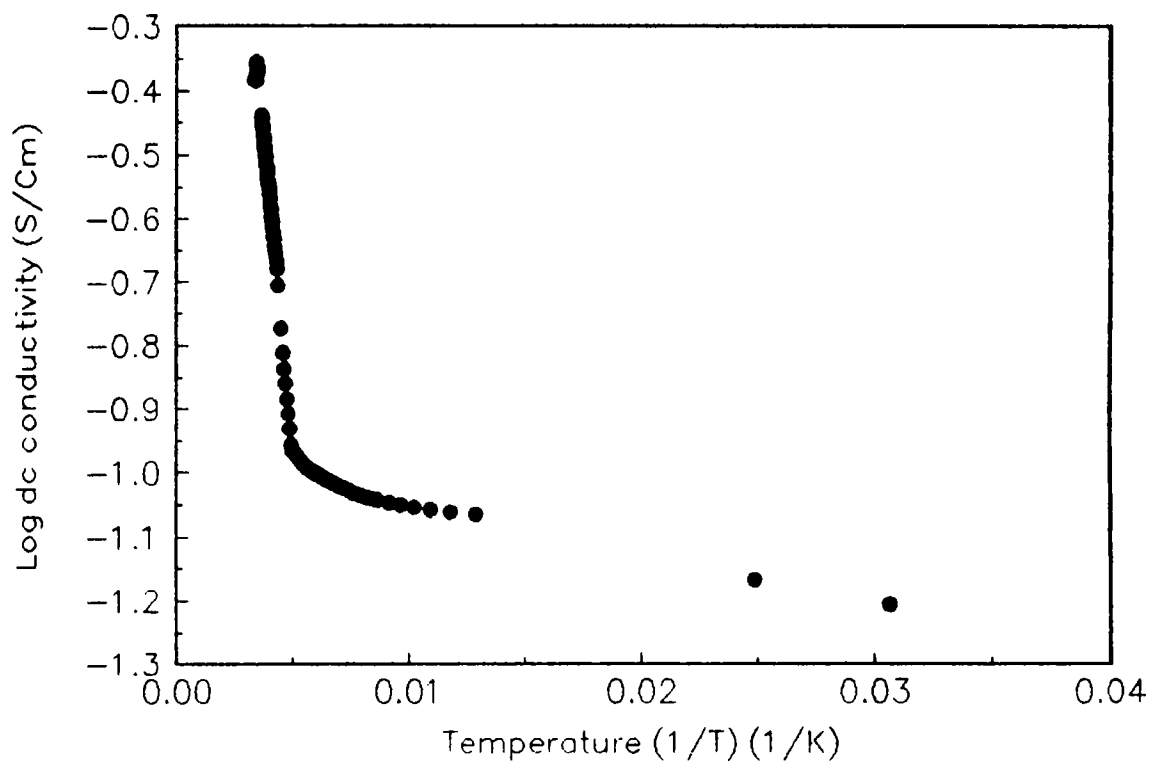


Figure 4.4c: Log conductivity versus 1/T plot for doped copolymer of aniline and anisidine.

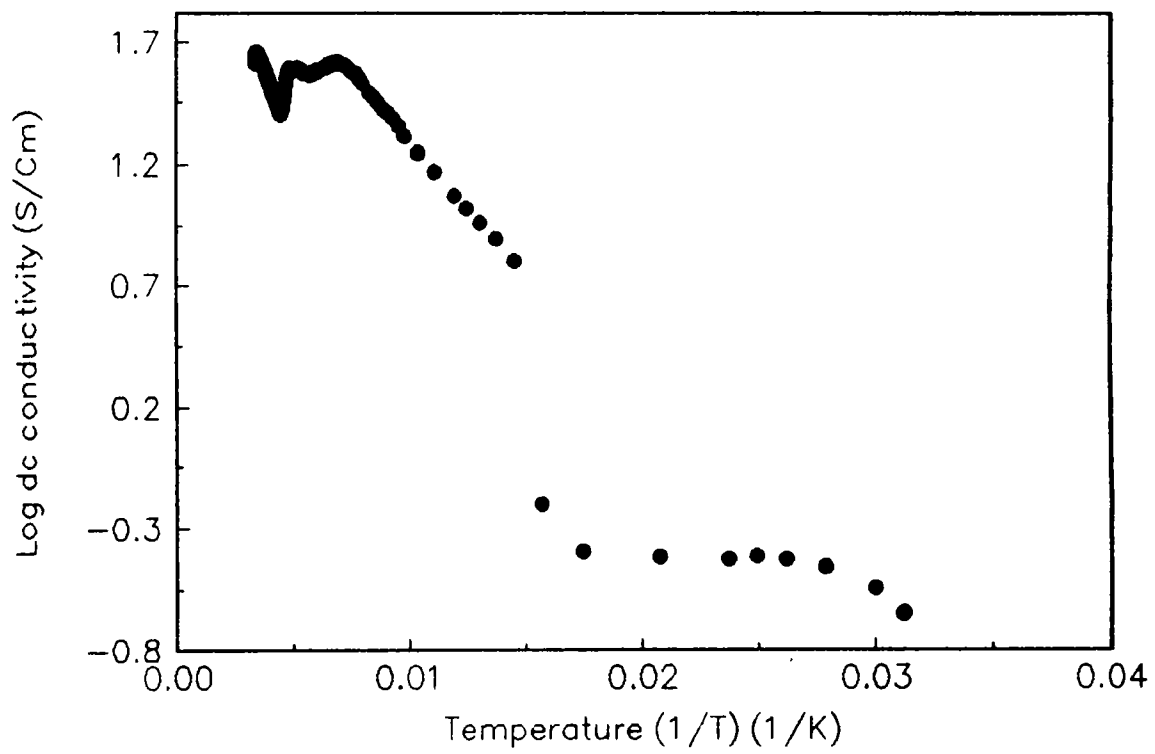


Figure 4.4d: Log conductivity versus 1/T plot for doped co polymer of aniline and benzidine.

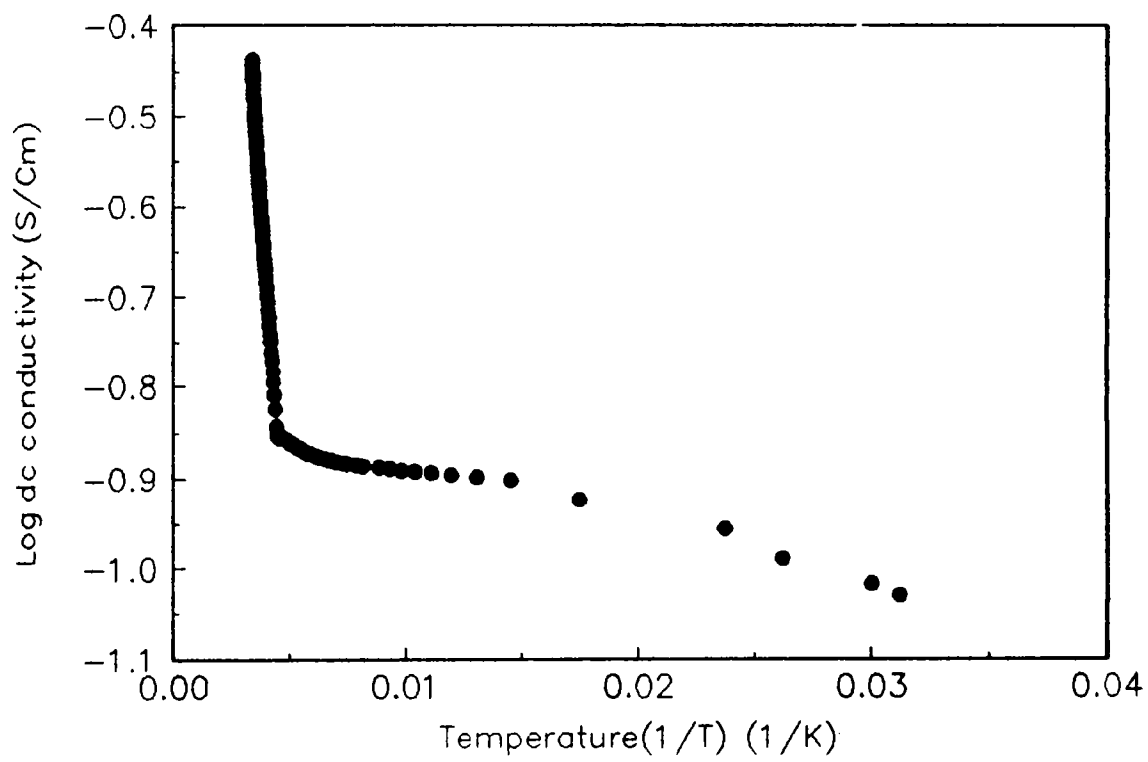


Figure 4.4e: Log conductivity versus 1/T plot for doped co polymer of anisidine and benzidine.

Figures 4.5a to 4.5e show the log conductivity versus $T^{-1/2}$ plot for all the polymers and copolymers we have studied. In these cases if the conduction is via variable range hopping one would expect to see a straight line fit. Figure 4.5 shows the plot of $\log \sigma$ as a function of $T^{-1/2}$. The data fits a straight line for the whole temperature range in the case of polyaniline. There are three possible models associated with this temperature dependence. First, it can be due to a one dimensional variable range hopping, but it can be excluded out since the material is heavily doped. The second possibility is that the system could be in a Fermi glass state. Assuming an electron-electron Coulomb interaction, one expects to see a decrease in the density of states around the Fermi level. However, the magnetic susceptibility measurements showed that there are no signature for the density of states at high doping level as having any anomalous decrease. The only possible model left is the charging energy limited tunneling between conducting segments proposed by Sheng et. al. [42]. According to this model, we write the conductivity as

$$\sigma = \sigma_0 \exp(-T_0/T)^{1/2}$$

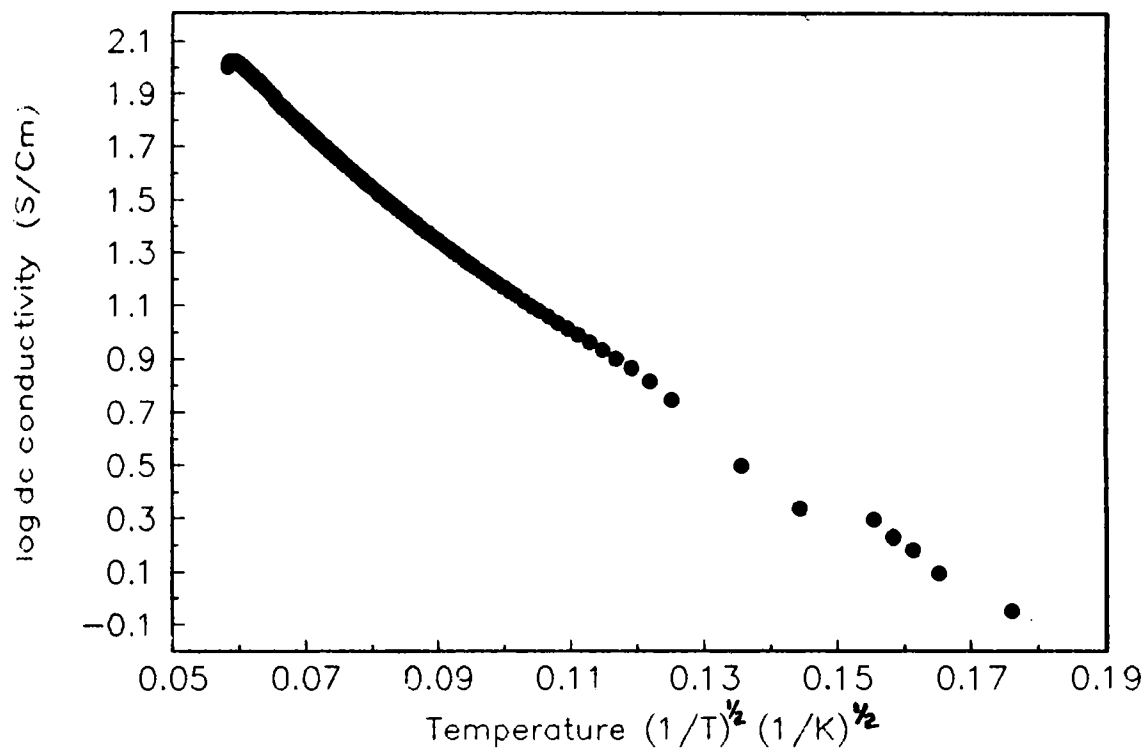


Figure 4.5a: Log conductivity versus $(1/T)^{1/2}$ plot for doped polyaniline.

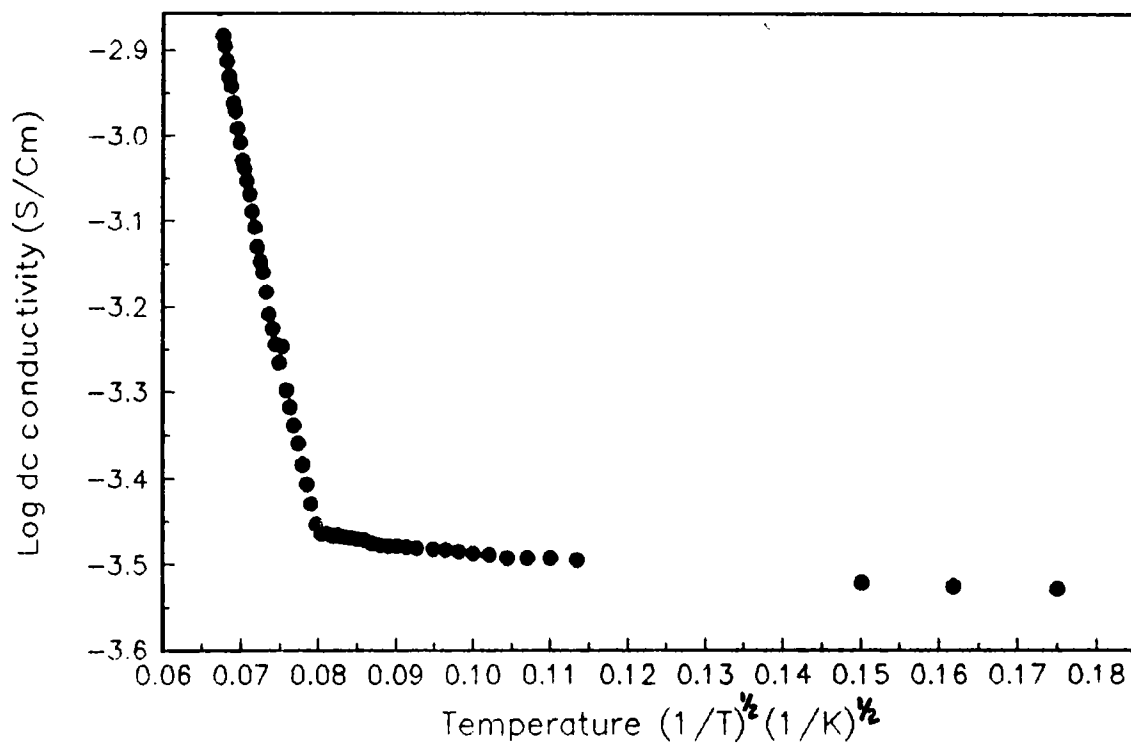


Figure 4.5b: Log conductivity versus $(1/T)^{1/2}$ plot for doped polyanisidine.

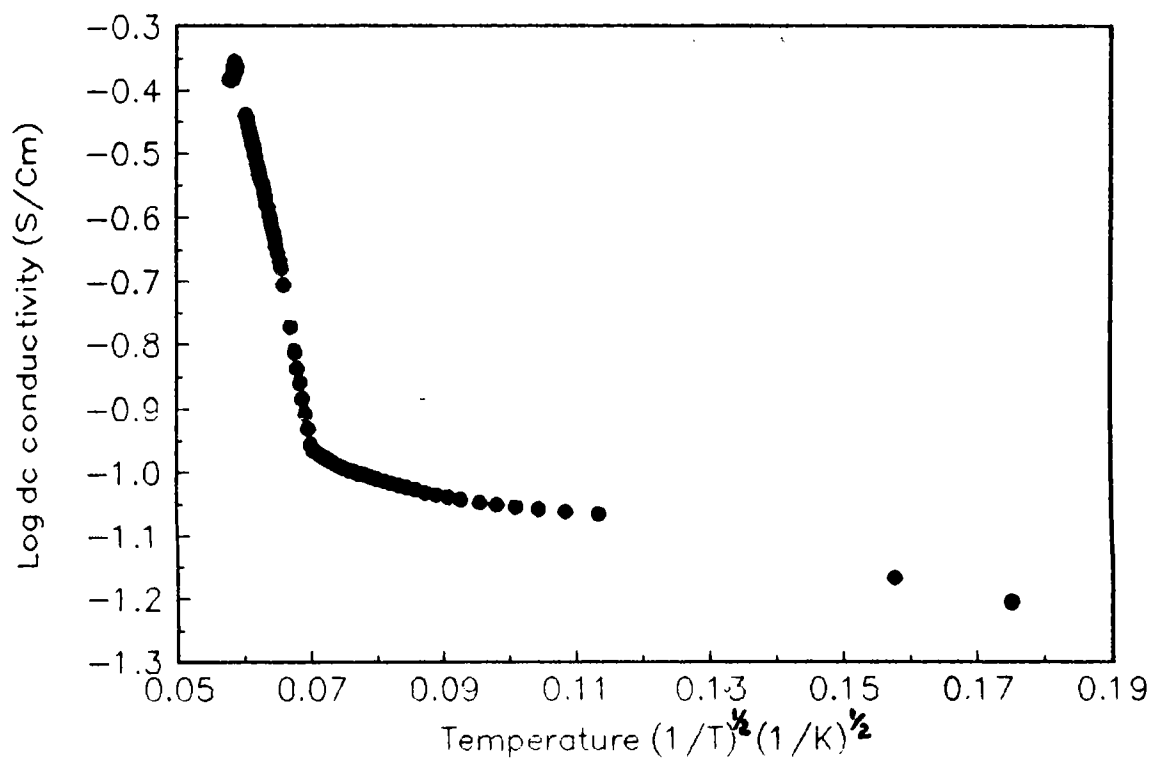


Figure 4.5c: Log conductivity versus $(1/T)^{1/2}$ plot for doped co polymer of aniline and anisidine.

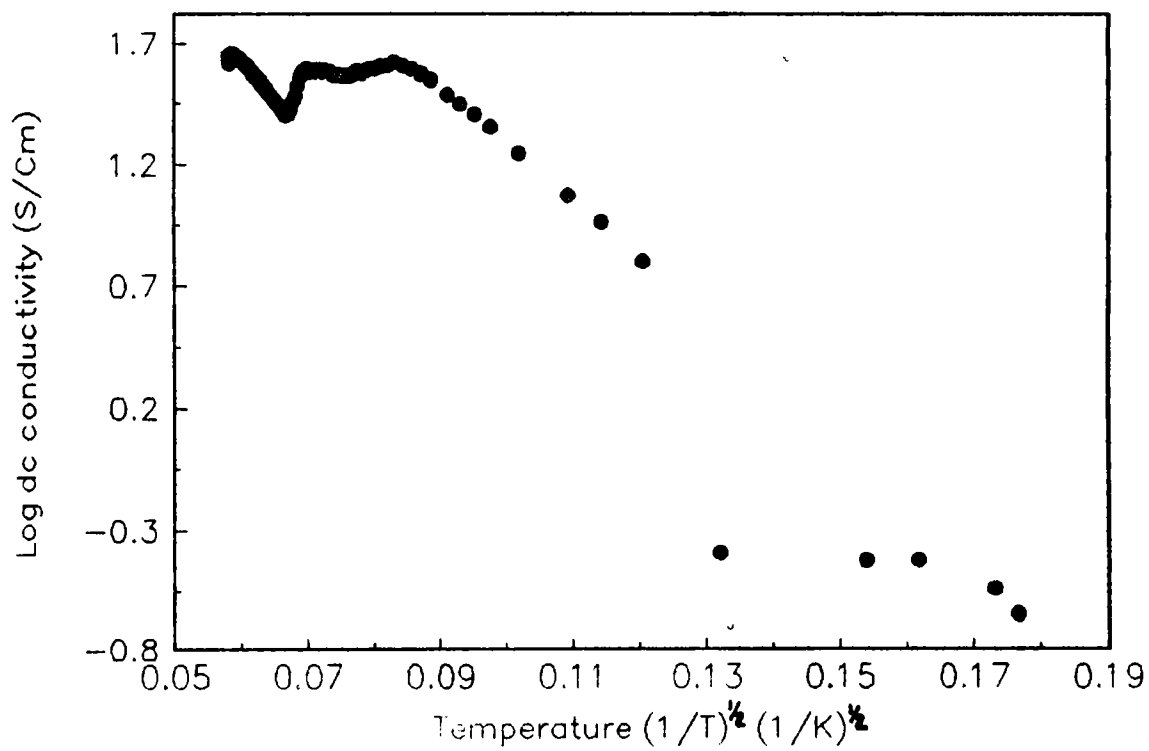


Figure 4.5d: Log conductivity versus $(1/T)^{1/2}$ plot for doped co polymer of aniline and benzidine.

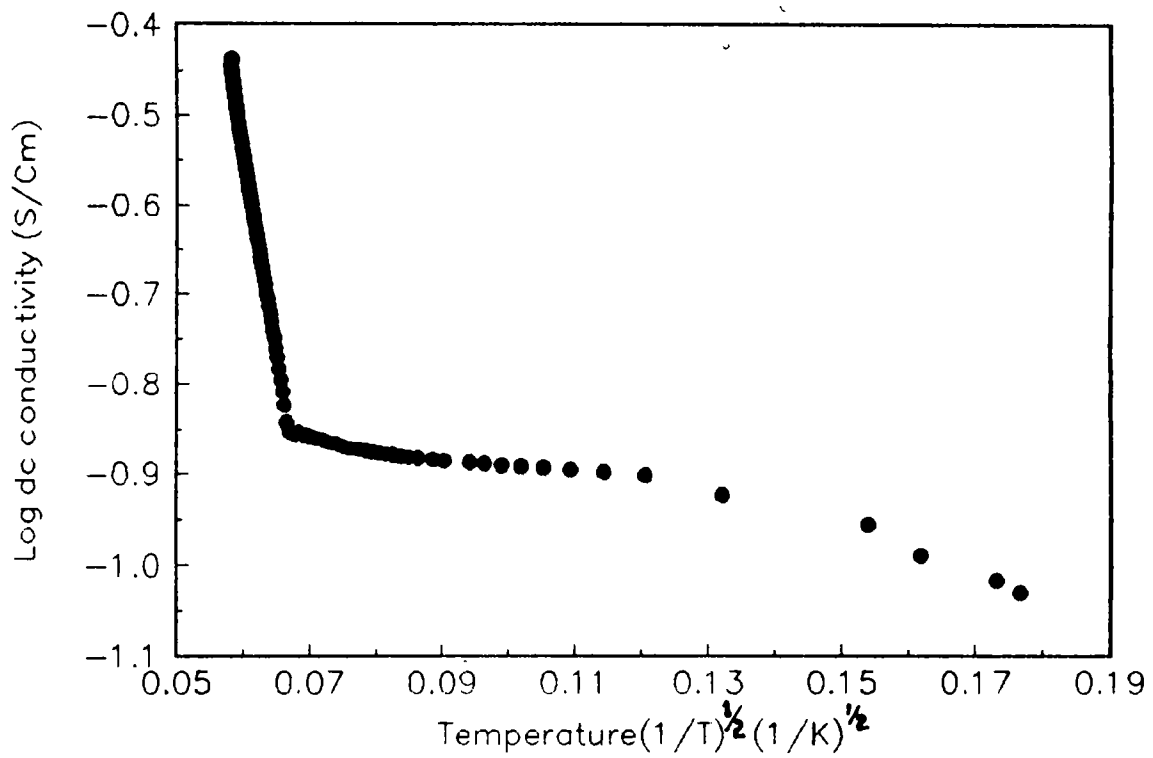


Figure 4.5e: Log conductivity versus $(1/T)^{1/2}$ plot for doped co polymer of anisidine and benzidine.

As discussed above the experimental data fits neither simple activation energy behaviour nor the one dimensional variable range hopping model with constant density of states at the Fermi level for all samples . The Sheng model seems to be the best fit for polyaniline. However the same is not applicable for the other samples. From the different plots we have come to the conclusion that all the three mechanisms discussed above are operating together in these samples.

4. 6 AC CONDUCTIVITY

Low frequency conductivity and dielectric relaxation measurements in the frequency range of up to 10^5 Hz have been found to be valuable in providing information on transport mechanism. These measurements provide additional information not provided by DC measurements. It is a major tool for the study of ionic conduction in glasses, ceramics, and polymeric materials. The pioneering work by Pollak and Geballe [43] on the low frequency hopping conductivity in n-type Si has provided valuable information for the understanding of hopping mechanisms of doped semiconductors in the semiconducting regime. We will review briefly in this section some of commonly used models.

From simple Drude model, the conductivity is related with mean relaxation time τ by [44]

$$\sigma(\omega) = [ne^2\tau/m] \cdot [1/1-i\omega\tau] \quad (4.32)$$

For highly conducting materials, the mean free path is much larger than the wave length of the AC signal, and the AC effect cancels out in the measurement. It is only for low conductivity materials, which have short mean free path, that hopping between localised states become important. It is easy to see from Drude's equations that if $\omega\tau \ll 1$, the conductivity is frequency dependent and the measured conductivity is bulk conductivity. If $\omega\tau \gg 1$, relaxations responsible for dc conductivity are negligible in ac measurements. What is measured is the contribution from localised states which has time scale of the relaxation process comparable to the applied frequency.

Consider a system with N dipoles per unit volume with dipole moment D per dipole. According to Debye's model, by thermally averaging the orientation with any dipole-dipole interaction one can get

$$\epsilon(\omega) - \epsilon_\alpha = (\epsilon_0 - \epsilon_\alpha) / (1 + \omega^2 \tau^2) = [4\pi D^2 N / 3k_B T] [1 / (1 + \omega^2 \tau^2)] \quad (4.33)$$

and the ac conductivity can be expressed as

$$\sigma(\omega) = \omega \epsilon_2(\omega) = [4\pi D^2 N / 3k_B T] [\omega^2 \tau / (1 + \omega^2 \tau^2)] \quad (4.34)$$

It should be mentioned that experimentally much more complex frequency dependence than single Debye type relaxation has been observed for different dielectric materials such as the empirical ones by Cole-Cole, Davidson-Cole, Havriliak-Neegami etc. [45].

4. 6a. ROLE OF VRH ON AC CONDUCTIVITY

The key concept in hopping conduction between localised states is that the relaxation rate is given by

$$1/\tau = \nu_{ph} \exp(-2\alpha R - \Delta W / k_B T) \quad (4.35)$$

The number of electrons taking part in the hopping is $N(E_F)k_B T$ per unit volume. Supposing that only hops of energy $\sim k_B T$ make important contributions, then $\exp(-\Delta W / k_B T)$

is of order unity. The number of vacant states into which an electron can jump is then $(NE_F)k_B T$. The important hops are those with $\omega\tau \approx 1$, where ω is the frequency of applied field, that is those for which the hopping distance is R , where

$$2\alpha R = \ln (\nu_{ph}/\omega) \quad (4.36)$$

This gives

$$\sigma(\omega) = A (e^2 / \alpha^5) N (E_F)^2 k_B T \omega [\ln (\nu_{ph} / \omega)]^4 \quad (4.37)$$

where $A = \pi^4/96$ [10].

A strong temperature dependence of AC conductivity can arise from thermal activation of charge carriers from the widely separated localised states in the band gap to the dense localised states in the valence or conduction band types. The temperature dependence of AC conductivity can be expressed as

$$\sigma(\omega) \approx f^\alpha T \exp (- E_a' / k_B T) \quad (4.38)$$

with $E_a' < E_a$. Here E_a is the activation energy of the extended states [33].

Hopping conduction of polarons also lead to strong T dependence for the AC conductivity. For weak coupling of charge to the lattice (large polaron), hops between states of large radius are involved. The hops involve the absorption and emission of minimum number of phonons requires for energy conservation. If the coupling is strong (small polaron), multiphonon processes dominate. The mobility ultimately becomes simply activated when the temperature exceeds the temperature characteristic of highest energy phonons with which the electronic states interact appreciably.

4. 7 EXPERIMENTAL TECHNIQUE FOR AC CONDUCTIVITY

It has been discussed earlier that at high doping level, a polaron band is formed due to an internal redox process, forming a granular polymeric metal. In the high doping region the, charge conduction obeys variable range hopping as it follows from temperature dependence of DC conductivity. In the emeraldine system the possible charge carriers are polarons and bipolarons. In order to further identify the hopping motions of these charged species, it is necessary to know the behaviour of the system with

applied alternating current in the audio frequency range as has been proved critical in the lightly doped polyacetylene case where Kivelson's intersoliton hopping model has been proposed. In this section we discuss the experimental results on AC conductivity on the highly protonated polyaromatic amine samples on which DC conductivity have been measured.

In the present study polyaniline, polyanisidine and co polymers of aniline and anisidine, co polymers of aniline and benzidine, anisidine and benzidine are employed for the measurements. All the polymers have been prepared under the same condition and doped with 1 M HCL.

Each of the samples is made in to a disk by pelletising, the diameter and thickness of which are 10 and 2 mm respectively. Both sides of the disk are coated with silver in order to ensure ohmic contact and the sample is fixed between the two terminal electrodes. The surroundings of the samples are electrostatically screened by an exterior brass cylinder. The container is then evacuated for an hour down to 5×10^{-4} Torr in order to remove the oxygen in the sample.

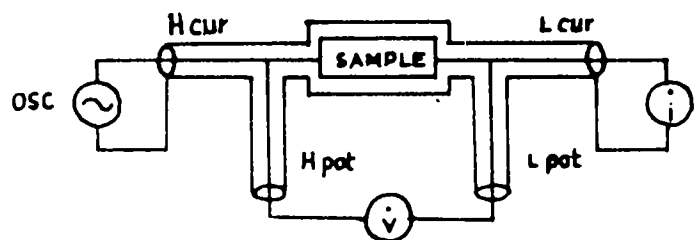
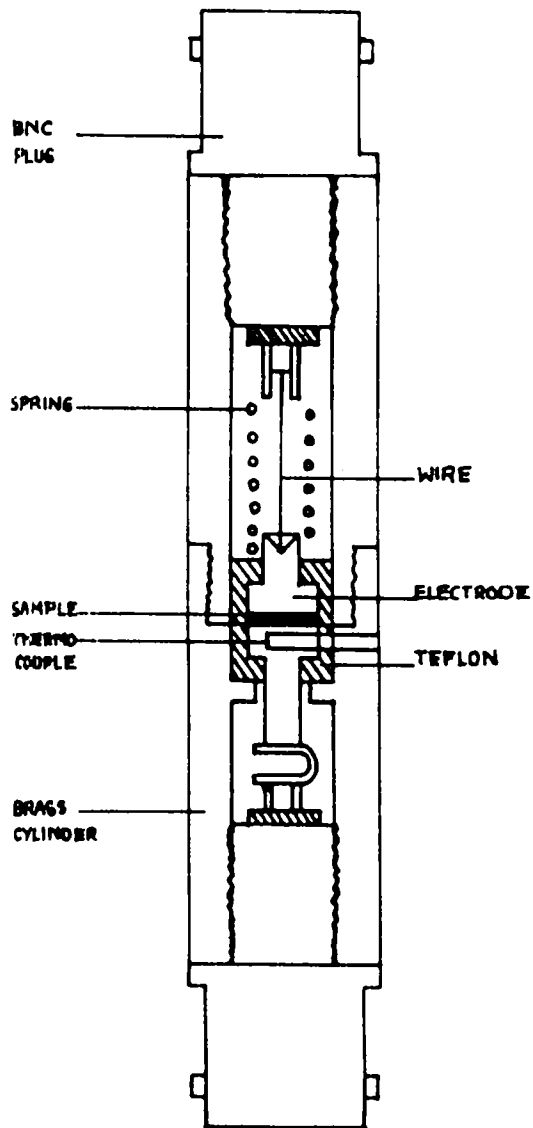


Figure 4.8: Experimental setup for ac conductivity measurements.

AC conductivity is obtained by the measurement of admittance by an impedance analyser. The four-probe construction shown in the Figure 4.6 was setup in order to remove the floating capacitance and or residual inductance of coaxial wire. The sinusoidal signal, the amplitude and frequency range of which are 10 V cm^{-1} and $10^3 - 10^7 \text{ Hz}$ respectively is imposed on the sample. Frequency is swept logarithmically where eight points per decade were sampled. The maximum error inherent in the observed conductivity is estimated to be 4%. The range of temperature applied for the measurement was from 80 to 300K and the measuring points are set approximately every 30K interval. Temperature is kept within $\pm 0.5\text{K}$ during the time of a frequency sweep series.

Different curves show the data taken at different temperatures, the highest temperature used in this work being 300K. With liquid nitrogen, the sample can be cooled to 77K. Data are taken at temperature intervals of the order of 30 degrees. All samples have been pumped for at least two to three hours before taking data to eliminate possible moisture influence on measurements.

4. 8 RESULTS AND DISCUSSION

Figures 4.7a to 4.7e show the experimental results on AC conductivity measurements on polyaniline, polyanisidine and their co polymers. The measurements have been done at different temperatures and frequencies as illustrated in the figures. The plots give AC conductivity as a function of frequency at different temperatures.

Our results show that the AC conductivity is almost independent of frequency at lower frequencies. The conductivity increases at higher frequencies. The rate at which conductivity increases at higher frequencies depend upon temperature. This behaviour is exhibited by all the conducting polymers we have investigated. It can also be noticed that in the case of polyanisidine, and co polymer of aniline with anisidine, the conductivity increases at very high frequencies indicating a threshold maximum in conductivity at a moderately high frequency. It is interesting to that the frequency which this threshold maximum occurs is independent of temperature. In the case of polyanisidine, the conductivity is independent of frequency at low temperatures. There is no increase in

at which conductivity increases at higher temperatures increase with temperature. The same behaviour is exhibited by the co polymer of aniline and anisidine, aniline and benzidine, and anisidine and benzidine. In the following paragraphs we give a qualitative interpretation for the experimental findings shown in Figures 4.7a to 4.7e.

When carriers are excited across the mobility edge in to the range of extended states in the samples, just as in a disordered semiconductor, the conductivity is independent of frequency. Here conductivity σ is proportional to the product of the density of excited state carriers and the temperature dependent mobility of the excited charge carriers. However, when carriers are not in extended states as in a disordered or inhomogeneous system, conductivity at higher frequency is generally larger than the DC conductivity. Physically, this is due to the presence of pairs of large clusters of anomalously close sites between which electrons can hop at a rate greater than that which characterizes the difficult hops necessary to traverse the sample for DC conductivity. Essentially our samples comprise a percolation network for which the above argument readily holds.. Such a marked frequency dependence of

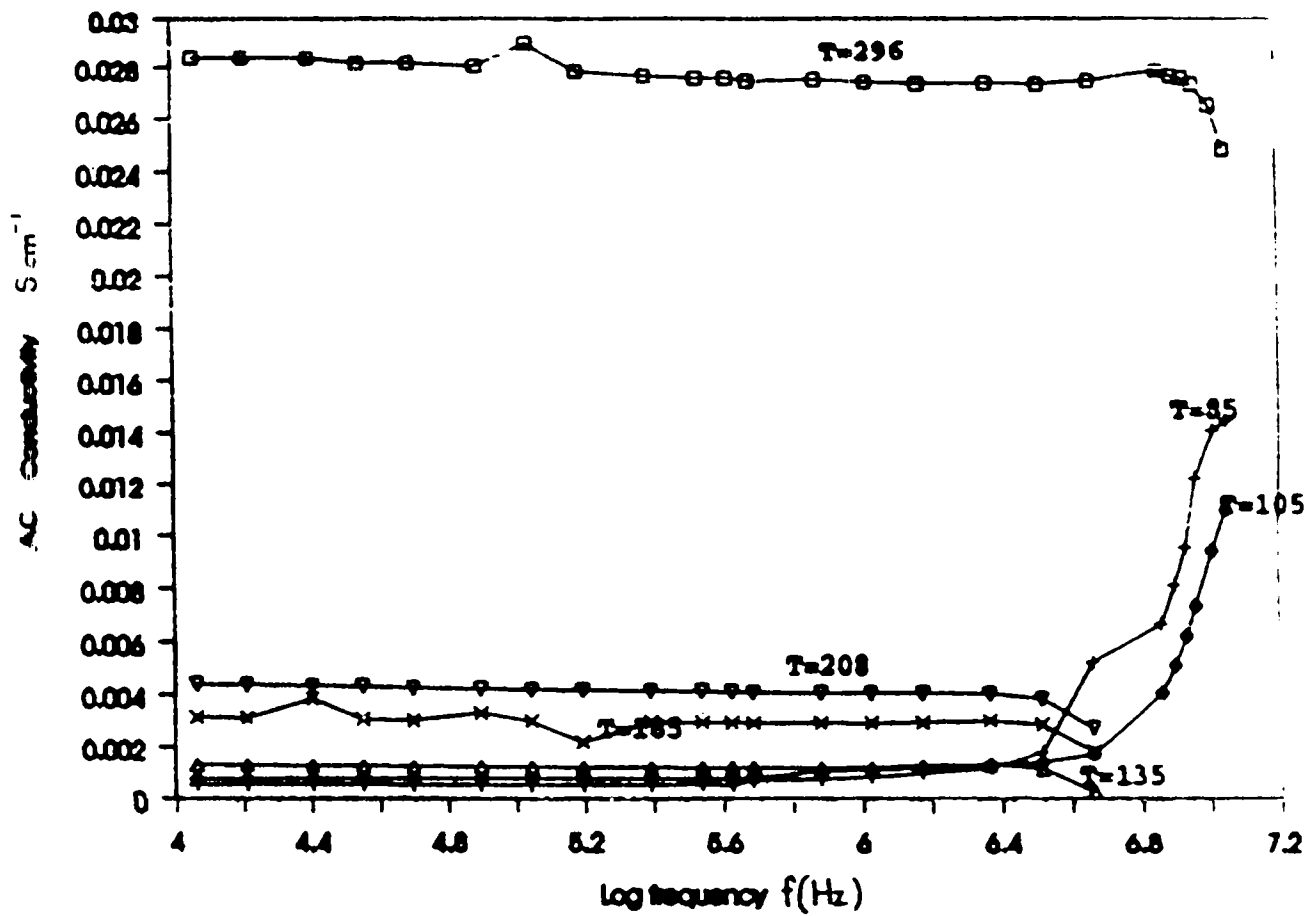


Figure 4.7a: Conductivity versus log frequency plot for doped polyaniline.

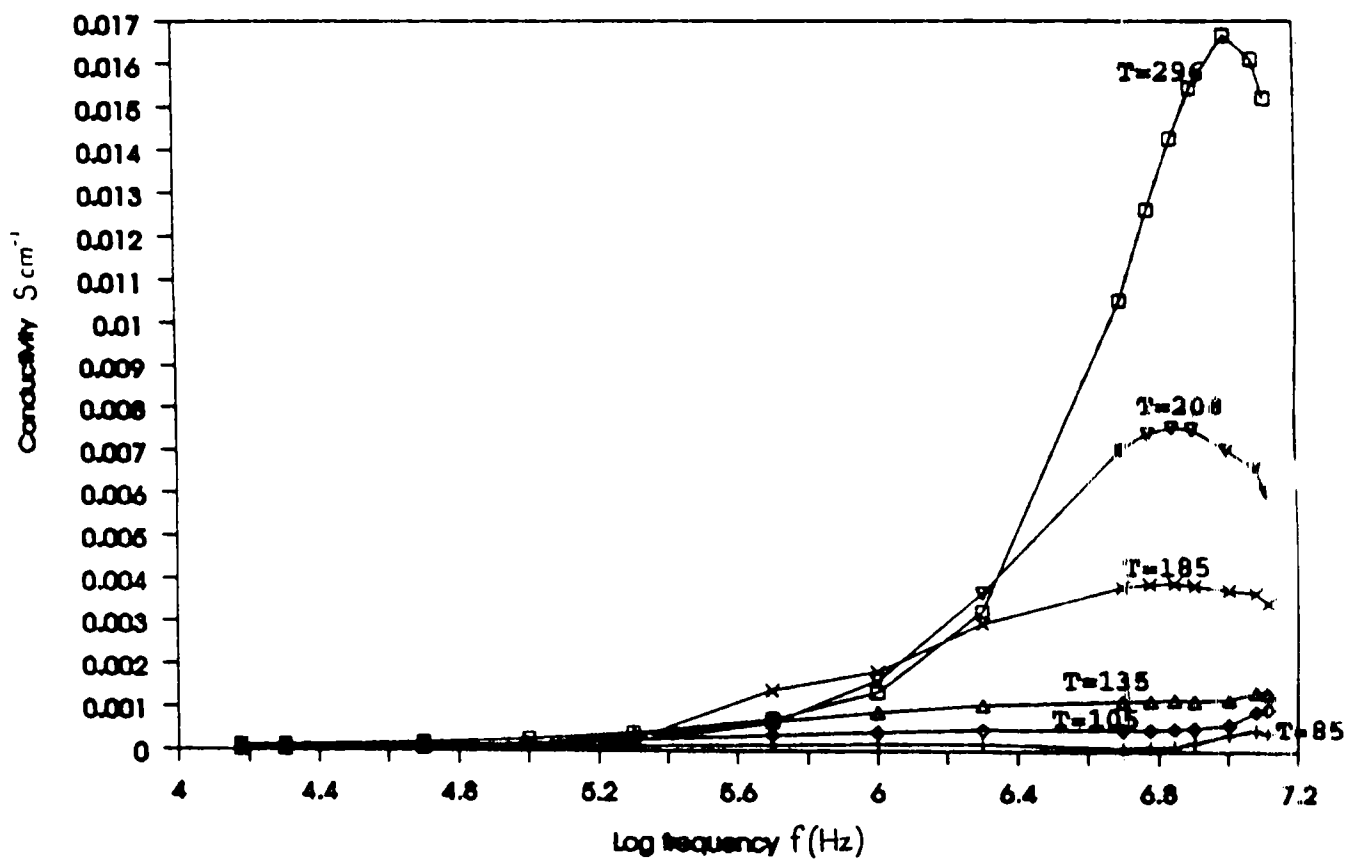


Figure 4.7b: Conductivity versus log frequency plot for doped polyanisidine.

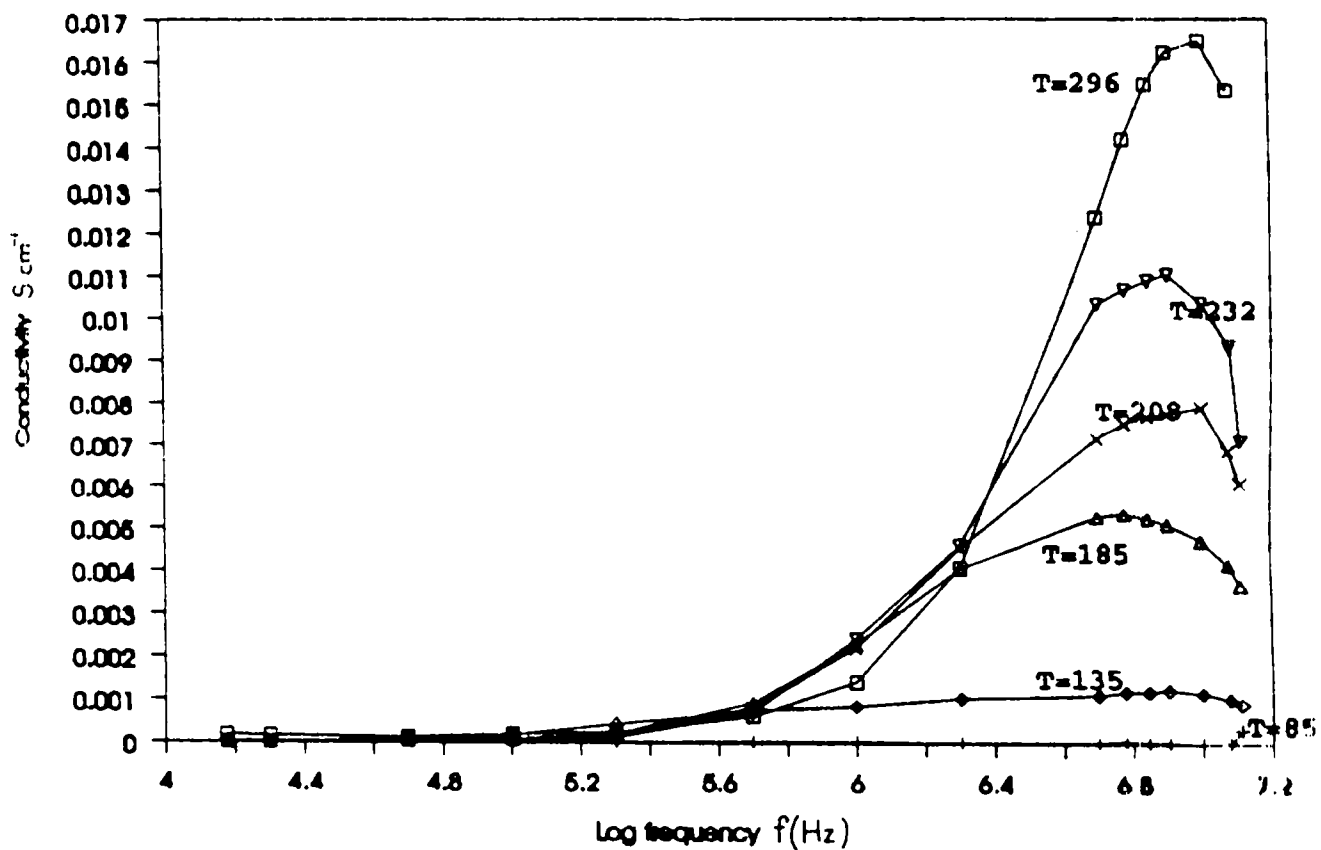


Figure 4.7c: Conductivity versus log frequency plot for doped co polymer of aniline and anisidine.

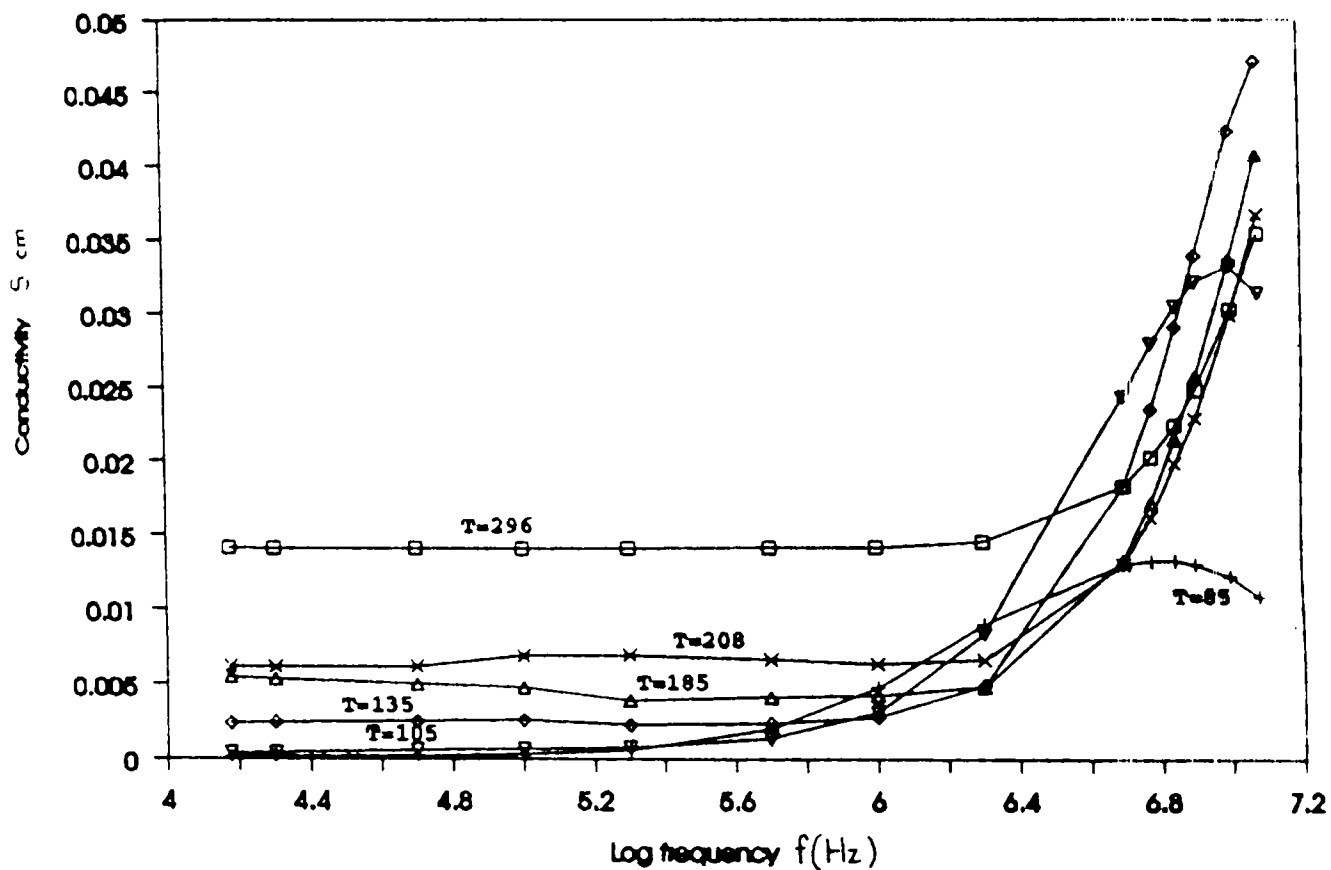


Figure 4.7d: Conductivity versus log frequency plot for doped co polymer of aniline and benzidine.

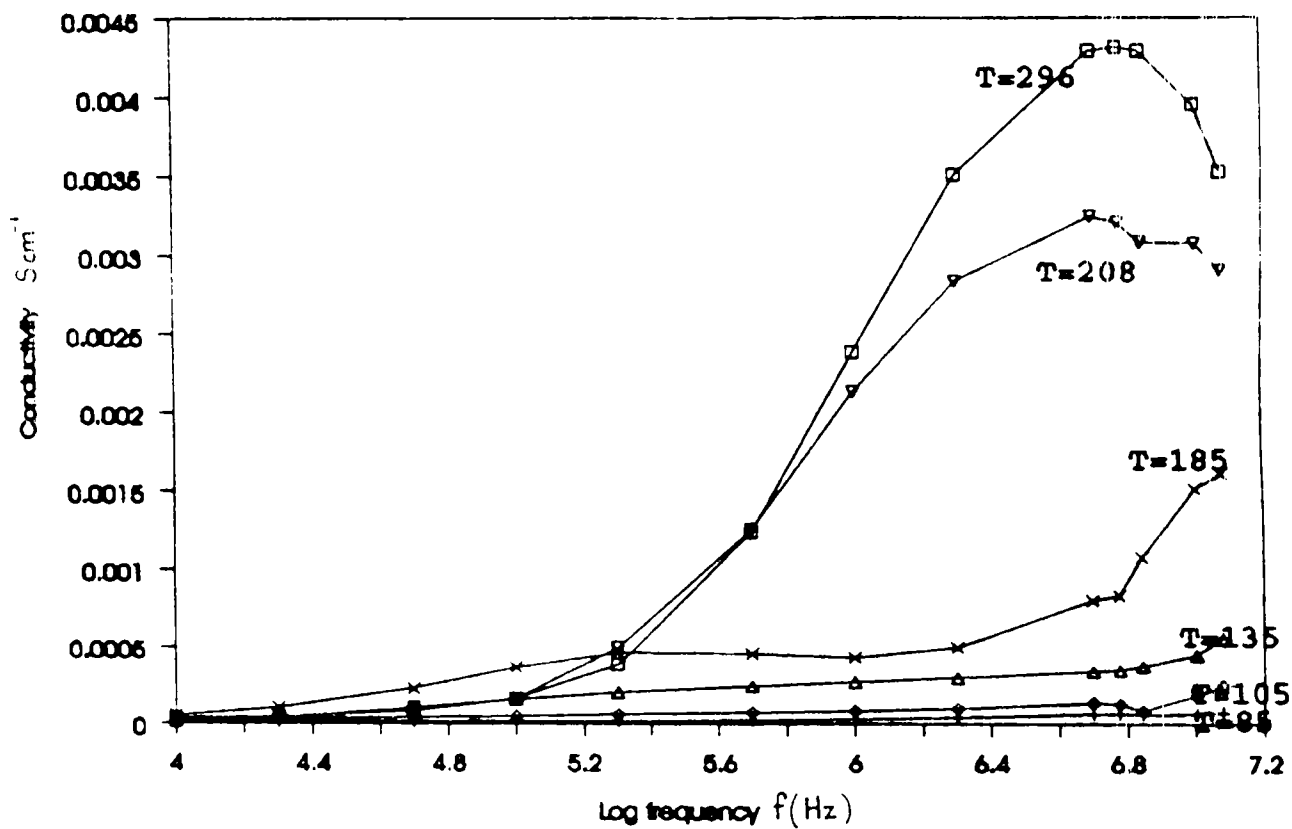


Figure 4.7e: Conductivity versus log frequency plot for doped co polymer of anisidine and benzidine.

the conductivity is common to a broad class of disordered semiconductors and insulators. Diverse physical mechanisms, including variable range hopping, presence of surface barriers, ionic dipoles, clusters of conductivity regions etc. can underlie this behaviour. This phenomenon can be understood better by calculating the DC conductivity using a percolation treatment while obtaining the frequency dependent contribution in the pair approximation. The interpolation formula

$$\sigma_{TOT} = \sigma_{DC}(T) + \sigma_{AC}(f,T)$$

can then be used to obtain the conductivity at finite frequency.

A strong temperature dependence for AC conductivity can arise from thermal activation of charge carriers from localized states in the gap to localised states in the valence or conduction band tails. The temperature dependence of σ_{DC} and σ_{AC} is determined largely by the number of charge carriers excited to the band tails.

Polaron hopping also lead to a strong temperature dependence for σ_{DC} and σ_{AC} . For weak coupling of the charge to the

lattice, hops between states of large radius are involved. The hops proceed with the absorption and emission of minimum number of phonons consistent with the requirements of energy conservation. If coupling to the lattice is strong, then multiphonon processes dominate . Ultimately the mobility becomes activated when the temperature exceeds the phonon temperature characteristic of the highest energy phonons with which electronic states interact appreciably. The strong temperature dependence of the hopping conductivity manifests itself in our AC Conductivity data.

REFERENCES

1. H. A. Pohl and E. H. Engelhardt,
J. Phys.Chem., 66 (1962) 2085.
2. V. P. Parini, Vysokomol. Soedin., 3 (1961) 1870.
3. V. I. Maleev, Vysokomol. Soedin., 4 (1962) 848.
4. M. Doriomedoff, F. H. Crisstofini, R. DeSurville, M. Josefowicz, L. T. Yu and R. Buvet,
J. Chim. Phys., 68 (1971) 1055.
5. L. T. Yu, J. Petit, M. Josefowicz, G. Belorgey and R. Buvet, C. R. Acad. Sci., Ser. C, 260 (1965) 5026.
6. L. T. Yu, M. S. Borredon, M. Josefowicz, G. Belorgey and R. Buvet, J. Polym. Sci., 10 (1987) 2931.
7. M. F. Combarel, G. Balorgey, M. Josefowicz L. T. Yu and R. Buvet C. R. Acad. Sci., Ser. C, 262 (1986) 459.
8. L. T. Yu, S. Borreton, M. Josefowicz and R. Buvet, Comm. Symp. Int. Chim. Macromol. IUPAC, Prague, 1965 A. 481.
9. M. Gohlamian and A. Q. Contractor, J. Electronal. Chem., 236 (1988) 126, 291.
10. J. P. Travers, J. Chroboczek, F. Devrex, F. Genoud, M. Nechtschein, A. A. Syed, E. M. Genies and C. Tsintavis, Mol. Cryst., Liq.Cryst. 131 (1985) 195.
11. A. G. MacDiarmid, J. C. Chiang, M. Halpern, W. S. Hung,

- S. L. Mu, N. L. D. Somasiri, W. Wu and S. I. Yaniger,
Mol. Cryst. Liq. Cryst., 121 (1985) 173.
12. A. G. MacDiarmid, N. L. D. Somasiri, W. R. Salaneck, I. Lundstrom, B. Liedberg, M. A. Hasan, R. Erlandsson, P. Konrasson, Springer Series in Solid State Sciences., Vol.63, Springer, Berlin, (1985)
 13. J. C. Chiang and A. G. Mac Diarmid,
Synth. Met., 13 (1988) 193.
 14. W. S. Huang, B. D. Humphrey and A. G. Mac Diarmid, J. Chem. Soc., Faraday Trans. 1,82 (1986) 2385.
 15. A. Brahma, Solid State Commun., 57 (1986) 673.
 16. A. Kitani, I. Izumi, J. Yano, Y. Hiromoto and K. Sasaki,
Bull. Chem. Soc. Jpn. 51 (1984) 2254.
 17. E. W. Paul, A. J. Ricco and M. S. Wrighton, J. Phys. Chem., 89 (1981) 1441.
 18. S. H. Glarum and J. H. Marshall, J. Electrochem. Soc., 134 (1987) 142.
 19. H. Shirakawa, E. J. Louis, A. G. Mac Diarmid, C. K. Chang, and A. J. Heeger,
J. Chem. Soc. Chem. Commun., (1977) 578.
 20. M. J. Rice, Phys. Rev. Lett. 71A (1979) 152.
 21. W. P. Su, J. R. Schrieffer, and A. J. Heeger,
Phys. Rev. Lett., 42 (1979) 1698.
 22. S. A. Brozovskii and N. N. Korova, Zh. Eksp. Teor.

- Fiz. Pisma Red. 33 (1981) 6
23. D. K. Campbell and A. R. Bishop,
Phys. Rev. B. 24 (1981) 4859.
 24. Y. Onodera, Phys. Rev. B 30 (1984) 775.
 25. A. G. Mac Diarmid, J. C. Chiang, A. F. Richter, and
A. J. Epstein, Synth. Met. 18 (1987) 285.
 26. J. P. Travers, J. Chroboczek, F. Devrex, F. Genoud, M.
Nechtschein, A. A. Syed, E. M. Genies and C. Tsintavis,
Mol. Cryst. Liq. Cryst., 131 (1985) 195.
 27. A. J. Epstein, J. M. Ginde, F. Zuo, R. Bigelow,
H. S. Woo, D. B. Tanner, A. F. Richter, W. S. Huang,
and A. G. Mac Diarmid, Synth. Met., 18 (1987) 303.
 28. J. M. Ginder, A. F. Richter, A. G. Mac Diarmid. and
A. J. Epstein, Solid State Commun., 63 (1987) 97.
 29. S. Stafstrom, J. L. Bredas, A. J. Epstein, H. S. Woo,
D. B. Tanner, W. S. Huang and A. G. MacDiarmid.,
Phys. Rev. Lett., 59 (1987) 1464.
 30. F. Zuo, M. Angelopoulos, A. G. Mac Diarmid and
A. J. Epstein, Phys. Rev. B. 36 (1987) 3475.
 31. F. Zuo, M. Angelopoulos, A. G. MacDiarmid and
A. J. Epstein, Phy. Rev. B. 36 (1987) 3475.
 32. N. F. Mott and E. A. Davis, "Electronic Processes in Non
Crystalline Materials" Clarendon, Oxford, (1979).
 33. P. Nagels, Top. Appl. Phys. 36 (1979) 114.

34. N. F. Mott and M. Kaveh, *Advances in Phys.* 30 (1986) 330.
35. D. Emin and K. L. Ngai, *J. Phys. Paris.* 44, (1983) C3-517.
36. A. R. Bishop, D. K. Campbell and K. F. Fesser, *Phys. Rev. B.* 26 (1982) 6862.
37. D. Emin, *Phys. Rev. B.* 33 (1986) 3973.
38. S. Kivelson, *Phys. Rev. B.* 25 (1982) 3798.
39. S. Kivelson and A. J. Epstein, *Phys Rev. B* 29, (1984) 3336.
40. M. H. Cohen and J. Jortner, *Phys. Rev. Lett.*, 15 (1973) 699.
41. B. Abeles, P. Sheng, M. D. Coutts and Y. Arie, *Adv. in Phys.* 24 (1975) 407.
42. P. Sheng, E. K. Sichel, and J. I. Gittleman, *Phys. Rev. Lett.*, (1978) 1197.
43. M. Pollak and T. H. Geballe, *Phys. Rev.*, 122 (1961) 1745
44. N. W. Ashcroft and N. D. Mermin *Solid State Physics* Saunder College (1976)
45. R. M. Hill and A. K. Jonscher, *Contemp. Phys.*, 24 (1983) 75.

CHAPTER 5

ELECTRICAL TRANSPORT PROPERTIES OF POLYAROMATIC AMINES - II. THERMO ELECTRIC POWER

5. 1 INTRODUCTION

With the fibrous morphology, a conducting polymer is not a continuous material and its dc conductivity is expected to be limited by interfibrillar connections. Under such circumstances the intrinsic metallic conductivity may be considerably higher than the measured bulk dc conductivity values. This difficulty is not present in thermoelectric power measurement, because there is no flow of current. The interfibrillar connections should play a minimal role allowing an evaluation of the intrinsic transport properties of the material.

The real morphology of conducting polymers is very complicated. The finite chain length, interchain crosslinkings, interfibrillar contact resistances, the sp^3 defects within a conjugated polymer chain etc. make carrier transport very complicated. Moreover, in doped polymers

there exist Coulomb potential of the doping ions and lattice vibrations (phonons) in the system giving rise to static and dynamic disorders. Because of the complex morphology, the conduction mechanism in highly conductive polymers is not yet well understood. Thermoelectric power (TEP) is basically a zero current transport coefficient. It measures the voltage drop across the sample due to the thermal gradient rather than the electrical current. Therefore, it is insensitive to complex morphological interruptions of the polymer chain and it can give a measure of intrinsic properties of conducting polymers.

There have been a large number of studies on the temperature dependence of the TEP of conducting polymers. Most of the work has been concentrated around polyaniline. A short review on the relation between structure and morphology of conducting polymers to their thermopower properties has been published by Park [1]. The TEP of As- doped polyacetylene was first reported by Park et al. [2,3] and a value of the order of $+900\mu\text{V/K}$ was reported. Later, several workers have obtained values of the order of $+1500\mu\text{V/K}$. Mases et al. [4] obtained TEP of trans-polyacetylene doped electrochemically with tetrabutylammonium which was n-type material.

The TEP of a number of conducting polymers have been reported. Park et al. [5] measured the TEP of FeCl_3 -doped polyacetylene and compared these results with those obtained on iodine and AsF_5 -doped polyacetylene in the heavily doped regime. Metal like behaviour has been reported by these authors. The temperature dependence of TEP of metallic polyaniline salts has been reported by Park et al [6]. These authors have reported that as the degree of protonation increases, the sign of TEP changes from positive to negative. Zuo et al [7] have measured the temperature dependence of TEP of polyaniline polymer as a function of protonation level. The TEP is found to change sign with protonation level and is found to be proportional to T. Conclusions regarding electron localization in methyl-ring substituted derivative of polyaniline viz poly-o-toluidine have been reached by Wang et al. [8,9] from TEP measurements. The temperature dependence of the TEP of the emeraldine salt form of polyaniline protonated with camphor sulfonic acid (PANI-CSA) has been measured [10] and TEP is found to increase linearly with temperature. The results have been discussed in the context of transport at the metal - insulator boundary.

We have measured the temperature dependence of TEP on the

conducting polymers which we have chosen for our investigations. The significance of TEP measurements, experimental technique used by us for our measurements and the results obtained are described in the following sections. A discussion of the results in terms of disorder and electron localization in those samples is given subsequently.

5.2. SIGNIFICANCE OF THERMOELECTRIC POWER

Thermoelectric power (TEP) is defined as $S = \Delta V / \Delta T$, the ratio of voltage drop to temperature gradient applied across the sample. It is a zero current transport coefficient since there is no electric current passing through the sample. The voltage drop ΔV is induced by the thermal gradient ΔT . So TEP is not limited by the contact resistances and can be used very effectively to probe the intrinsic conduction mechanism of the system.

Thermoelectric power can be viewed as measure of entropy per carrier; it is positive or negative depending on the sign of the charge carrier. Since it is a zero current measurement i.e. there is no electrical current passing through the sample during measurements it is a powerful

probe to investigate the mechanism of intrinsic electronic conduction in any system. Without going through the detailed expressions for TEP, one can intuitively understand this point by considering the distribution of the thermally driven carriers. For a nondegenerate system, it is purely the configurational entropy that determines the magnitude of TEP and the magnitude of TEP for semiconductors is large. For the completely degenerate system, the configurational entropy is zero, so that the magnitude of TEP for a metal is small. For this reason, TEP can measure the semiconductor-metal transition of a system.

The sign of TEP usually indicates the majority carriers of the system because TEP measures the voltage drop due to thermally driven carriers and hence the net signal is dominated by the majority carriers. One should notice here the sign of TEP is often complicated to understand, depending on the materials. For noble metals, positive TEP is observed even though the majority carriers are electrons. The complex Fermi surface at the Brillouin zone boundary could have a hole like structure and the Unklapp processes could reverse the sign of TEP. Nevertheless, one could use the measured sign of TEP as a first pointer to the type of majority carriers in the system.

Another important feature of TEP measurement is that it is a very sensitive probe to the scattering mechanisms of charge carriers with static disorders such as dopants, impurities or with dynamic disorder such as phonons. In the case of semiconductors, there are only few charge carriers contributing significantly to configurational entropy, so that the effect of charge carrier scattering is not very significant. But in metals, there are a large number of degenerate carriers which are localized throughout the sample, and hence the magnitude of TEP is small. Therefore, the effect of charge carrier scattering, whether due to static or dynamic disorder, is significant. This scattering is the intrinsic property of the material and is entirely different from the scattering causing contact resistance of the experimental system. Hence thermoelectric power measurements in conducting polymers give very good information regarding metal - insulator transitions and mechanisms responsible for charge transport in this system.

The temperature dependence of the high electric field dependence of conductivity show that there are two different transport mechanisms responsible for the two different doped regimes in the case of polyaniline. One of them is at the

light protonation level where the transport is dominated by charge hopping between localised states, similar to variable range hopping. The other is through charging energy limited tunneling between conducting segments separated by insulating regions. The system is a granular polymeric metal in the second regime. The origin of the insulating species between conducting segments may lie in the fact that the emeraldine form of polyaniline does not really have the exact stoichiometry of three benzene rings to one quinoid ring. The barriers in the system limit the measurement of the absolute intrinsic conductivity of the system and its temperature dependence. Consequently there have been limitations on testing the proposed polaronic model based on experimental data on absolute conductivity and its temperature dependence. One way to get over the problem is to measure the dependence of thermopower on temperature which is least affected by the carriers in the regions between conducting islands because there is no current flow in the thermopower measurements. So these measurements do not involve long range carrier transport in the system. We have performed thermopower measurements on the HCl doped polyaromatic amine polymers in search of the intrinsic polaron metal at high doping level in these systems.

The temperature dependence of TEP gives information about the nature of charge transport in conducting polymers. The temperature dependence of the TEP for trans-polyacetylene has been explained as due to carrier hopping among a set of localised states [3] and is given by the Heikes formula

$$S = +(k_B/|e|) \ln [(1-\rho)/\rho] \quad (5.1)$$

Where $\rho = n/N$ is the ratio of the number of holes n to the number of available sites N . This expression applies to spinless Fermi ions. Experimental value of S gives $\rho \approx 10^{-4}$ or a carrier concentration of $2 \times 10^{18} \text{ cm}^{-3}$ in undoped polyacetylene. Later, Mases et al. [4] analysed the temperature independence of TEP in the temperature range of 230-280K and interpreted the results in terms of intersoliton hopping transport given by modified Kivelson's equation [18,19].

In the metallic state, doped polyacetylene has nearly filled bands. The thermopower then can be written as

$$S = (+\pi^2 k_B^2 / 3 |e|) k_B T \left[d \ln \sigma(E) / dE \right] \quad (5.2)$$

Where $\sigma(E) = n(E) |e| \mu(E)$ and $n(E)$ is the number of

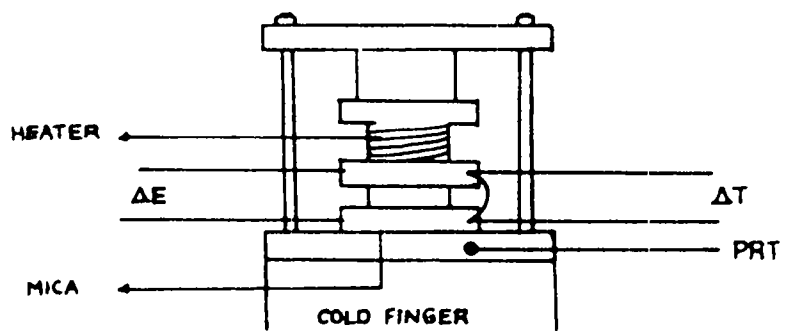
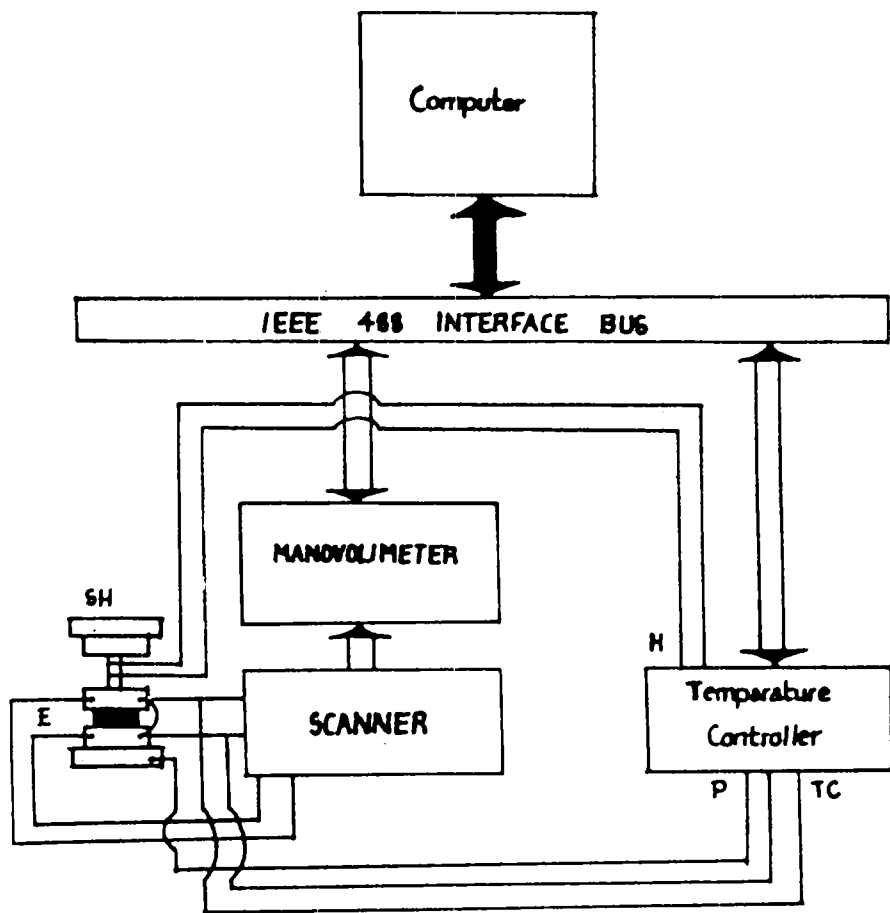
carriers contributing to $\sigma(E)$, $dn(E)/dE$ is the density of states and $\mu(E)$ is the charge-dependent mobility. Several authors have used these equations to explain the temperature dependence of TEP and have drawn conclusions regarding the nature of charge transport in several conducting polymers.

5.3 EXPERIMENTAL METHOD

A fully automated thermoelectric power (TEP) measurement setup was used to measure the TEP of all samples down to 30K. An indigenously developed closed cycle helium refrigerator at Centre for Advanced Technology, Indore, was used for this purpose. The sample holder consists of two copper blocks. The top one having a heater and the bottom one was attached to the cold finger of the refrigerator with delta bond so that it is electrically isolated but thermally conducting. Samples in the form of pellets of size 10 mm diameter and 2 mm thickness were kept between the two copper blocks and the temperature difference between the two, ΔT , was measured by a Copper-Constantan thermocouple or by a Chromel-Alumel thermocouple. Two high purity copper wires glued to the copper blocks by means of conducting silver

paint was used to measure the potential difference ΔE . TEP of the sample was determined after subtracting the contribution from copper.

Temperature difference ΔT was controlled in a differential mode using a Lake shore model DRC 93C temperature controller with 9305 thermocouple input card and the sample temperature was measured by calibrated platinum resistance thermometer using the same temperature controller. Data collection was made while warming using a locally available IEEE 488 interface card and a PC. A Schlumberger nanovoltmeter with a scanner was used to measure ΔE . A schematic diagram of the TEP measurements and sample holder is shown in figure 5.1.



Thermopower Sample Holder (Schematic)

Figure 5.1: Schematic diagram of thermoelectric power measurements and sample holder.

5. 4 RESULTS AND DISCUSSION

Figure 5.2a to 5.2c shows the temperature dependence of thermoelectric power of HCl doped polyaniline. The shape and sign change of TEP obtained in the temperature variation of thermoelectric power is similar to the results reported by different authors earlier [11,12]. As can be seen, the sign changes from positive to negative at 283.88 K. The temperature dependence of the TEP of polyanisidine is shown in Figure 5.3a to 5.3c. The temperature variation of the thermopower of polyanisidine is also similar to that of polyaniline. However, the sign change close to room temperature is sharper here. The U shaped behaviour in the variation of TEP, seen at low temperatures is also similar to that of polyaniline, but the temperature at which the minimum occurs is different. The value of the thermopower of polyanisidine is much higher than that of polyaniline. In addition to this there is a small hump near 120 K. The sign changes from positive to negative at a temperature of 289.32 K. The curve obtained for the co-polymer of anisidine and aniline is shown in Figure 5.4a to 5.4c. The U shaped behaviour is retained in this polymer also. The sign change is again sharp in this case and it occurs at a

temperature of 287.27K. In addition, the hump seen in the case of polyanisidine is also present in this co polymer prominently. In Figure 5.5a to 5.5c we show the plot obtained for the co polymer of aniline and benzidine. This curve is very much similar to the curve of polyaniline, however the sign changes from positive to negative at 288.44 K in this case. The variation of TEP with temperature for the co polymer containing anisidine and benzidine is shown in Figure 5.6a to 5.6c. Here, instead of a U shaped behaviour, a W shaped behaviour is seen. The transition from positive to negative is again very sharp and occurs at a temperature of 283.23 K.

The temperature dependence of thermopower shows aspects of U shaped or partially U shaped behaviour in all the polymers studied. These U shaped behaviour shows different shifts in Y axis, reflecting constant contributions to the different polymers. Though these constant term varies in different polymers. all those have negative values as reported [9].

At high temperatures the thermoelectric power, $S(T)$ is proportional to T ie, $S(T) = CT$. The proportionality constant C is independent of the orientations of the crystallites in the polymers [9]. For the polymers

investigated in this study, C values are different for each of them. At low temperatures, the relation between temperature and thermopower can be expressed by the equation $S(T) = S_0 + B/T$. This relation is followed by all the samples. However, in the case of polyanisidine a small hump is observed near 100 K and it is prominent in all the copolymers containing anisidine. In general the U shaped behaviour can be represented by the equation

$$S(T) = S_0 + B/T + CT. \quad (5.3)$$

This general behaviour is followed only up to room temperature. At room temperature the sign of the TEP changes from positive to negative value in all these polymers.

The U shaped behaviour of the temperature dependence of TEP suggest that the conduction mechanism in these polymers is of the one-dimensional variable range hopping ID-VRH type [13]. It also suggests the existence of three dimensional metallic region in the polymer. The low temperature behaviour, ie. $S(T) = S_0 + B/T$, is consistent with the quasi ID-VRH, since $S_0 < 0$ and $B/T > 0$ are contributions from inter chain and intra chain VRH conduction respectively [14]. At

higher temperatures, $S(T) = CT$ where C is a constant. This constant component indicates that inter chain hopping still plays a role in the conduction process. It is well known that $S(T)$ is proportional to T/E_f for free electrons. For the high temperature region, since the linear dependence is independent of orientations of the sample, this may be due to the contribution of nearly free electrons taking part in transport in 3D metallic regions of the polymer.

Thermoelectric power at room temperature shows the sign cross over for all the polymer samples under investigation which is already reported in polyaniline [15]. In the case of polyaniline the sign change is explained in the following way. The protonated form of polyaniline is viewed as a degenerate solid with non zero density of states at the Fermi level. for the metallic case, Fritzsche [14,16,17] points out that the sign of the thermoelectric power is determined by whether electronic conduction is supported predominantly by states above ($S > 0$) the Fermi level. According to the equation of Fritzsche,

$$S = - \frac{k}{e} \frac{\int (E - E_f) \sigma(E) dE}{kT \sigma(E)} \quad (5.4)$$

The fractional contribution, $\sigma(E)dE/\sigma$ depends both on the density of states, $N(E)$ and the mobility $\mu(E)$ immediately above and below the Fermi level. Assuming conduction within a band of states and neglecting for the moment the effects of mobility, it can be shown that a higher density of states below the Fermi level will result in a positive thermopower. The observed sign crossover and the low value of the thermopower suggest, therefore, that the Fermi level is in a region of near constant density of states for samples with high doping level. From the simplest point of view, such a near constant density of states would be consistent with a half filled band having the Fermi level at the point of crossover in the energy-wave vector diagram from positive to negative curvature.

The above explanation for the sign crossover in TEP is valid in the case of polyaniline and one of the co polymers of aniline and benzidine in our investigations. However, our investigations show that in polyanisidine and other co polymers very high values of TEP are observed and, moreover, the transitions are very sharp in these polymers compared to polyaniline and its co polymer containing benzidine. So the above model cannot be applied and generalised to the polyaromatic amine family of conducting polymers.

Our experimental results indicate that the transport mechanism in the conducting polymers and co polymers we have studied is very complex. Several mechanisms came into play as the temperature is varied from 50 K to room temperature. At low temperature our result suggest that there exist three dimensional metallic regions in the samples and the thermopower follows the relation

$$S(T) = S_0 + B/T \quad (5.5)$$

where S_0 is always negative and B/T is always positive [11]. This behaviour is in accordance with quasi-one dimensional variable range hopping. For inter chain hopping S_0 is negative and for intra chain hopping B/T is positive. When inter chain hopping dominates we have $S(T)$ decreasing with temperature. As the degree of orientation increases as temperature decreases, the intra chain contribution decreases. For higher temperatures $S(T)$ becomes proportional to T , except for a constant. This indicates that $S(T)$ at higher temperatures is dominated by intra chain contributions even though inter chain contribution plays a significant role. In the high temperature regime, there is a contribution from nearly free electrons transporting in

3-dimensional metallic regions of the polymer because $S(T) \propto T/E_f$ for free electrons, where E_f is the Fermi energy. The competition between inter chain and intra chain variable range hopping and the free charge carriers in the metallic regions give rise to the observed U shaped behaviour in the $S(T)$ versus T curve.

The thermoelectric power of the co polymers is further complicated by the side chains present in the structure. These side chains act as paths for the transport of charge carriers between chains leading to enhanced inter chain hopping of the carriers with a complex temperature dependence as exhibited by the W-shaped behaviour in the co polymer of anisidine and benzidine, aniline and anisidine. The effect is more prominent in co polymer containing anisidine and benzidine.

The aromatic amine family of conducting polymers make a very interesting group of samples which are very complex from electrical transport point of view. The materials contain conducting regions separated by amorphous regions. Charge transport has several contributions; inter chain and intra chain variable range hopping, tunneling across the conducting regions through amorphous regions, transport of

free carriers within the conductive regions and charge transport through side chains. All these with different temperature dependence make the temperature dependence of thermoelectric power very complicated and interesting.

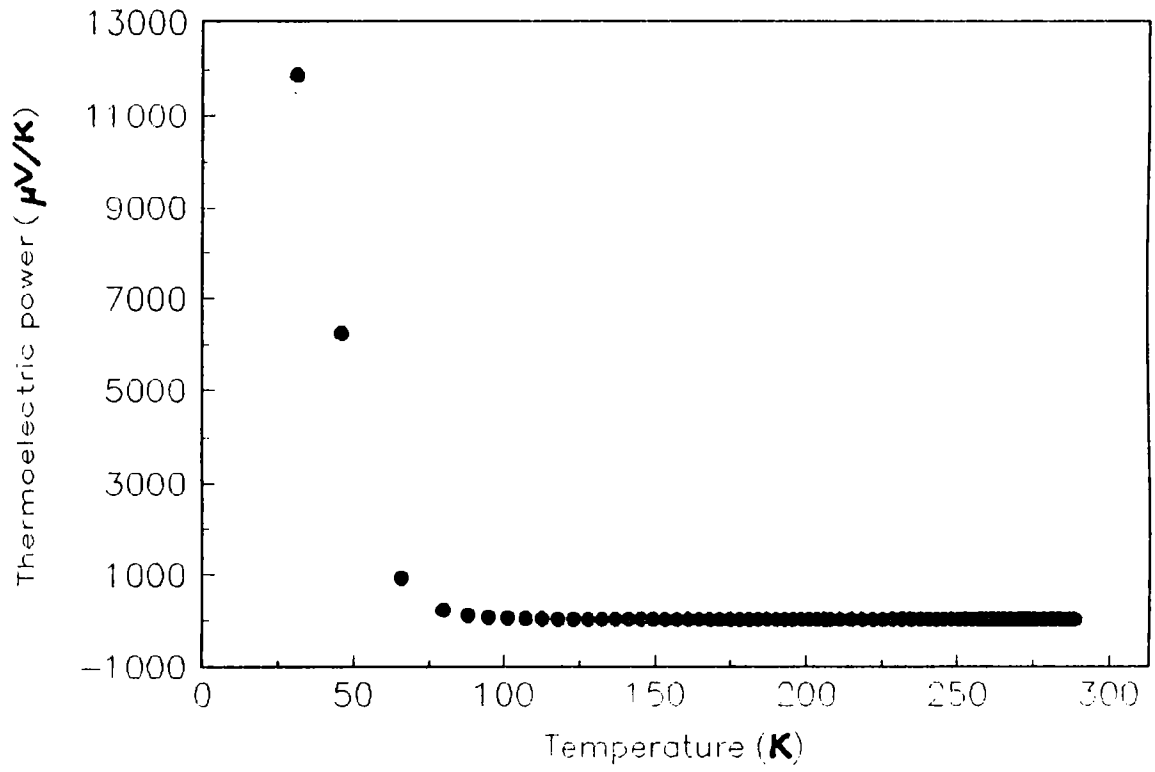
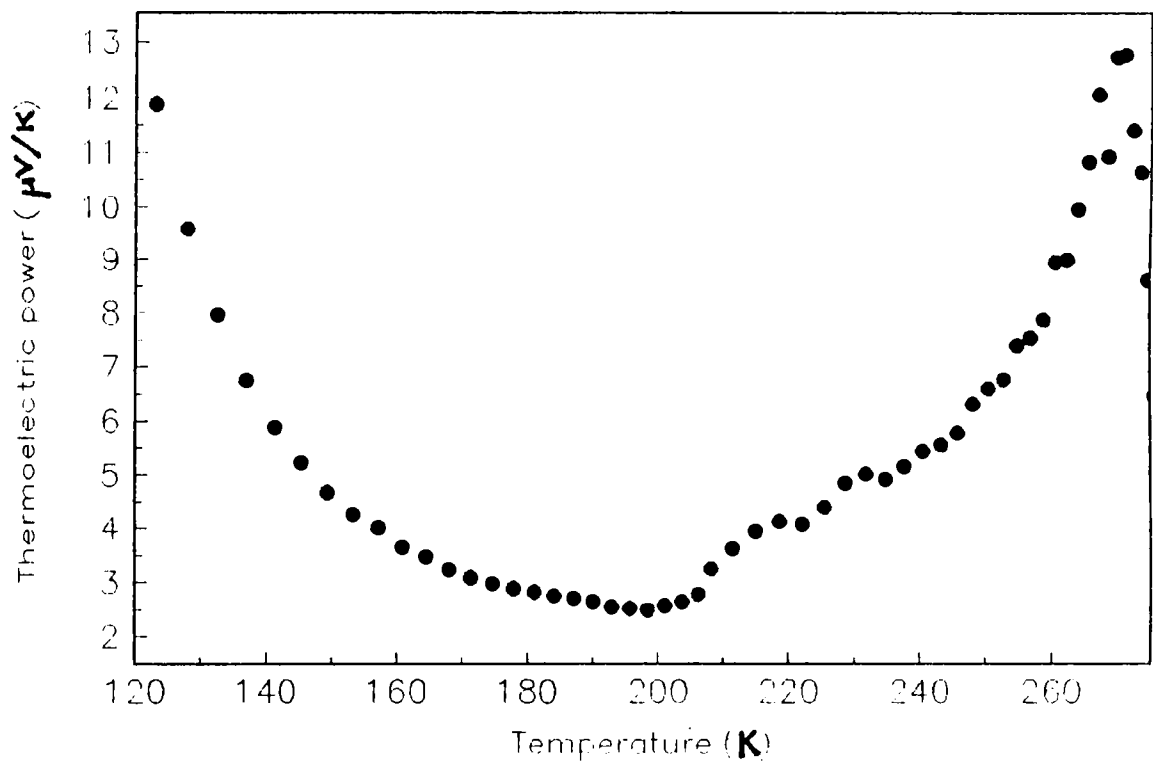


Figure 5.2a: The temperature dependence of thermoelectric power of doped polyaniline.



· **Figure 5.2b: The U shape temperature dependence of thermoelectric power of doped polyaniline.**

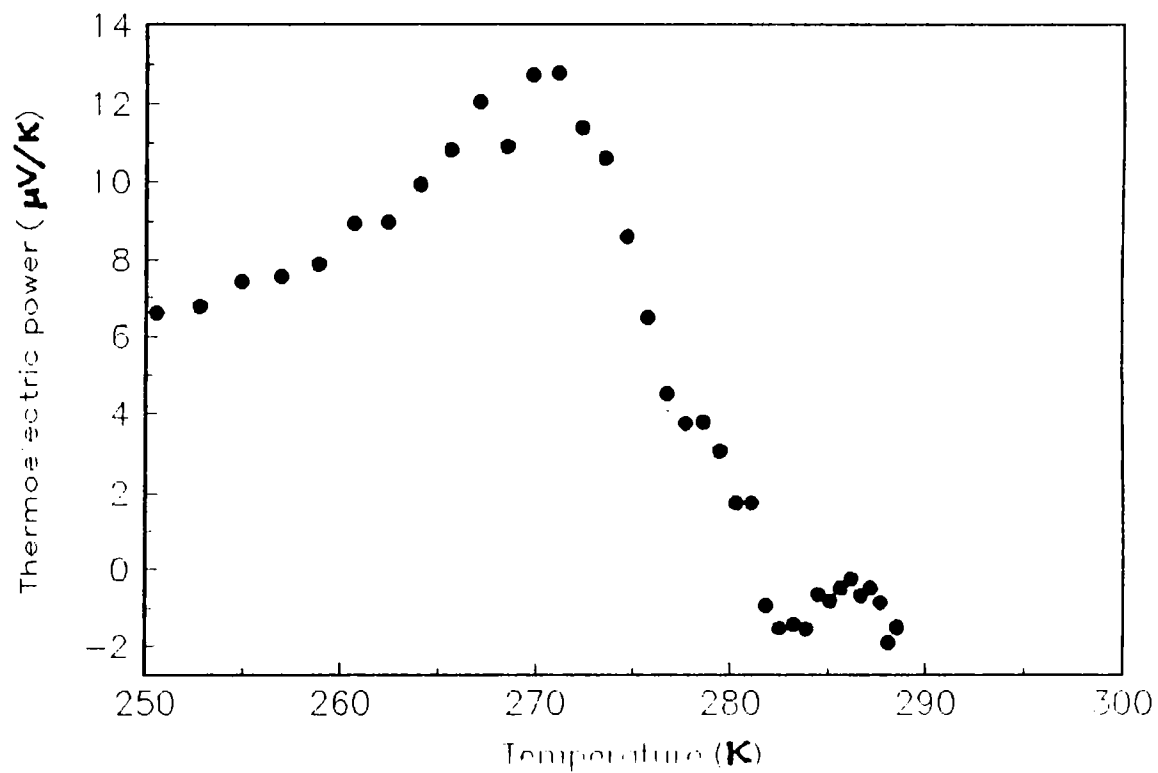


Figure 5.2c: The sign change of thermoelectric power of doped polyaniline.

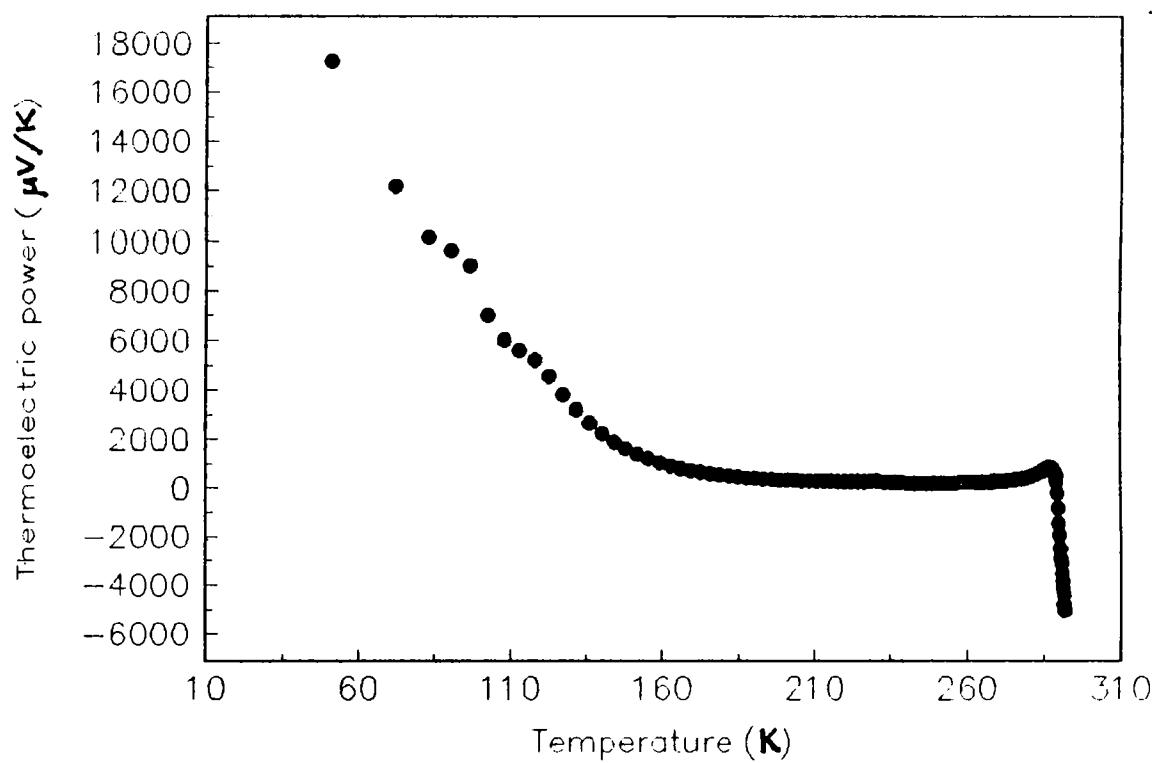


Figure 5.3a: The temperature dependence of thermoelectric power of doped polyanisidine.

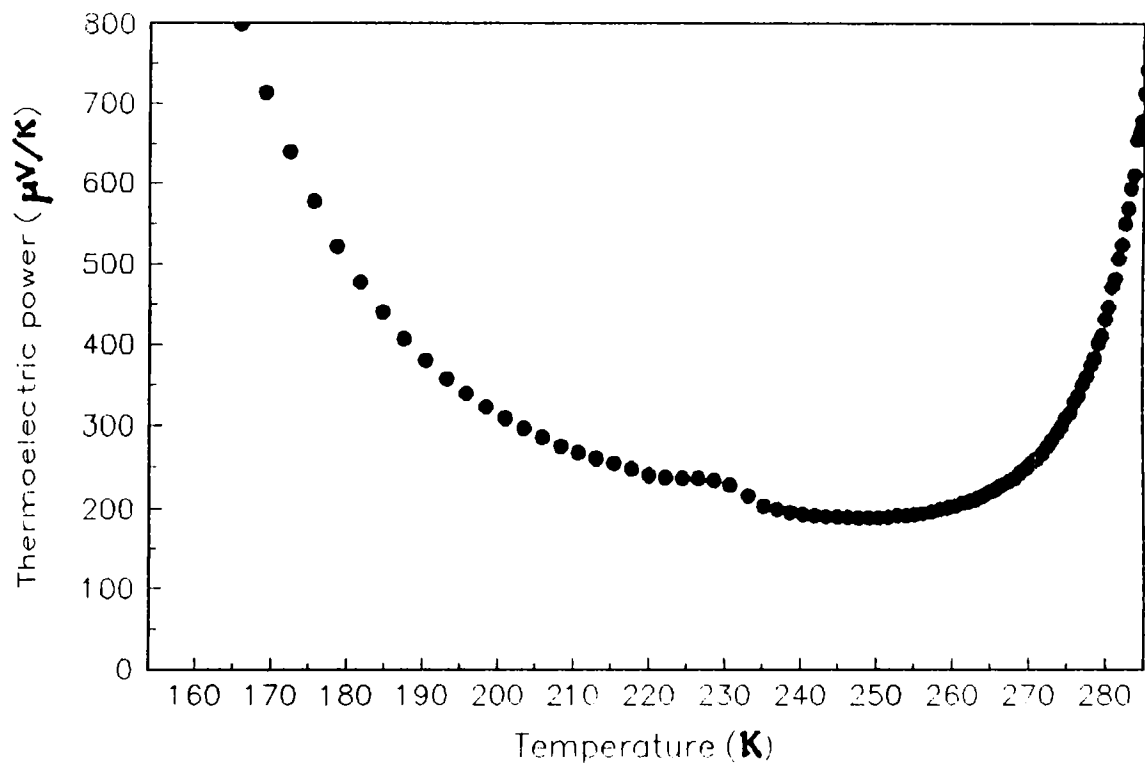


Figure 5.3b: The U shape temperature dependence of thermoelectric power of doped polyanisidine.

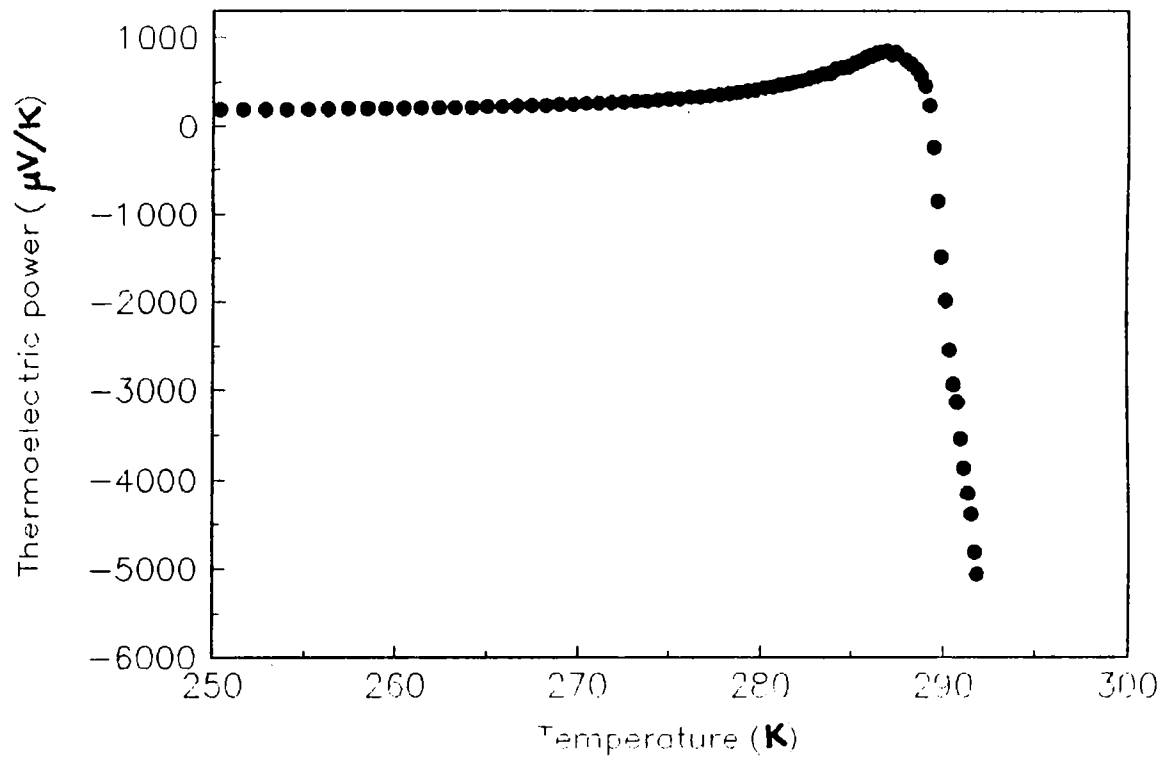


Figure 5.3c: The sign change of thermoelectric power of doped polyaniline.

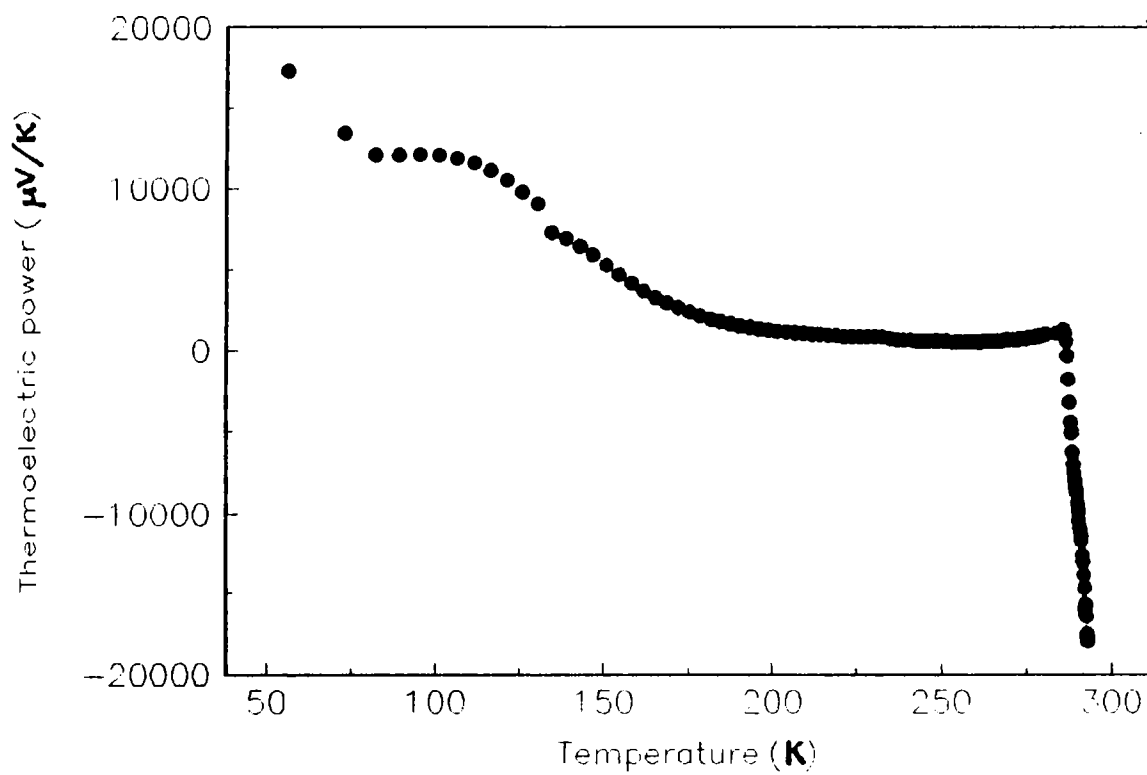


Figure 5.4a: The temperature dependence of thermoelectric power of doped co polymer of aniline and anisidine.

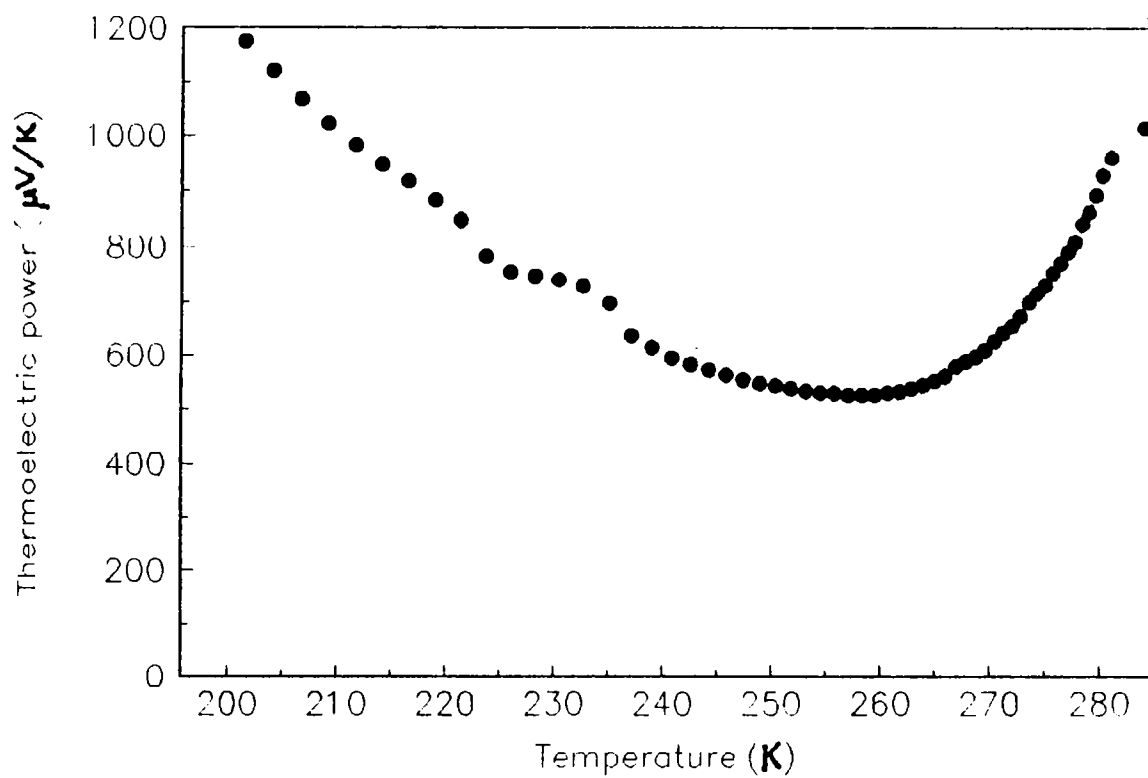


Figure 5.4b: The U shape temperature dependence of thermoelectric power of doped co polymer of aniline and anisidine.

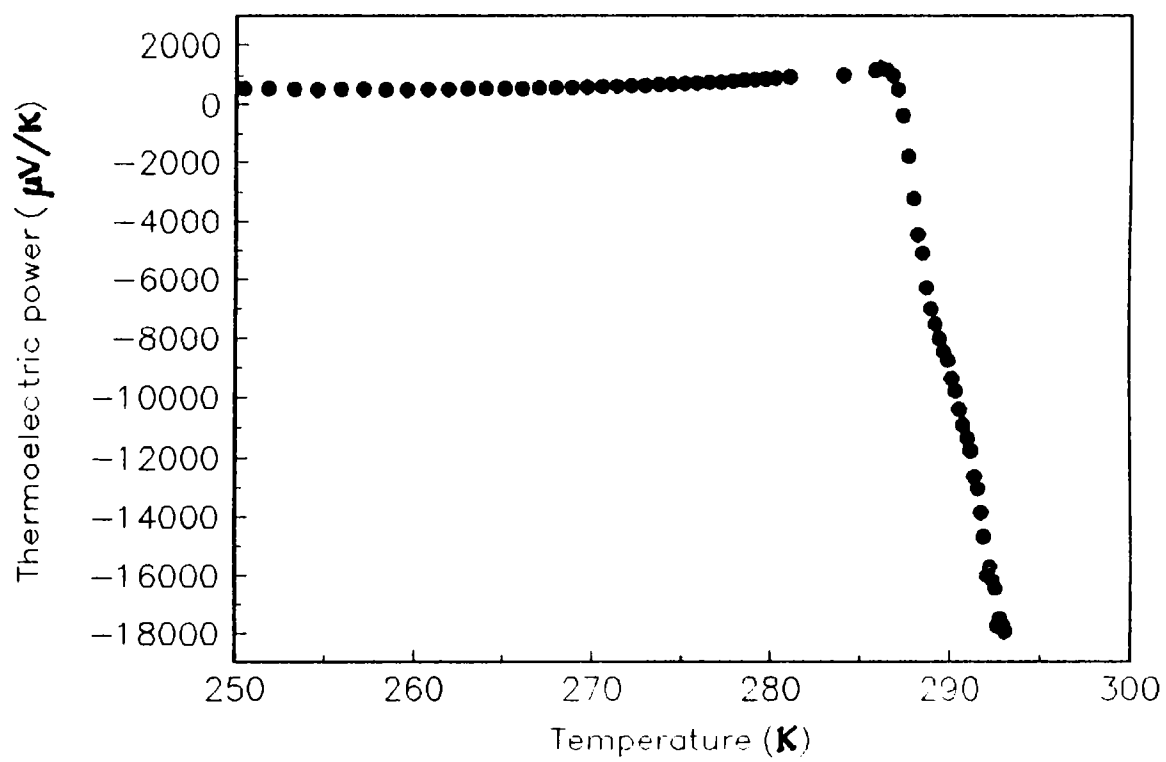


Figure 5.4c: The sign change of thermoelectric power of doped co polymer of aniline and anisidine.

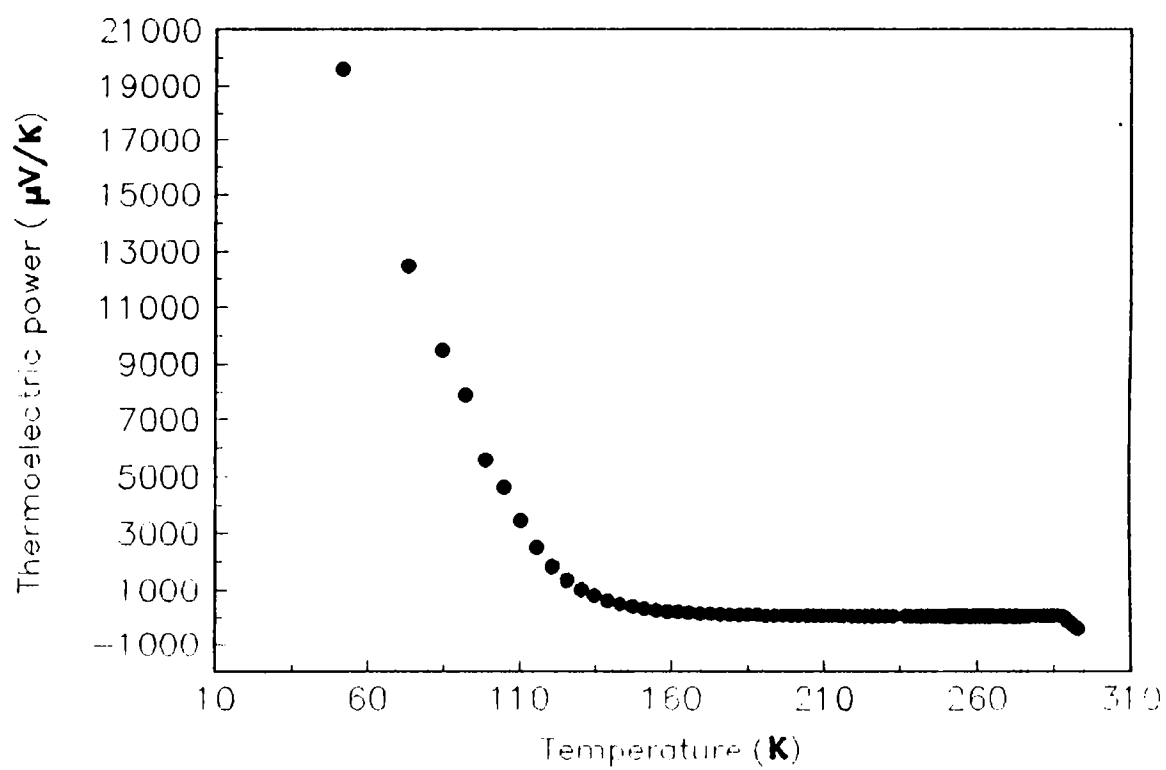


Figure 5.5a: The temperature dependence of thermoelectric power of doped co polymer of aniline and benzidine.

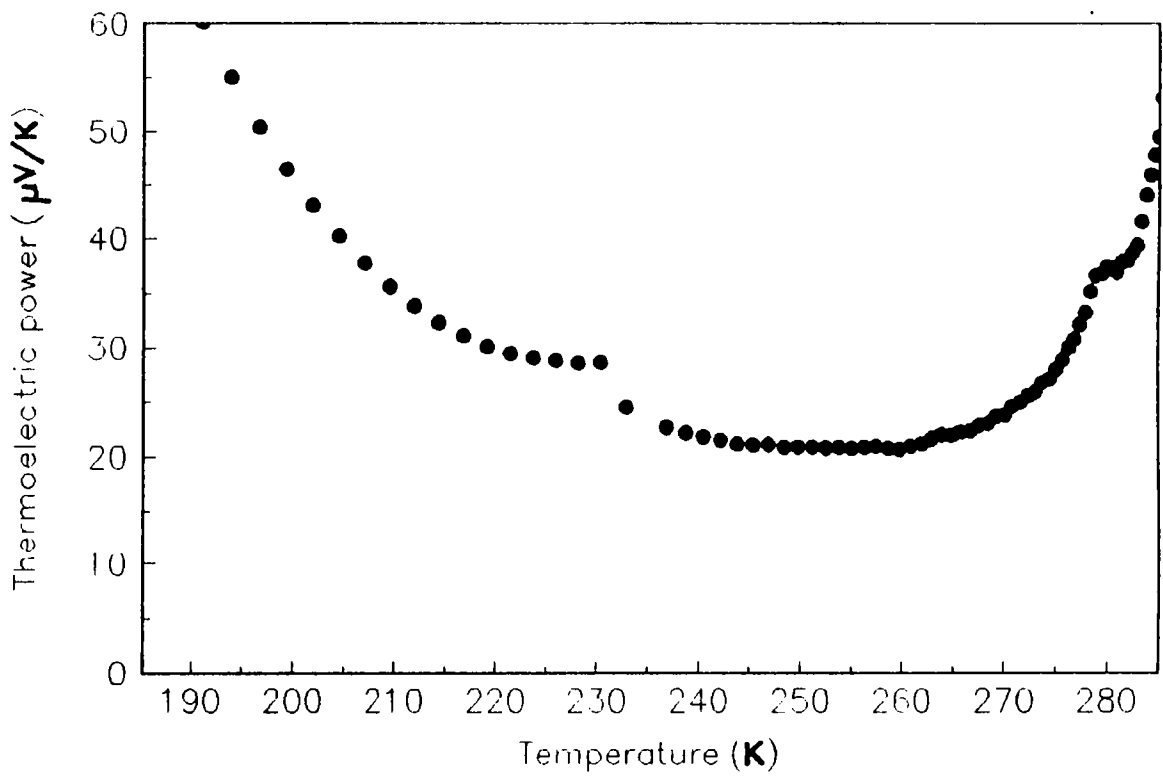


Figure 5.5b: The U shape temperature dependence of thermoelectric power of doped co polymer of aniline and benzidine.

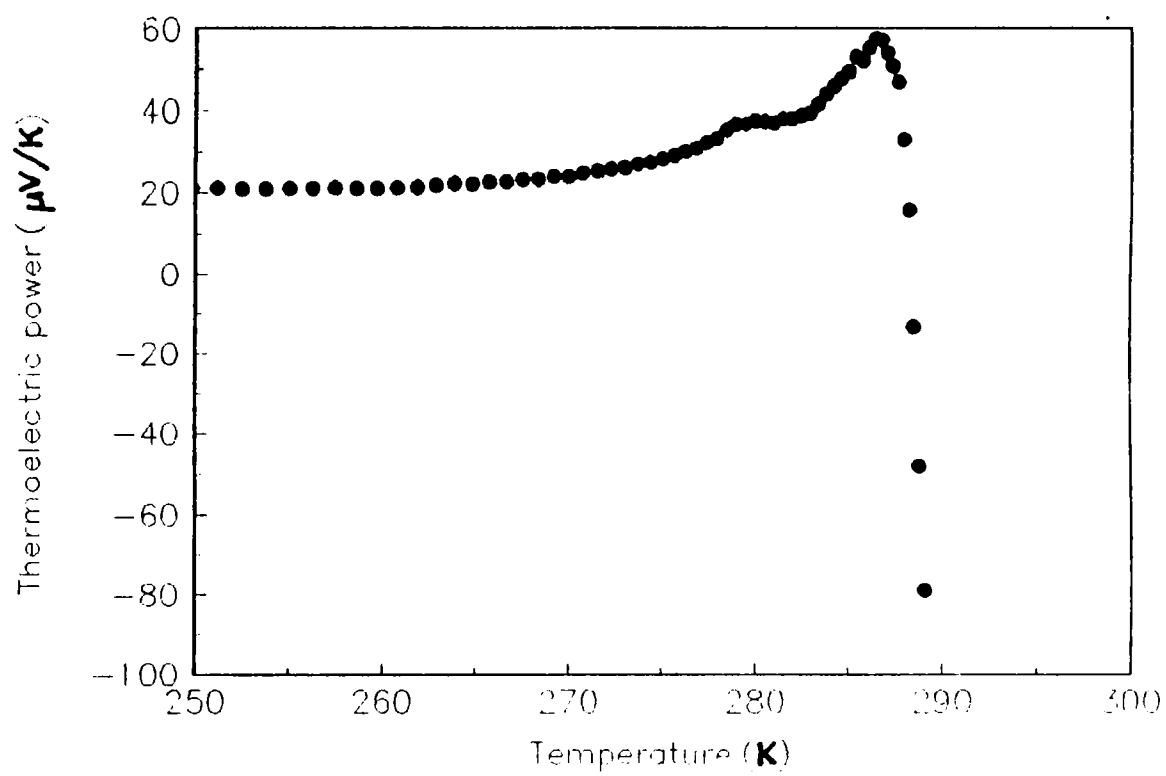


Figure 5.5c: The sign change of thermoelectric power of doped co polymer of aniline and benzidine.

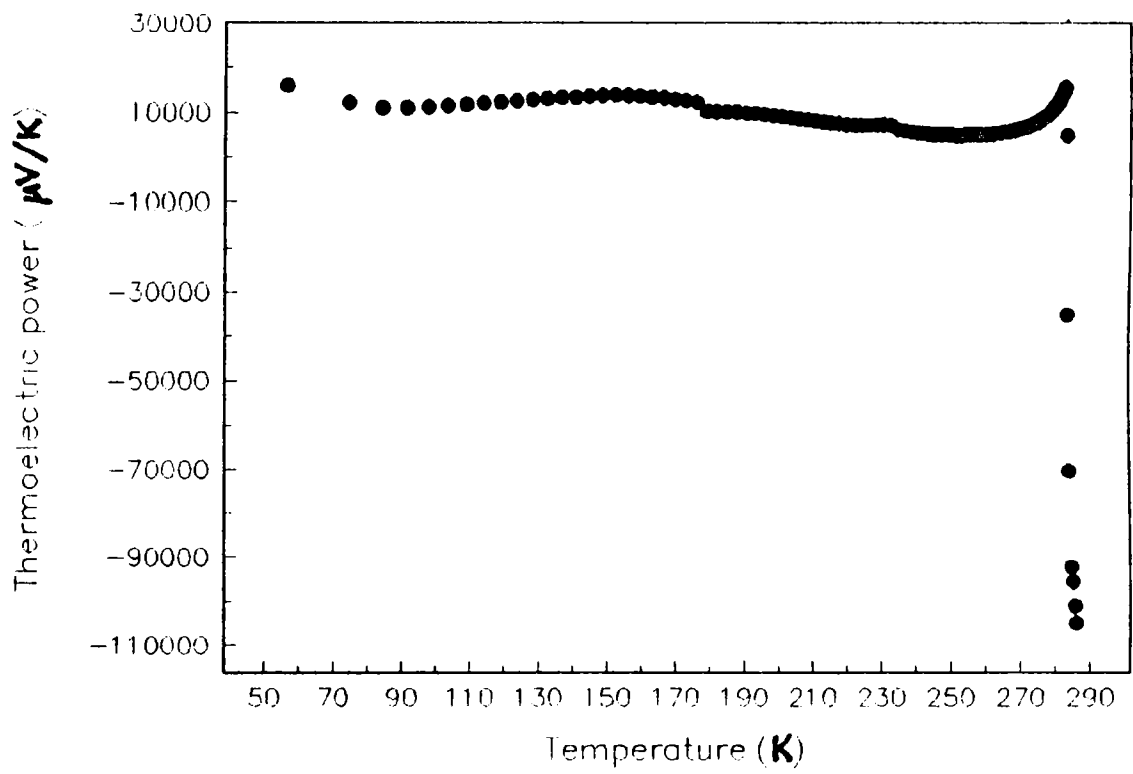


Figure 5.6a: The temperature dependence of thermoelectric power of doped co polymer of anisidine and benzidine.

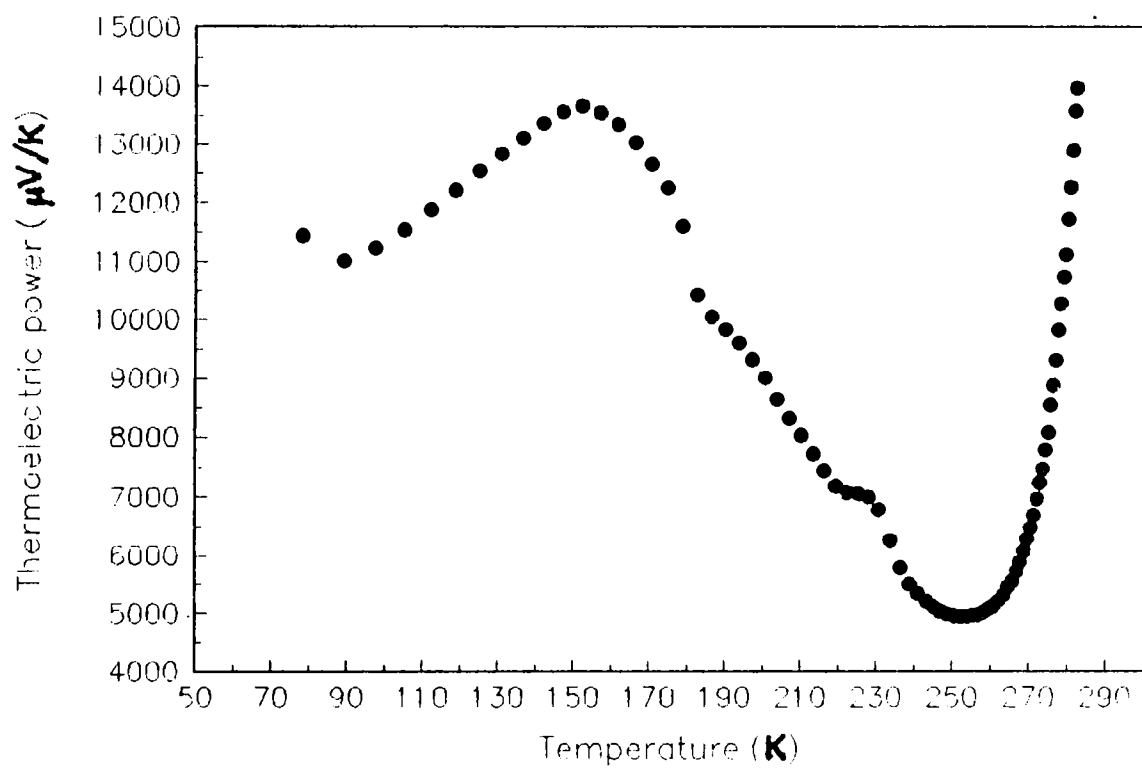


Figure 5.6b: The W shape temperature dependence of thermoelectric power of doped co polymer of anisidine and benzidine.

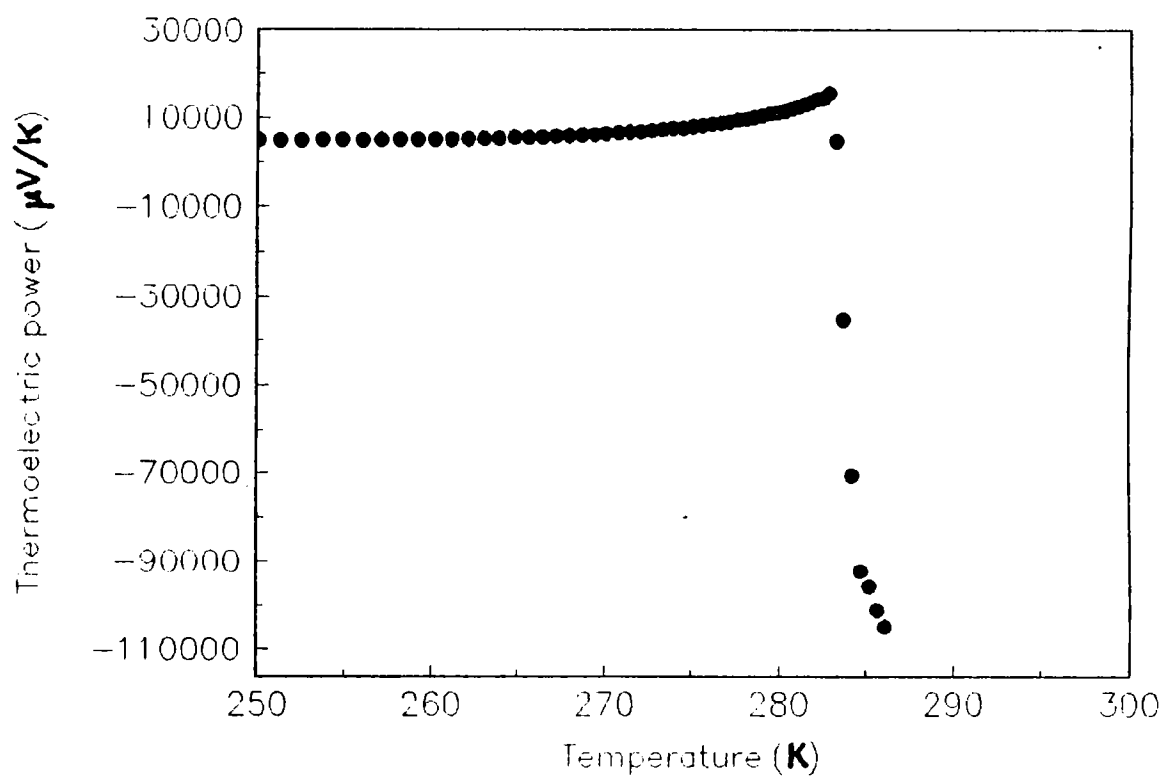


Figure 5.6c: The sign change of thermoelectric power of doped co polymer of anisidine and benzidine.

REFERENCES

1. Y. W. Park, Workshop on the Materials Science of Conductive Polymers, Atlanta, 173 (1991).
2. Y. W. Park, A. Denenstein, C. K. Chiang, A. J. Heeger and A. G. MacDiarmid, Solid State Commun. 29, (1979)745.
3. Y. W. Park, A. J. Heeger, M. A. Drug and A. G. Mac Diarmid, J. Chem. Phys. 73, (1980)946
4. D. Mases, J. Chen, A. Denenstein, M. Kaveh, T. C. Chung, A. J. Heeger and A. G. Mac Diarmid, Solid State Commun. 40, (1981)1007.
5. Y. W. Park, W. K. Han, C. H. Choi and H. Shirakawa, Phys. Rev. B 30, (1984)5847.
6. Y. W. Park, Y. S. Lee, C. Park ,L. W. Shacklette and R. H. Baughman Solid State Commun. 63, (1987)1063.
7. F. Zuo, M. Anglopoulos, A. G. Mac Diarmid and A. J. Epstein. Phys. Rev. B 36, (1987)3475.
8. Z. H. Wang, H. H. S. Javadi, A. Ray, A. G. Mac Diarmid and A. J. Epstein, Phys. Rev. B 42, (1990)5411.
9. Z. H. Wang, A. Ray, A. G. Mac Diarmid and A. J. Epstein, Phys. Rev. B 43,(1991)4373.
10. C. O. Yoon, M. Reghu, D. Moses, A. J. Heeger and Y. Cao, Phys. Rev. B 48, (1993)14080.

11. Z. H. Wang, C. Li, E. M. Scherr, A. G. Mac Diarmid and A. J. Epstein, Phys. Rev. Lett. 66, (1992)1745.
12. Q. Li, L. Cruz and P. Phillips, Phys. Rev. B 47 (1993)1840.
13. Z. H. Wang, E. M. Scherr, A. G. Mac Diarmid and A. J. Epstein, Phys. Rev. B 45 (1992)4150.
14. N. F. Mott and E. A. Davis, Electronic Processes in Noncrystalline Materials (Clarendon, Oxford, 1979)
15. J. P. Travers, J. Chrovoczek, F. Devreux, F. Genoud, M. Nechtschein, A. Syed, E. M. Genies and C. Tsintavis, Mol. Cryst. Liq. Cryst. 121, (1985)195.
16. N. W. Ashcroft and N.D.Mermin, Solid State Physics (Saunders College 1976).
17. P. Nagels, Topics in Appl. Phys. 36, (1979)114.
18. S. Kivelson, Phys. Rev. Lett. 46, (1981)1344.
19. S. Kivelson, Phys. Rev. B 25, (1982)3798.

CHAPTER 6

THERMAL PROPERTIES OF CONDUCTING POLYMERS - POLYANILINE, POLYANISIDINE AND CO-POLYMERS

6. 1 INTRODUCTION

Measurement of the thermal properties is as important as electrical properties for solid state materials. Thermal properties such as heat capacity and thermal conductivity are basic parameters which determine several physical properties of materials. It is well known that, in general, good electrical conductors are good thermal conductors as well which leads to realisation of the well known Wideman-Franz law. In a solid, thermal energy is carried by both electrons and phonons. Consequently, there is electronic and phononic contributions to thermal conductivity. In good electrical conductors, where there is a large number of free electrons, thermal conductivity is dominated by the electronic part. In insulators there are no free electrons to carry heat and thermal conductivity is dominated by phonon contribution. Since phonons are elementary excitations for lattice vibrations, phononic

contribution is basically lattice contribution. One can distinguish between electronic and phononic part of thermal conductivity from the temperature dependence of thermal conductivity.

Thermal conductivity in a solid is limited by various scattering mechanisms. If we consider the phononic part of thermal conductivity, its value is limited by scattering of phonons by electrons, other phonons and defects. Scattering of phonons from boundaries, interstitials etc. also contribute to thermal resistance. In general, following Casimir, one can write an expression for thermal conductivity as

$$K = (1/3) C \bar{v} l \quad (6.1)$$

where C is the heat capacity, \bar{v} is the average velocity of phonons and l is the mean free path for phonons. Theoretical techniques have been developed to evaluate thermal conductivity of a solid and to separate the electronic and phononic contributions.

Several experimental techniques have been developed to measure thermal conductivity of solids very accurately. These methods can broadly be classified as transient and periodic heat flow methods. The details of these techniques can be found in several text books. While making measurements, one must account and correct for radiative heat losses. Otherwise the heat losses can cause significant errors in measurements. The corrections will vary with the sample because radiative heat loss from a sample depends on surface emissivity, surface area etc.

Another parameter closely related to thermal conductivity is thermal diffusivity. Thermal diffusivity is related to thermal conductivity through the relation

$$\alpha = K/\rho C \quad (6.2)$$

where α is the thermal diffusivity, K is the thermal conductivity, ρ is the density and C is the heat capacity of the sample. Measurement of thermal diffusivity is rather insensitive to heat losses and is particularly suited to poor heat conductors. Just as conductivity, diffusivity can also be measured by either transient or periodic heat flow techniques. Of late, periodic heat flow techniques have

become more popular due to the accuracy and fastness with which measurements can be made.

Of the different periodic heat flow techniques used to measure thermal diffusivity, the photoacoustic technique has gained wide acceptance and popularity because the measurements are accurate and fast and due to the fact that the technique can be adapted to a wide variety of samples. This technique makes use of the photoacoustic (PA) effect which is the generation of an acoustic signal when a sample, kept in an enclosed volume, is irradiated by an intensity modulated beam of light. When modulated light, at a modulation frequency f , falls on the sample, it absorbs whole or part of the light energy and the internal energy levels, electronic, vibrational or both depending upon the sample, get excited. Nonradiative decay of these levels gives rise to thermal fluctuations in the sample which also have a frequency f . These periodic thermal fluctuations propagate through the sample and reach the boundary. These thermal waves cause a periodic heating of the sample boundary which causes a corresponding periodic expansion of the gas medium adjacent to the sample surface which in turn induce corresponding pressure fluctuations in the gas medium surrounding the sample. These pressure waves can be

detected as acoustic waves with a sensitive microphone kept inside the PA cell. The mechanism of PA effect in condensed media involves conversion of light into heat by absorption, thermal diffusion through the sample and conversion of heat waves into sound waves by acoustic piston effect. The theory is rather involved and is discussed in detail in literature [1,2,3]. The photoacoustic amplitude is a measure of the optical absorption and thermal diffusion properties of the sample whereas the PA phase gives very accurate information about thermal diffusion in the sample. The technique can be adapted to a wide variety of samples and is particularly useful with samples for which conventional techniques often fail.

Measurement of PA amplitude and phase can be performed with a photoacoustic spectrometer which consists of a source of light, an optical chopper, a photoacoustic cell in which the sample is kept and necessary signal processing instruments such as a lock-in amplifier. A schematic diagram of a typical setup is shown in Fig. 6.1. The technical details can be found in several articles and papers [3,4]. The thermal diffusivity of a sample can be determined by by amplitude or phase. Here, the sample, with an appropriate thickness is kept in the PA cell and the incident light

chopping frequency is varied so that the sample which is thermally thin at lower frequencies becomes thermally thick at higher frequencies . For a thermally thin sample,

$$l_s \cdot a_s < 1 \quad (6.3)$$

where a_s is the thermal diffusion coefficient of the sample.

As the sample goes from a thermally thin regime to a thermally thick one, there will be a distinct change in the slope in PA amplitude versus frequency plot. The frequency at which this happens is called the characteristic frequency f_c . Moreover, the PA phase ceases to vary above the characteristic frequency. The characteristic frequency can be determined accurately from PA amplitude or phase measurement. Once the characteristic frequency is determined, the thermal diffusivity can be evaluated from the relation

$$\alpha = f_c / l_s^2 \quad (6.4)$$

More details about this technique and the results obtained on several samples can be found in literature [5,6].

We have used a modified phase lag measurement technique to determine the thermal diffusivity of conducting polymer samples. The experimental technique used and the results obtained are described in the following sections. A discussion of the results follows these sections. We have carried out the measurements on polyaniline, polyanisidine and co polymers of aniline, anisidine and benzidine.

6. 2 EXPERIMENTAL METHOD

We have used a modified photoacoustic phase lag measurement technique to determine the thermal diffusivity of conducting polymers. This technique involves measurement of the photoacoustic phase lag between the signals generated from the front and rear surface of the sample. Illumination of the front and rear surfaces with chopped beam of the same light is achieved by a smooth rotation of the PA cell by 180° . The technique is analogous to the two-beam technique in which two separate beams of light derived from the same source are used to illuminate the front and rear surfaces of the sample simultaneously and measuring the PA amplitude

ratio or phase difference. It is found that measurement of the phase lag is straightforward and it leads to very good results. The experimental details are given in reference [7].

Starting with the one dimensional theory of Rosencwaig and Gersho [1] one can write an expression for the complex envelope of the photoacoustic signal from a sample from which the amplitude and phase terms can be separated. This equation when applied to a thermally thick sample illuminated on the front surface first and then on the rear surface leads to the following expressions for the PA phases from the two surfaces respectively [7,8].

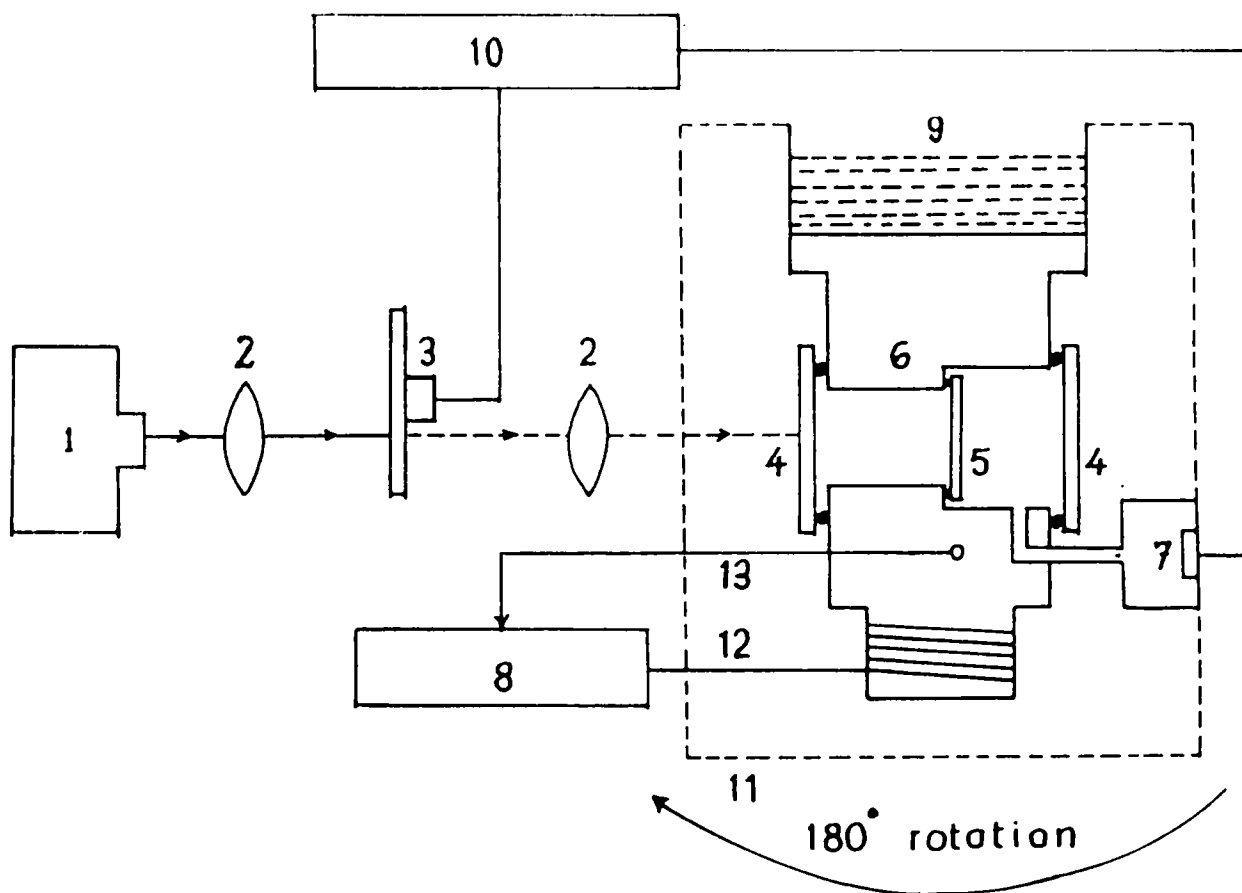


Figure 6.1. Schematic diagram of the experimental setup.

1-Source, 2-Lenses, 3-Chopper, 4-Cell windows, 5-Sample,
 6-Sample holder, 7-Microphone, 8-Temperature
 controller,
 9-Liquid nitrogen chamber, 10-Lock-in amplifier,
 11-Outer chamber, 12-Heater, 13-Temperature sensor

$$\phi_r = \tan^{-1}[\cosh(a_s l_s) \sinh(a_s l_s) / \cos(a_s l_s) \sin(a_s l_s)] \quad (6.5)$$

$$\phi_r = \tan^{-1}[\cos(a_s l_s) \sinh(a_s l_s) / \cosh(a_s l_s) \sin(a_s l_s)] \quad (6.6)$$

where l_s is the thickness of the sample and $a_s = (\pi f / \alpha)^{1/2}$ is the thermal diffusion coefficient of the sample at frequency f . α is the thermal diffusivity of the sample which we want to measure. From equations (1) and (2), an expression for phase difference can be written as

$$\tan(\phi_r - \phi_r) = \tanh(a_s l_s) \tan(a_s l_s) \quad (6.6)$$

This equation is used to evaluate α after measuring the phase difference $(\phi_r - \phi_r)$. This technique has been tested on a number of samples whose thermal diffusivities are known and is found to work very well on samples with different thermal diffusivity values. Results on some standard samples can be found in reference [7].

We have followed the above technique to determine thermal diffusivity of our conducting polymer samples. Pelletised samples, cut into thin discs of diameter about 6mm and

thickness about 2mm have been used in the measurements. The two sides of the samples have been hand lapped and polished before mounting in the PA cell for measurements. Since the samples are dark they give good photoacoustic signals so that phase difference between the front and rear surface illuminations in each case could be measured accurately. As in any measurement, experimental errors are there due to various experimental limitations. Uncertainties in measurement have been estimated in each case and recorded.

6. 3 RESULTS AND DISCUSSION

The measured values of thermal diffusivity for polyaniline, polyanisidine, co-polymers of aniline and anisidine, aniline and benzidine , and anisidine and benzidine at room temperature are tabulated in Table 6.1. The tabulated values show that the thermal diffusivity of these samples are comparable to that of normal nonconducting polymers. Since the thermal diffusivity of these samples have not been reported before, we could not make any comparison. The variation of thermal diffusivity with temperature also could not be measured which we intend to do later.

The thermal diffusivity data on our conducting polymer samples indicate that even though doping enhances their electrical conductivity, thermal diffusivity do not get enhanced likewise. This means that Wideman-Franz law is not followed by these samples. It is an expected result because Wideman-Franz law is followed by systems which exhibit free electron conductivity. Since electrical conduction in conducting polymers is due to a variety of mechanisms such as electron tunneling, variable range hopping, inter chain and intra chain hopping which are phenomena responsible for electrical transport in disordered systems, one need not expect thermal conductivity to follow electrical conductivity behaviour. The low values of thermal conductivity indicate that the primary heat carriers in conducting polymer samples are phonons. Even though our samples are good electrical conductors, basically it is a disordered system containing a very large number of scattering centers. The phonon mean free path is limited by scattering from these scattering centers limiting the values of thermal conductivity to those of ordinary nonconducting polymers .

Since we could not make measurements on the temperature variation of thermal diffusivity/conductivity, we are not able to say anything more about the scattering processes that limit the thermal conductivity values to the measured ones. Experimental data on heat capacity, temperature variation of heat capacity, sound velocities etc. are also needed to throw more light on the mechanism of thermal transport in these complex systems.

Table 6.1

The measured values of the thermal diffusivity of polyaromatic amines.

Sample.	Measured.	Standard deviation.
Polyaniline.	5.6172×10^{-3}	0.2159×10^{-3}
Polyanisdine	4.5137×10^{-3}	0.1426×10^{-3}
Co-polymer of aniline and anisidine.	4.7602×10^{-3}	0.1935×10^{-3}
Co-polymer of aniline and benzidine.	3.3445×10^{-3}	0.2146×10^{-3}
Co-polymer of anisidine and benzidine.	4.6762×10^{-3}	0.1165×10^{-3}

REFERENCES

1. A. Rosenswaig and A. Gersho, *J. Appl. Phys.*,
47 (1976) 64.
2. F. A. McDonald and G. C. Wetsd Jr, *J. Appl. Phys.*, 49
(1978) 2313.
3. A. Rosenswaig in *Photoacoustics and Photoacoustic
Spectroscopy* (John Wiley & Sons 1981).
4. K. N. Madhusoodhanan, J. Philip, G. Parthasarathy, S.
Asokan and E. S. R. Gopal, *Phil. Mag.*, B 58 (1988) 123.
5. P. Charpentier, F. Lepoutre and L. Bertrand, *J. Appl.
Phys.*, 53 (1982) 608.
6. K. N. Madhusoodanan, M. R. Thomas and J. Philip,
J. Appl. Phys., 62 (1987) 1162.
7. Sheenu Thomas, Johnney Issac and J. Philip, *Rev.
Scientific Instruments*, 66 (1995) 3907.
8. O. Pessoa Jr., C. L. Cesar, N. A. Patel, H. Vargas,
C. C. Ghizone and L. C. M. Miranda,
J. Appl. Phys., 59 (1986) 1316.

CHAPTER.7

SUMMARY AND CONCLUSION

The work reported in the previous chapters of this thesis is basically centered around the following conducting polymers - polyaniline, polyanisidine, copolymers of aniline and anisidine, aniline and benzidine, and anisidine and benzidine. Chemical polymerisation techniques have been adopted for the synthesis of these polymers. The polymers have been characterised using UV-Vis absorption measurements, Fourier transform IR absorption measurements, Nuclear magnetic resonance spectra, and X-Ray diffraction. The characterisation of the material using FTIR, UV-Visible and NMR spectroscopy show that polyaniline and polyanisidine have similar structure as reported earlier. The copolymers based on the different monomers show differences in the spectra which indicate that the copolymers have lower structural order in comparison to their parent polymers.

The dc and ac conductivity and thermoelectric power measurements have been made on doped samples over a temperature range of 30 K to 295 K. Computer controlled

measurement systems have been used in these experiments. We have got some very interesting and new results from these measurements. The observed reduction in conductivity and the differences in the temperature dependence of conductivity of copolymers is in support of the structural disorder of these materials. Polymers having methoxy substituents on the aromatic ring show interesting temperature behaviour in dc conductivity. The variation of the conductivity with temperature in these polymers has two different regions. Measurements on the temperature variation of conductivity in some of these polymers are reported for the first time and so are the measurements on thermoelectric power. The thermoelectric power measurements show that all the polymers show a sign change around room temperature. The temperature behaviour of thermoelectric power is similar to that reported in the case of polyaniline. An exception is observed in the case of co-polymers containing anisidine and benzidine. In addition we have measured the ac conductivity of our samples. The results are interesting and reported for the first time in these samples.

In addition to electrical properties, we have studied selected thermal properties of our samples. The thermal diffusivity of the samples pelletized into disc form have

been measured using the photoacoustic technique. Only very limited work had been reported so far on the thermal properties of conducting polymers and our results are the first of this kind on polyaromatic amines.

The interesting results obtained by us in our samples are of great value for future workers on conducting polyaromatic amines and these will be published soon in journals in the relevant area.

There is plenty of scope for doing further work in this area. Many more polyaromatic amines remain to be made conducting by doping. It is very valuable and important to investigate their electrical transport as well as other physical properties. Some of them might find practical applications. The applications depend very much on their properties.

Even in the case of the polyaromatic amines we have investigated, several more things remain to be done. The theoretical explanations provided for the measured conductivity and thermoelectric power behaviour is not complete. More measurements would be required to provide a thorough quantitative explanation for our experimental

findings. Complicated interplay of different processes such as variable range hopping, tunneling across the conducting regions, transport within the conducting regions etc. make the situation very complex. Only very few measurements have been done on the thermal properties of these materials. There is plenty of scope for doing frontline work in this area.

The subject of conducting polymers is very vast and we have just entered this field. With the possession of exciting electrical and optical properties, conducting polymers are poised to become materials of not too far away future.

